INVESTIGATION OF THE EFFECTS OF DIFFERENT ADDITIVES ON PYROLYSIS LIQUID PRODUCT PROPERTIES

Ahmed AYYASH

Master's Thesis

Department of Chemical Engineering

Programme in Process and Reactor Design

Supervisor: Prof. Dr. Esin APAYDIN VAROL

Eskişehir

Eskişehir Technical University

Institute of Graduate Programs

June 2022

FINAL APPROVAL FOR THESIS

This thesis titled INVESTIGATION OF THE EFFECTS OF DIFFERENT ADDITIVES ON PYROLYSIS LIQUID PRODUCT PROPERTIES has been prepared and submitted by Ahmed AYYASH in partial fulfillment of the requirements in "Eskişehir Technical University Directive on Graduate Education and Examination" for the Degree of Master's in Chemical Engineering Department has been examined and approved on 21/06/2022.

Committee Members		Title, Name and Surname	Signature
Member (Supervisor)	:	Prof. Dr. Esin APAYDIN VAROL	
Member	:	Prof. Dr. İlker KIPÇAK	
Member	:	Doç. Dr. Elif Begüm ELÇİOĞLU	

Prof. Dr. Murat TANIŞLI

Director of the Institute of Graduate Programs

21/06/2022

SUPERVISOR APPROVAL

Master's student Ahmed AYYASH, whom I supervise, has completed this thesis titled INVESTIGATION OF THE EFFECTS OF DIFFERENT ADDITIVES ON PYROLYSIS LIQUID PRODUCT PROPERTIES. According to my inspections, the work is scientifically and ethically appropriate for the student to the thesis defense exam.

Supervisor

Prof. Dr. Esin APAYDIN VAROL

ABSTRACT

INVESTIGATION OF THE EFFECTS OF DIFFERENT ADDITIVES ON PYROLYSIS LIQUID PRODUCT PROPERTIES

Ahmed AYYASH

Department of Chemical Engineering

Eskişehir Technical University, Institute of Graduate Programs, June 2022

Supervisor: Prof. Dr. Esin APAYDIN VAROL

In this thesis, the effect of aging under different conditions (7 days at room temperature, and 24 and 168 hours at 80 ºC), and the addition of chemicals on the characteristics and rheological behavior of olive pomace-based bio-oil were investigated. Bio-oil was produced via slow pyrolysis at 500 ºC. Methanol, furfural, and tetrahydronaphthalene were used as the solvent additives at 5, 10, and 15 wt.%. Ultimate analysis, FT-IR, TGA, and GC-MS analyses were conducted on pre- and post-aged samples to analyze the characteristics of bio-oil and a rheometer was used to analyze the rheological behavior of each sample under different shear rates and temperatures. Shear rate ramp was increased from 5 to 580 s^{-1}, and temperature ramp was applied from 20 to 60 ºC.

Bio-oil was found to be unstable after a certain period under all storage conditions and durations. GC-MS results showed that chemical reactions occur during storage and the additives trigger several chemical reactions between the compounds in the bio-oil. The rheological behavior of bio-oil was found to be Newtonian. Solvent addition to bio-oil improved the dynamic viscosity. The addition of 10% methanol decreased the dynamic viscosity of non-aged bio-oil by 34.54% and after 168 hours of accelerated aging by 33.90% at 40 ºC. Among the chemicals used in this study, methanol was found to be the best additive for the long-term stability of bio-oil.

As a result, storage temperature, compared to storage duration has a higher effect on the stability of olive pomace-based bio-oil.

Keywords: Pyrolysis, Olive pomace, Bio-oil, Characterization, Additives, Rheology.

ÖZET

FARKLI KATKI MALZEMELERININ PIROLIZ SIVI ÜRÜNÜ ÖZELLIKLERINE ETKISININ ARASTIRILMASI

Ahmed AYYASH

Kimya Mühendisliği Anabilim Dalı

Proses ve Reaktör Tasarımı Bilim Dalı

Eskişehir Teknik Üniversitesi, Lisansüstü Eğitim Enstitüsü, Haziran 2022

Danışman: Prof. Dr. Esin APAYDIN VAROL

Bu tezde, pirinadan elde edilen piroliz sıvı ürünün özelliklerine ve reolojik davranışına farklı koşullar altında (oda sıcaklığında 7 gün ve 80 ºC'de 24 ve 168 saat) depolamanın ve kimyasal eklenmesinin etkileri araştırılmıştır. Sıvı ürün, 500 ºC'de yavaş piroliz yöntemi ile üretilmiştir. Çözücü katkı maddeleri olarak metanol, furfural ve tetrahidronaftalin ağırlıkça %5, %10 ve %15 oranında kullanılmıştır. Piroliz sıvı ürünün karakterizasyonu için depolama öncesi ve sonrası her numuneye, FT-IR, TGA ve GC-MS analizleri yapılmıştır, aynı zamanda reolojik davranışını farklı kayma hızları (5'ten 580'e s^{-1}) ve farklı sıcaklıklar altında analiz etmek için reometre kullanılmıştır. Sıcaklık artış testi ise 20'den 60 ºC'ye uygulanmıştır.

Tüm depolama koşulları ve süreleri altında belirli bir süre sonra sıvı ürünün stabil olmadığı saptanmıştır. GC-MS sonuçlarına göre depolama sırasında kimyasal tepkimelerin oluştuğu ve katkı maddelerinin eklenmesiyle gerçekleşen tepkimelerin farklılaştığı görülmüştür. Piroliz sıvı ürünün reolojik davranışının Newtonian olduğu saptanmıştır. Katkı malzemeleri eklendiğinde piroliz sıvı ürünün dinamik viskozitesini iyileştiği belirlenmiştir. %10 metanol eklenmesi ile, ham sıvı ürünün 40 ºC'de dinamik viskozitesinde %34,54, 168 saat hızlandırılmış depolamanın ardından ise %33,90 oranında azalma olduğu görülmüştür. Bu çalışmada kullanılan kimyasallar arasında, piroliz sıvı ürününün uzun süreli stabilizesi için en iyi katkı maddesi metanol olarak bulunmuştur.

Sonuç olarak, depolama sıcaklığı, pirina bazlı biyo-yağın stabilitesi üzerinde depolama süresine göre daha yüksek bir etkiye sahiptir.

Anahtar Sözcükler: Piroliz, Pirina, Biyo-yağ, Karakterizasyon, Reoloji.

ACKNOWLEDGEMENTS

I would like to express my gratitude to my supervisor, Prof. Dr. Esin APAYDIN VAROL, who guided me throughout this study. I am also thankful to Assoc. Prof. Gamzenur ÖZSİN and Dr. Murat KILIÇ for their help during my experiments.

A special thanks to my family, especially my parents. Their belief in me has kept my spirits and motivation high during this process. I would also like to thank my beloved wife for encouraging me throughout this experience.

Ahmed AYYASH

21/06/2022

STATEMENT OF COMPLIANCE WITH ETHICAL PRINCIPLES AND RULES

I hereby truthfully declare that this thesis is an original work prepared by me; that I have behaved in accordance with the scientific ethical principles and rules throughout the stages of preparation, data collection, analysis and presentation of my work; that I have cited the sources of all the data and information that could be obtained within the scope of this study, and included these sources in the references section; and that this study has been scanned for plagiarism with "scientific plagiarism detection program" used by Eskişehir Technical University, and that "it does not have any plagiarism" whatsoever. I also declare that, if a case contrary to my declaration is detected in my work at any time, I hereby express my consent to all the ethical and legal consequences that are involved.

Ahmed AYYASH

CONTENTS

Page

LIST OF TABLES

Page

LIST OF FIGURES

Page

GLOSSARY OF SYMBOLS AND ABBREVIATIONS

FT-IR	:	Fourier Transform Infrared Spectroscopy
TGA	:	Thermogravimetric Analysis
GC-MS	:	Gas Chromatography–Mass Spectrometry
Pa	:	Pascal
h	:	Hours
s	:	Seconds
HDO	:	Hydrodeoxygenation
τ	:	Shear stress (Pa)
cP	:	CentiPoise
η	:	Dynamic viscosity (cP)
η_T		Transformed dynamic viscosity
$\dot{\gamma}$	:	Shear rate (s^{-1})
E	:	Activation energy ($J.mol^{-1}$)
R	:	Universal gas constant ($J.\ mol^{-1}.\ K^{-1}$)
θ	:	Angle (degree)
ω	:	Angular velocity ($rad.s^{-1}$)
d	:	Cone and plate gap (m)
N.m	:	Newton-meter
F	:	Force (N)
A	:	Surface area (m^2)
V	:	Velocity (m/s)
cst	:	Centistokes
NMR	:	Nuclear Magnetic Resonance
L	:	Liter
wt.%	:	Percentage by weight
ASTM	:	American Society for Testing and Materials
Hz	:	Hertz

PID	:	Proportional-Integral Derivative
Q_{GCV}	:	Gross calorific value (MJ/kg)
DAF	:	Dry and Ash-Free
ND	:	Not detected
AI	:	Aging index
NA	:	Not available
NNP	:	Normal Probability Plot
ANOVA	:	Analysis of variance

1. INTRODUCTION

One of the main crucial fuels to the transportation industry is hydrocarbons, especially liquid and gaseous fuels. The desirable hydrocarbons being produced from fossil fuel sources caused severe global problems by increasing the concentration of carbon dioxide (CO_2) in the atmosphere [1]. With the growing demand for fuel used to produce electricity and used in transportation, increasing the percentage use of renewable sources for energy purposes become an urgent need [2]. Biomass, which is a cheap and abundant source, is considered to be one of the renewable energy resources that could be recycled to produce bio-oil [3,4]. The development and application of bio-oil derived from various biomass wastes have been investigated extensively in the last decades [5–7].

Various processes can be used to produce bio-oil. Pyrolysis and hydrothermal liquefaction have become the two most common methods [8]. Pyrolysis is the thermal decomposition of biomass occurring in the absence of oxygen and with or without nitrogen as a flowing gas, has been accepted as a potential method regarding reasonable cost, simple operation, and high liquid yields [9,10].

Although bio-oil is being used in several applications such as direct combustion for diesel engines [11], boilers [12,13], and gas turbines [14–16], the commercial application of bio-oil hasn't reached the desired level yet, because of its technical lacking, economical return, and instability during storage. The instability of bio-oil is typically called "aging" which describes the changes in bio-oil over time [17]. The chemical and physical properties of bio-oil may change during storage and multiphase behavior may occur, making it challenging to storage, transportation, and upgrade [18]. Chemical and physical methods could be applied to bio-oil to reduce the effects of aging. These methods include, but not limited to, biomass drying, solvent addition, emulsification, removal of solid char, esterification, mild hydrogenation, catalytic cracking, and so on [19].

In this thesis, to overcome the stability problems that occurred during storage, the chemical upgrading method represented by solvent addition was investigated to measure the influences on slowing the aging mechanism which causes bio-oils instability. Bio-oil produced via slow pyrolysis method at 500 ^{o}C from olive biomass was used. The effects of aging under different conditions and adding different solvents with various ratios were investigated. Pre-

and post-aged bio-oil samples were characterized and the rheological properties were measured. Ultimate analysis, FT-IR, TGA, and GC-MS were used to analyze and characterize bio-oil samples and a rheometer was used to analyze the rheological behavior under different shear rates and temperatures.

2. BIOMASS

Biomass word refers to any living organism that includes both the above- and the belowground parts of plants, animals, and microorganisms. It also refers to cellulose, lignin, sugars, fats, and proteins from a biochemical perspective [20].

Mankind used biomass energy or bioenergy (the energy from organic matter) for thousands of years since fire was founded and used to cook food or to keep warm. Today, wood is still our largest biomass energy source [21]. In addition to wood and wood processing wastes, agricultural crops and waste materials (e.g., corn, soybeans, sugar cane, switch grass, palm, and olive pomace, etc.), animal manure and human sewage and biogenic materials are examples of biomass sources used to produce energy.

Pollution is considered one of the biggest issues worldwide due to increasing energy consumption from fossil sources. This forces mankind toward renewable energy sources including biomass. Although biomass produces the same amount of carbon dioxide as fossil fuels, carbon dioxide is removed during plant growth. In the process of photosynthesis, plants capture and use radiant energy from the sun to convert water, carbon dioxide, and minerals into oxygen and energy-rich organic compounds (Figure 2.1) [21–23].

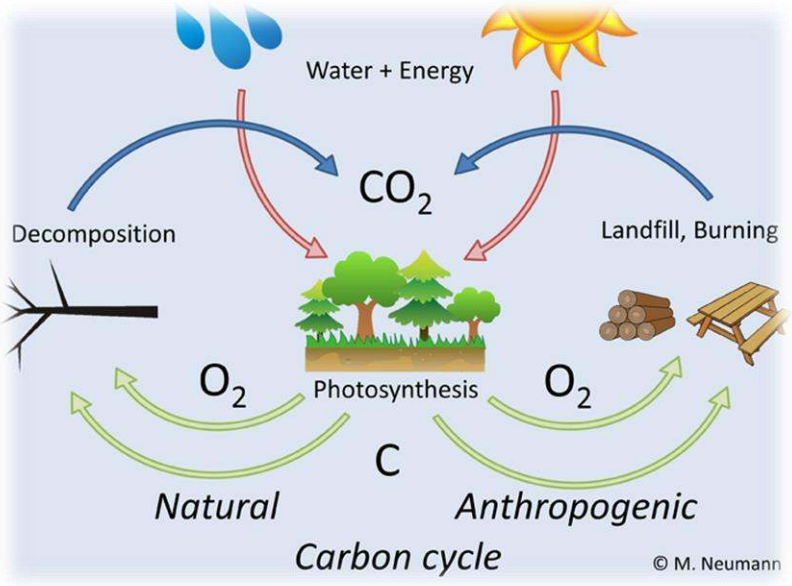

Figure 2.1. *Biomass carbon cycle* [24]

2.1. Olive Pomace

The olive tree is among the oldest known cultivated trees in the world. It seems certain that the olive tree, as it is known today, had its origin about 5,000 years ago in the region corresponding to ancient Persia and Mesopotamia and from there it spread to Syria and Palestine [25].

The olive tree is mainly used for oil and canned fruit production. The leaves due to their high phenolic compound content as oleuropein and hydroxytyrosol are used in medicine as herb tea, which are beneficial in nutrition and medicine [26].

Olive production worldwide varies from year to year, however, it shows an increment each year. 90% of the worldwide olive cultivation is done in the Mediterranean basin and the rest is in Latin American countries. Approximately 17 million tons of grain olives are obtained from 900 million olive trees in around 10 million hectares of land in the world. The average worldwide annually olive oil production, according to the last 5 seasons, is around 3 million tons/year. The largest olive and olive oil-producing countries are Spain, Italy, Greece, Turkey, Tunisia, and Morocco [27].

Olive average production during the period 2016-2020 in Turkey was 1,634,419 tons, with 449,000 tons used as table olive, and the rest (1,185,419 tons) used to produce olive oil [28].

Olive pomace is the main residue of the olive oil extraction process that is a thick dark brown sludge. It is the remaining pulpy material after removing most of the oil from the olive paste and it consists of pieces of skin, pulp, stone, and olive kernel [29]. Of the total olive weight, the pulp makes up about 70–90%, the stone about 9–27%, and the seed about 2–3% [30].

Depending on the production line, the moisture percentage of olive pomace is close to 70% in the two-phase and about 45% in the three-phase decanter. Besides water, olive pomace contains carbohydrates, lipids (remaining oil), phenols, and several inorganic compounds with an average pH of 4.8–5.2. Cellulose, hemicellulose, and lignin are the main components; however, fat and protein are also present in significant quantities [29].

2.2. Thermochemical Conversion

Biomass fuels and residues can be converted to energy via thermochemical and biological processes. Generally, compared to biological processes, thermochemical processes have higher efficiencies in terms of the lower reaction time required [31].

In thermochemical conversion, numerous technologies are applicable to biomass (Table 2.1). Pyrolysis is considered to be an industrial realized process for biomass conversion. Depending on the heating rate, reaction temperature, and residence time, pyrolysis can be classified into slow, fast, and flash pyrolysis. Typically, slow pyrolysis has a lower reaction temperature and a longer residence time and would produce a higher yield of solid char product. In contrast, fast pyrolysis has a very short residence time and a higher reaction temperature compared to slow pyrolysis. And hence, fast pyrolysis results in a higher yield of liquid product. Moreover, gasification is a process that converts carbonaceous biomass into combustible gases with specific heating values in the presence of a partial oxygen supply or suitable oxidants such as steam. In other words, gasification can be viewed as a special form of pyrolysis, taking place at higher temperatures to achieve higher gas yields [32–34]. Thermochemical conversion technologies and the main differences among them are highlighted in Table 2.1

.

Table 2.1. *Processes for the thermochemical conversion of biomass* [35]

Technology	Temperature	Heating rate	Pressure reaction	Reaction time	Medium	Target product
Torrefaction	200–300 °C	-	Atmospheric	<2 h	Oxygen-free atmosphere	Torrefied biomass
Slow pyrolysis	>300 °C	<20 °C.min^{-1}	Atmospheric	Hours–months	Oxygen-free atmosphere	Char
Fast pyrolysis	>300 °C	Up to 1000 °C.min^{-1}	Atmospheric or vacuum	<2 s	Oxygen-free atmosphere	Bio-oil
Flash carbonization	<800 °C	-	1 Mpa	<30 min	Oxygen-free atmosphere/air	Char
Gasification	600–1800 °C	-	0.1–8 Mpa	-	Steam and oxygen or air	Gas
Hydrothermal carbonization	180–220 °C	-	Water saturation pressure	Hours	Water	Char
Wet torrefaction	200–260 °C	-	Water saturation pressure	5 min	Water	Char
Hydrothermal liquefaction	300–350	-	15–20 Mpa	5–15 min	Water	Bio-oil
Supercritical water gasification	>650	-	>22 Mpa	-	Supercritical water	Gas
Plasma pyrolysis	>3000	-	-	-	Ionized gas	Gas

2.3. Slow Pyrolysis

Pyrolysis is a thermal decomposition occurring at high temperatures (>300 ^{o}C) in the absence of oxygen. Temperature and residence time play a major role in the pyrolysis products ratio. Low temperature and longer residence time increase the production of solid char product. High temperature and longer residence time enhance gas production and moderate temperatures with short residence time are the optimum conditions for producing liquids [36].

Slow pyrolysis has been used for thousands of years to produce charcoal. The process of slow pyrolysis is typically heating biomass to about 500 ^{o}C at slow heating rates (up to 10-20 ^{o}C.min^{-1}), with a residence time between 5 to 30 minutes [37]. In pyrolysis, biomass is converted to char and volatiles during the heating process. The volatiles contain low and high molecular weight hydrocarbon gases, some of which can be condensed at 0 ^{o}C and quenched as bio-oil (liquid product). Non-condensable gases such as CO_2, CH_4, CO, and H_2 are the gaseous products of the slow pyrolysis process. Char is the pyrolysis solid product, that is rich in carbon content. The relatively simple single particle pyrolysis model is shown in Figure 2.2.

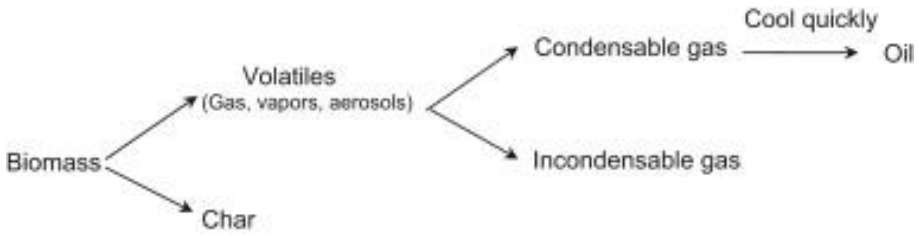

Figure 2.2. *Reaction pathway for the biomass pyrolysis process* [38]

3. BIO-OIL

Bio-oil is the liquid product from the condensation of the condensed fragments of the cellulose, hemicellulose, and lignin present in the feedstock. It's a dark brown liquid, its color and heating value depend on the chemical composition of the feedstock.

Bio-oil has undesirable properties represented by high viscosity, thermal instability, high moisture content, and high acidity that limit its usage except in direct boiler applications, possibly for some types of turbine and diesel applications after being modified and in some applications in the chemical industry [39–42]. Furthermore, the properties of bio-oil are connected to its feedstock and to any variations in the pyrolysis process. Several studies mentioned that the parameters such as feedstock chemical composition, particle size, moisture content, final pyrolysis temperature, holding period, and heating rate, significantly, affect the bio-oil yield and properties [43–48]. Therefore, to understand the properties of bio-oil characterization, it is vital to understand the kind of upgrading method that should be used to produce high-quality transportation fuels and chemicals [1].

3.1. Storage Stability of Bio-oil

The viscosity of bio-oil produced by pyrolysis of biomass is considered to be low, especially, if it is produced under conditions of rapid heating and short reactor residence times. In order to use bio-oil as an alternative fuel, bio-oil should retain its initial physical and chemical properties during storage, shipment, and use. Unfortunately, the viscosity of bio-oil rapidly increases during storage at room temperature and much faster at higher temperatures [41,49].

Bio-oil is not a product of thermodynamic equilibrium during pyrolysis [50], it is produced with short reactor times and rapid cooling. This produces a condensate that is also not at thermodynamic equilibrium at storage temperatures. Bio-oil contains a large number of oxygenated organic compounds with a wide range of molecular weights, typically in small percentages [51]. During storage, the chemical composition of the bio-oil changes toward thermodynamic equilibrium, resulting in changes in the viscosity, molecular weight, and co-solubility of its many compounds [52].

The chemical composition, physical and chemical properties of fresh oil play a major role on the aging processes of bio-oil. As can be seen from Figure 3.1, all these properties depend on each other mutually [53].

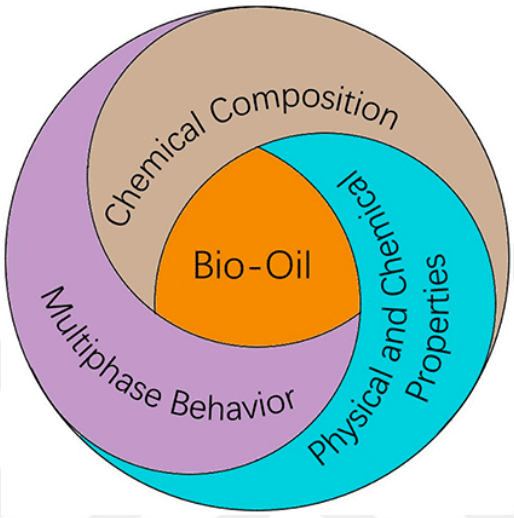

Figure 3.1. *Mutually dependent chemical composition, chemical and physical properties, and multiphase behavior of bio-oil* [53]

3.2. Chemical Changes During Storage

Bio-oil is a mixture containing more than a hundred organic compounds that make it impossible to determine all possible reactions taking place during storage. However, based on the theoretical background, the main reactions that may be responsible for bio-oil aging can be briefly described below:

3.2.1. Esterification

The reaction of alcohols with organic acids forms esters and water:

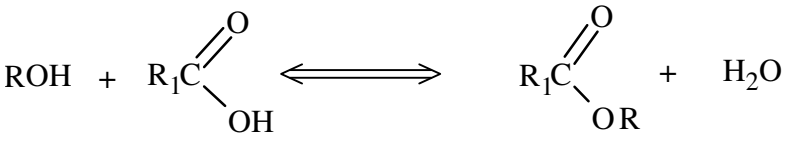

Figure 3.2. *Esterification reaction*

where R and R_1 are alkyl groups.

Esters are well known for their aromas. These reversible ester-forming reactions can take place over the course of several years. They are catalyzed by acids, which are of interest in bio-oil with their naturally low pH of 2.3 to 3.0 [52,54].

3.2.2. Transesterification

The transesterification reaction is the exchange of alcohol and acid groups in a mixture of two or more esters:

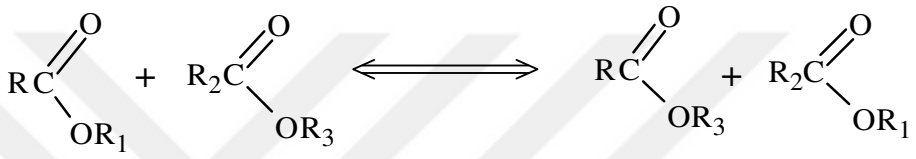

Figure 3.3 *Transesterification reaction*

This reaction is catalyzed similarly to esterification. In a mixture of esters, transesterification is thought to occur. Because esterification is reversible, acids and alcohols can also be reacted with esters to form new esters, acids, and alcohols [52,54].

3.2.3. Homopolymerization

Aldehydes can react with each other to form polyacetal oligomers and polymers [52,54]:

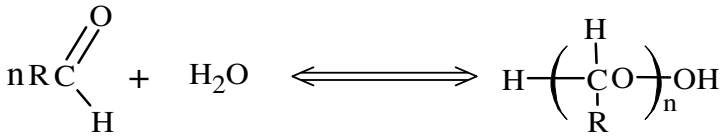

Figure 3.4. *Homopolymerization reaction*

3.2.4. Hydration

Aldehydes or ketones mixed with water react to form hydrates, also referred to as glycols [52,54]:

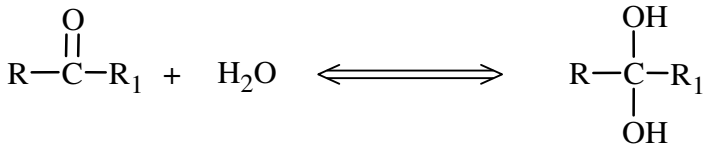

Figure 3.5. *Hydration reaction*

where R and R_1 are hydrogen or alkyl groups.

3.2.5. Hemiacetal formation

When alcohol is mixed with an aldehyde, hemiacetal is formed with a significant amount of heat liberating, it is notable that this reaction takes place relatively quickly and without catalysis [52,54]:

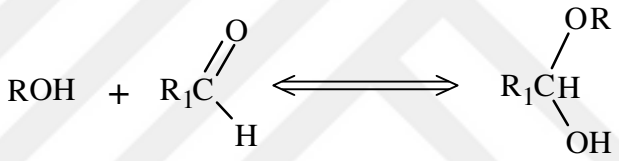

Figure 3.6. *Hemiacetal formation*

3.2.6. Acetalization

Aldehydes and alcohols react to form acetyls as shown by the following reactions:

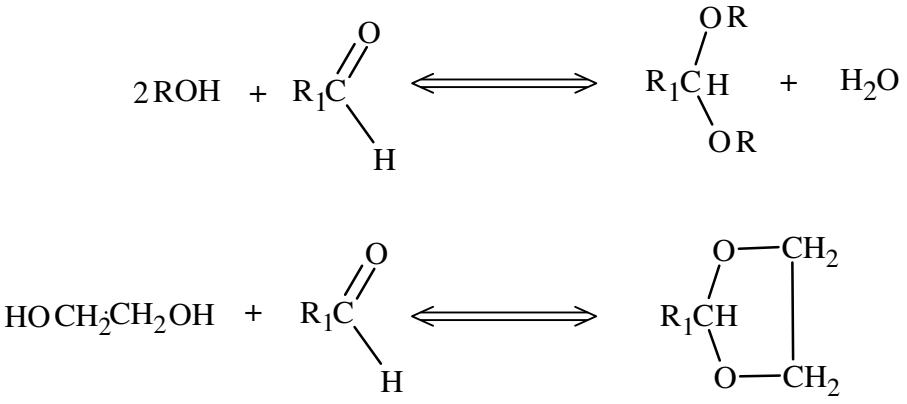

Figure 3.7. *Acetalization reactions*

In the presence of acid catalysts, stable formals are formed by the reaction of aldehydes and the hydroxyl groups of sugars, starches, and cellulose. Cellulose reacted with formaldehyde

and an acid catalyst creates a cross-linked polymer that resists swelling in water and dyes [52,54].

3.2.7. Phenol/Aldehyde reactions and resins

Phenol reacts as alcohol with formaldehyde to form the hemiformal in the absence of catalysts, or, phenols and substituted phenols react with aldehyde hydrates to form novolak resins and water [52,54]:

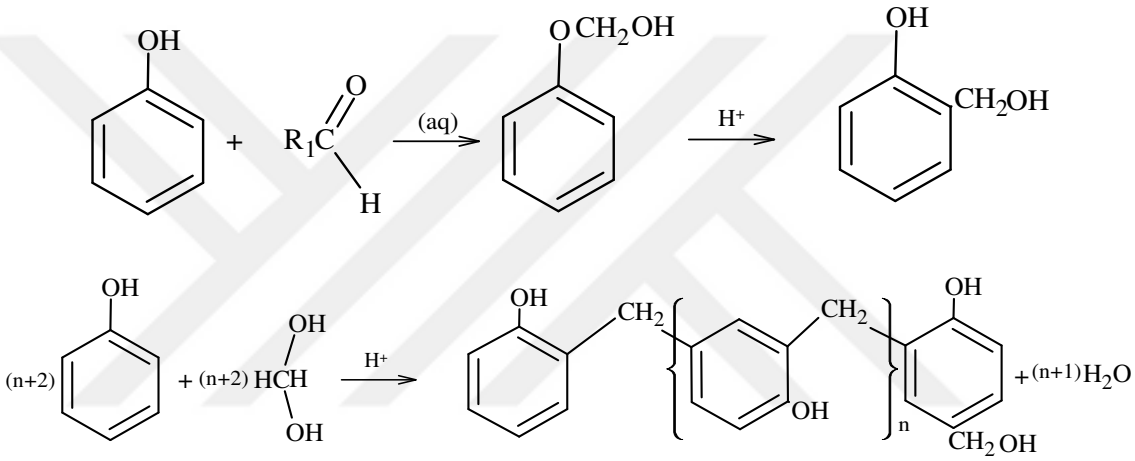

Figure 3.8. *Phenol/aldehyde reactions*

3.2.8. Oxidation

The exposure of bio-oil to air can oxidize the alcohols and aldehydes to carboxylic acids. However, a more important reaction that affects the storage of pyrolysis oils is that of forming hydroperoxides and alkylperoxides by autoxidation with air.

Hydroperoxides can be formed by reacting air with olefins, ethers, ketones, nitrogen compounds, aldehydes, and organic acids. Peroxides are sources of free-radicals, which can catalyze olefinic polymerization. The ease of forming hydroperoxides is related to the ease of breaking the C-H bonds involved. Thus, for hydrocarbons the relative ease of forming hydro peroxides increases in the following order: *n*-alkanes < branched alkanes < aralkanes ≅ alkenes < alkynes [52,54].

3.3. Bio-oil Upgrading Methods

Bio-oil upgrading methods are divided into two different categories; physical and chemical methods:

3.3.1. Physical methods

3.3.1.1. *Biomass drying*

Biomass materials often have a high content of moisture. This moisture will be transferred into bio-oil during the condensation portion of pyrolysis. In addition to this, a considerable amount of water will be produced in the pyrolysis process. Removing water from biomass will decrease the amount of moisture in bio-oil. Therefore, a drying pretreatment of biomass is essential for the reduction of the water content to an acceptable level [54,55].

3.3.1.2. *Emulsification*

Emulsification of bio-oil with other petroleum fuels, such as diesel is one of the promising methods to decrease bio-oil viscosity.

Emulsification involves two immiscible liquids in which droplets of one phase (the dispersed or internal phase) are encapsulated with in a layer of another phase (the continuous or external phase) with the help of agitation and emulsifying agent (also known as surfactant). The quality of the final mixture is highly dependent on agitation intensity, surfactant concentration, operation temperature, and bio-oil to bio-diesel ratio [56].

3.3.1.3. *Removal of solid char residue*

The solids content in bio-oil includes coke, char and ash attained during the pyrolysis process. While the most common inorganic elements found in biomass ash are potassium, calcium, sodium, magnesium, silicon, phosphorus, and chlorine, a higher concentration of them may catalyze polymerization and condensation of reactive species and consequently increase the viscosity of bio-oil [53,56–59].

The removal of ash, char and especially metallic ions may lead to improving the stability of bio-oil [18,54,60].

3.3.2. Chemical methods

Chemical methods can improve the stability of bio-oil. Catalytic cracking, catalytic hydrogenation, and catalytic esterification are the main methods [54].

3.3.2.1. *Solvent additions*

One of the most effective and easiest methods for improving the stability of bio-oil is adding soluble organic solvents [54]. Solvents added to bio-oil influence the viscosity of bio-oil primarily by the following 3 types of mechanisms: (1) physical dilution; (2) reducing reactant concentration or changing micro- structure of bio-oil to reduce the reaction rate; and (3) formation of an ester or acetal based on reacting with active components in bio-oil to prevent the generation of macro molecule polymer. One of the most disadvantages of this method is that the mechanisms involved in adding solvent are not quite understood yet [38,61].

3.3.2.2. *Esterification*

Esterification of bio-oil with low molecular weight alcohols has been demonstrated as an effective approach to mitigate the deleterious properties of bio-oil. After treating bio-oil, the acidity, density, heating value, and storage stability could be improved remarkably [62,63].

3.3.2.3. *Mild hydrodeoxygenation*

The presence of oxygenated compounds in bio-oil is another factor influencing the aging of bio-oil [64,65]. Therefore, the removal of oxygenated compounds can improve the stability of bio-oil by mild hydrogenation. Mild hydrogenation is the process of hydrodeoxygenation (HDO) of bio-oil carried out at a mild temperature using catalysts and high hydrogen pressure [66–69].

Mild hydrogenation can result in lower levels of chemically unstable compounds, oxygenates, and water, thus slowing the aging rate of the bio-oil and improving its stability. Despite the benefit of reducing the oxygen content in the bio-oil, mild hydrogenation can result in a significant decrease in liquid yield and appears to be a cost-effective technique. [53].

3.3.2.4. *Catalytic cracking*

Hydrocarbons are usually formed in very low yields during fast pyrolysis of biomass, but using proper cracking catalysts with deoxygenation capability can increase hydrocarbons formation [70]. Zeolite catalysts (such as HZSM-5, HY, etc.) are very effective to convert the highly oxygenated crude bio-oils or pyrolysis vapors to hydrocarbons that are dominated by several light aromatic hydrocarbons (benzene, toluene, xylene, and naphthalene) [71,72].

4. RHEOLOGY

Rheology means the study of the deformation and flow of matter. Flow properties of liquids are crucial in our lives. This importance ranges from the viscosity of the blood flowing around our bodies, through the thickness of the liquids that we swallow, to the grade of the oil used in car engines [73].

Rheology is the science of flow and deformation [30] and can be defined as the behavior of a fluid as a function of stress, strain, the rate of strain, and time. The field of rheology could be considered as understanding the behavior of complex fluids under various conditions [31].

4.1. Major Fluid Types

The function of viscosity involves shear rate and shear stress. The relationship between them can be obtained from experimental data. Behavior is visualized as a plot of shear stress versus shear rate, and the resulting curve is mathematically modeled using various functional relationships (Figure 4.1).

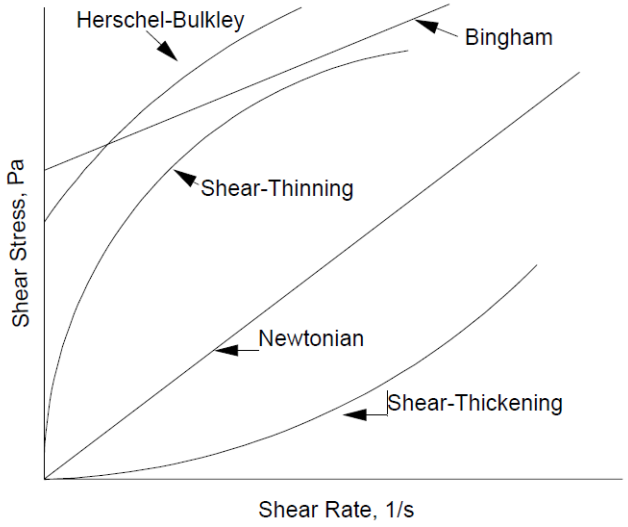

Figure 4.1. *Typical time-independent fluid curves* [74]

4.1.1. Newtonian fluids

The simplest type of substance to consider is the Newtonian fluid where shear stress is directly proportional to shear rate.

$$\tau = \eta\dot{\gamma} \quad (4.1)$$

where τ is the shear stress (Pa), η is the dynamic viscosity (Pa.s) and $\dot{\gamma}$ is the shear rate (s^{-1}).

Newtonian fluids, by definition, have a straight-line relationship between the shear stress and shear rate with a zero intercept. This shows that the dynamic viscosity is a constant of proportionality appropriate. A low viscosity Newtonian liquid such as water or alcohol would have a line with a small slope closer to the horizontal, while a high viscosity Newtonian fluid would have a line with a greater slope closer to the vertical [73].

All fluids which do not exhibit this behavior may be called non-Newtonian fluids.

4.1.2. Non-Newtonian fluids

Focusing on the relationship between shear stress and shear rate, the curves obtained from experimental data are nonlinear and does not start from the origin (intercept refers to yield stress), this kind of fluids are non-Newtonian fluids.

Dispersions, emulsions, and polymer solutions are considered non-Newtonian fluids. The viscosity of non-Newtonian fluids is not constant, it is a function of shear rate and time. According to this, fluid behavior is divided into two subgroups time-independent and time-dependent. In the first, the viscosity may increase with shear rate, and such behavior is called shear-thickening or dilatant, for the vast majority of cases, viscosity decrease with shear rate, and such behavior is called shear-thinning or pseudoplastic. This type of fluids may show a Newtonian behavior with an intercept value to indicate a Bingham plastic behavior. In the second (time-dependent), thixotropic or rheopectic, behaviors may be seen as, decreasing (thixotropic) and increasing (rheopectic) shear stress over time at a fixed rate of shear. In other words, thixotropy is time-dependent thinning and rheopexy is time-dependent thickening. Both phenomena may be irreversible, reversible, or partially reversible.[74]

4.2. Arrhenius-Type Relation for Newtonian Fluids

The linear relationship between dynamic viscosity and inverse temperature can be measured and modeled using an Arrhenius type relation [73,75–77] as given in Eq. 4.2:

$$\eta = Ae^{\frac{E}{RT}} \quad (4.2)$$

where η is the dynamic viscosity of bio-oil (cP); A is a constant (cP); E represents the flow activation energy ($J.mol^{-1}$) and R is the universal gas constant (8.314 $J.\ mol^{-1}.\ K^{-1}$). To achieve a linear relationship between viscosity and temperature, the Arrhenius equation is linearized as in Eq. 4.3.

$$\ln(\eta) = \ln(A) + \frac{E}{RT} \tag{4.3}$$

The above equation can be plotted as a straight line with ln(η) versus 1000/T. The slope of the straight lines is the activation energy E which is related to the rate of vaporization of the bio-oil [75] and/or to the amount of energy required to move the liquid [78].

4.3. Rheometers

Rheometry is the measuring technology used to measure rheological data, which includes, measuring systems, instruments, and test and analysis methods [79]. Although each rheometer has limits to the type of tests and the range of each test that can perform, modern rotational rheometers give the user the ability to apply a wide variety of tests (i.e., shear stress and shear rate controlled viscometry, shear stress, and shear strain controlled oscillation rheometry, creep test/creep recovery and stress relaxation) on dispersions, polymers, pastes, gels, and complex fluids. Some rheometers can perform temperature-controlled tests if equipped with the appropriate instrument. Coming with an easy-to-use user interface software, rheometers became a powerful tool to do rheological tests and analyses.

4.3.1. Geometries

Modern rheometers give the ability to use more than one geometry to measure the viscosity of a liquid. Each geometry has its design and properties. In the rheometer device, the commonly used ones are cone-plate, plate-plate, and bob-cup geometries (Figure 4.2) [80].

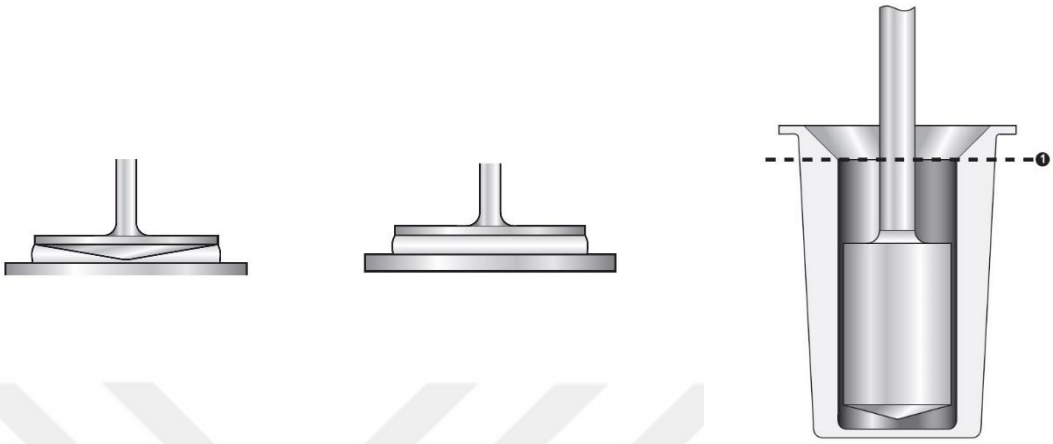

Cone and plate Plate and plate Bob and cup

Figure 4.2. *Vertical cross sections of common geometries used in rheometers* [81]

4.3.1.1. *Cone and plate*

Cone and plate geometry (Figure 4.3) are the most commonly used geometries for obtaining primary normal stress. In cone-plate geometry, the shear rate is distributed equally along with the radius of the geometry and the material needed to complete the measurement is lower compared to other geometries.

Cone has an angle of 4 degrees and 40 mm diameter, made from stainless steel 316 with a fixed gap equal to 0.15 mm during measurements.

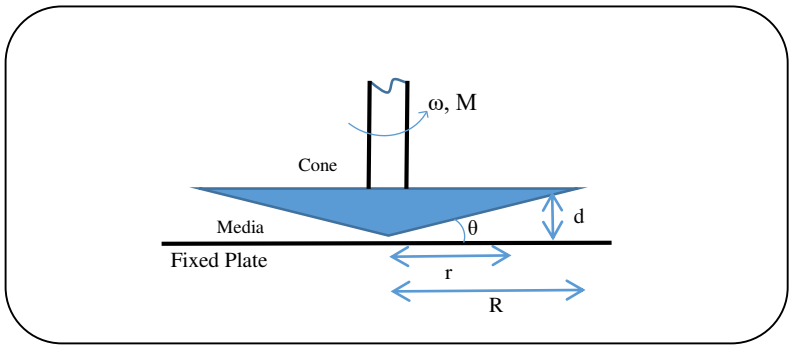

Figure 4.3. *Cone and plate system*

The cone is rotating at a known ω angular velocity (rad.s^{-1}) and M the resulting torque (N.m) is measured through the cone which translates to a F force (N) acting over A the surface

area (m) of the fixed plate to give τ a shear stress (F/A, Pa). In response to an applied τ, the sample will flow with $\dot{\gamma}$ a shear rate (s^{-1}). If the measurement gap (d) is accurately known, then the $\dot{\gamma}$ (V/d) can be determined from the measured ω of the cone, and its radius (r). Since V = r.ω, d = r.tan(θ), and with the small angel, tan(θ)=θ, the shear rate can be written as;

$$\dot{\gamma} = \frac{V}{d} = \frac{r\omega}{r tan(\theta)} = \frac{\omega}{\theta} \tag{4.4}$$

To develop an expression for shear stress, the differential torque on an annular ring of thickness dr is considered as;

$$dM = (2\pi r dr)\tau r \tag{4.5}$$

Integrating over the radius to find the total torque response will result in:

$$\int_0^M dM = \int_0^R (2\pi r^2 \tau) dr \tag{4.6}$$

Since the shear rate is constant in the gap, the shear stress is also constant in that area so $\tau \neq f(r)$. Then, Eq. 4.6 can be simplified to

$$M = 2\pi\tau \int_0^R r^2 dr \tag{4.7}$$

Hence,

$$\tau = \frac{3M}{2\pi R^3} \tag{4.8}$$

This result shows that shear stress, like shear rate, is constant throughout the gap [82].

5. LITERATURE REVIEW

5.1. Bio-oil Characterization

Bio-oil characteristics produced from different biomasses have been studied by researchers (Table 5.1).

E. Varol et al. [83], using pistachio shells as biomass, investigated the effects of pyrolysis temperature on the product yields and bio-oil characteristics. Five different temperatures were tested (300, 400, 500, 550, and 700 ^{o}C). The maximum liquid yield found to be obtained at around 500-550 ^{o}C, bio-oil produced at the optimum temperature was characterized using elemental analysis, column chromatography, FT-IR, and GC/MS.

B. Uzun et al. [84], studied the main characteristics of bio-oil produced from tea waste biomass using fast pyrolysis method. The effect of the pyrolysis temperature (673, 773, 823, 973 K), sweeping gas flow rate (100, 200, 400, 800 $cm^3.min^{-1}$), and heating rate (5, 300, 500, 700 $K.min^{-1}$) on pyrolysis yields were studied. The highest yield of liquid product was obtained under a heating rate of 500 $K.min^{-1}$, pyrolysis temperature of 773 K, and 200 $cm^3.min^{-1}$ of nitrogen flow rate. The ratio of pyrolytic oil products was found to be 30%. Bio-oil obtained at the optimum temperature was characterized using elemental analysis, FT-IR, ^{1}H NMR, and GC/MS. FT-IR results showed that some functional groups, e.g., hydroxyl and carbonyl groups disappeared at high pyrolysis temperatures.

C. Acikgoz [85], studied the characterization of slow pyrolysis bio-oil obtained from linseed (Linum usitatissimum L.) biomass. The main scope was to determine its elemental composition and calorific value. Moreover, chromatographic and spectroscopic techniques have been used to determine bio-oil chemical composition (GC, FT-IR, and ^{1}H NMR). Using liquid column chromatographic fractionation, the chemical composition of bio-oil was determined. Elemental analysis results showed that the ratios of C, H, N, and O were 74.2, 10.5, 1.5, and 13.8%, respectively. The calorific value was calculated as 34.58 MJ/kJ.

N. Özbay et al. [86], studied the main characteristics of bio-oil produced using slow pyrolysis from apricot pulp biomass. The optimum temperature for bio-oil yield was found at 550 ^{o}C, produced bio-oil at this temperature was characterized using elemental analysis, FT-IR, ^{1}H NMR, and GC/MS. Elemental analysis results showed that the ratios of C, H, N, and O were 61.50, 7.80, 1.74, and 28.96%, respectively. The calorific value was calculated

as 26.82 MJ/kJ. Phenols, acids, and aldehydes were found to be the main compounds in the bio-oil product according to GC/MS results.

R. Yin et al. [87], studied the main characteristics of bio-oil produced using a fluidized bed reactor fast pyrolysis system from sweet sorghum biomass. The reactor temperature was set at 500 ºC, and the flow rate of carrier gas was 60 $L.min^{-1}$. The pyrolysis gasses first passed through a cyclone to remove char. Then, they were passed to four fractional condensers and an electrostatic precipitator to trap the liquid oil. The bio-oil samples were collected from four condensers and the electrostatic precipitator separately, the samples were named 1, 2, 3, 4, and 5, respectively. Elemental analysis, water content, acidity, density, viscosity, GC/MS, and FT-IR analyzing methods were used for bio-oil characterization. Viscosity was measured at four different temperatures, i.e., 30, 40, 50, and 60 ºC. At 40 ºC, the viscosity was reported to be 1.89, 41.39, 90.15, 445.86 $mm^2.s^{-1}$ for 1, 2, 4 and 5 bio-oil samples.

Table 5.1. *Literature review on bio-oil characterization*

Biomass source	Type of pyrolysis	Type of reactor	Temp. (°C)	Bio-oil characterization	Reference
Pistachio shell	Slow pyrolysis	Fixed bed reactor	500-550	Elemental analysis, column chromatography, FT-IR, and GC/MS.	[83]
Tea waste	Fast pyrolysis	Fixed bed reactor	500	Elemental analysis, FT-IR, 1H NMR, and GC/MS	[84]
Linseed	Slow pyrolysis	Fixed bed reactor	550	Elemental analysis, column chromatography, FT-IR, GC, and 1H NMR.	[85]
Apricot pulps	Slow pyrolysis	Fixed bed reactor	550	Elemental analysis, FT-IR, 1H NMR, and GC/MS	[86]
Sweet sorghum	Fast pyrolysis	Fluidized bed reactor	500	Elemental analysis, water content, Acidity, Density, Viscosity, GC-MS, and FT-IR	[87]

5.2. Bio-oil Upgrading Studies Using Solvent Addition Method

Previous studies have shown that bio-oil is a valuable product that is renewable and can be used as an alternative to fossil fuels. In addition, bio-oil can be a source of chemical compounds since it consists of different functional groups and chemical compounds. Due to its complexity, some chemical reactions may occur in bio-oil during storage. This affects the stability of bio-oil in terms of physical and chemical properties.

Several studies have been reported in the literature on bio-oil stability and the ways to upgrade bio-oil to improve its stability during storage. In this manner, several methods have been proposed, e.g. hot-vapor filtration, solvent addition, emulsions, catalytic hydrogenation, etc. Among them, solvent addition is the easiest and the most economical way to minimize some undesired properties of bio-oil [88].

W. Yi et al. [40] studied the effects of adding ethanol, ethyl acetate, and mixtures of both on the stability of bio-oil obtained through the pyrolysis of rice husk. The bio-oil viscosity, moisture content, and organic composition were recorded and analyzed as characteristic parameters of the aging process. The accelerated aging process was carried out at 80 ºC for 24 hours. It was observed that the addition of ethanol and ethyl acetate at a mass ratio of 1:1 significantly improved the stability of the fractional bio-oil, and the resulting modified bio-oil was found to be rich in high value-added components, such as 2-methyl-3-buten-2-ol, furfural, and phenol. During the aging process, the kinematic viscosity of the modified bio-oil increased by 9.3%, whereas 31.7% for pure bio-oil aged under the same condition.

Lu Qiang et al. [78] studied the effect of adding methanol with 5 wt.%, 10 wt.%, and 15 wt.% on bio-oil produced from rice husk biomass using fast pyrolysis method. Bio-oil samples were aged using the accelerated aging technique at 50 and 80 ºC for 12 h, 24 h, 48 h, 72 h, and 120 h. Elemental analysis, FT-IR, GC/MS, kinematic viscosity, and water content were analyzed. The addition of methanol effectively slowed the aging rates of the bio-oil. For the four samples stored at 50 and 80 ºC for 120 h, the increase in viscosity after the addition of 5 wt.%, 10 wt.%, and 15 wt.% of methanol reduced from 31.7% to 21.7%, 16.3%, and 11.9%.

Fei Wenting et al. [88] studied the addition of methanol on crude rice straw-based bio-oil at different mass concentrations (1, 6, 11, 16, 21 wt.%). pH value, water content, and viscosity (at 40 ºC) were measured regularly during 91 days of storage period. They found that the addition of 21 % of methanol improved the pH value from 2.97 to 3.88 and decreased the water content after storage (91 days) by 35%. They emphasized that according to GC/MS analysis results, methanol could inhibit aging reactions such as polymerization and esterification. FT-IR and NMR analysis showed that methanol caused some structural changes in bio-oil. Compared to fresh bio-oil, the kinematic viscosity of the treated groups

decreased after 91 days of storage by 14.19%, 49.33%, 67.06%, 75.75%, and 81.35%, respectively. The ideal concentration of methanol addition was found to be 11 wt.%.

Diebold et al. [89] studied the effects of additives (10 wt % ethyl acetate; 5 wt % methyl isobutyl ketone and 5 wt % methanol; 10 wt %ethanol; 5 wt % acetone and 5 wt % methanol; 10 wt % acetone; and 10 wt % methanol) to stabilize the viscosity of bio-crude. Methanol was found as the best additive among the others and bio-oil containing 10% methanol was still a single-phase liquid and still met the ASTM No. 4 diesel fuel specification for viscosity even after 96 hours of accelerated aging at 90 °C. However, the aging of pure bio-crude without additives would have exceeded the allowable ASTM No. 4 viscosity after only 2.6 hours of aging at the same temperature. The bio-oil was produced from poplar biomass using fast pyrolysis method. The viscosity of fresh pure bio-oil was measured as 22.2 cP.

Ethanol, acetonitrile, and methyl acetate were added to bio-oils to assess the effects of these additives on the stability of bio-oil using a D-optimal experimental mixture design by Yin et al. [90]. A systematic analysis of the influence of different proportions of composite additives on bio-oil properties such as viscosity, water content, and pH was carried out. They found that the optimum additive formulation consisted of 6.58 wt.% ethanol, 1 wt.% acetonitrile, and 2.42 wt.% methyl acetate in terms of lower viscosity, water content, and higher pH. Moreover, the composite additive was better compared to a single additive in 24 hours of accelerated aging at 80 ^{o}C storage conditions. Bio-oil viscosity without additives increased from 211.80 $mm^2.s^{-1}$ to 550.2 $mm^2.s^{-1}$, but with the optimal composite additive the viscosity was reduced by 33–47% compared to the bio-oil with a single additive; while reduced by 95% with no additives. GC–MS analysis showed that several compounds such as 4-hydroxy-Butanoic acid, p-Cresol, and Vanillin were virtually eliminated in bio-oil with the addition of the chemicals.

In another study, Calophyllum inophyllum seed cake was used to produce bio-oil in a fixed bed reactor at 500 ^{o}C under a constant heating rate of 30 ^{o}C.min^{-1}. 10% of methanol was used as an additive, where the aging process was carried out for 24 hours at 80 ^{o}C. Pre and post-aged bio-oil with and without methanol was characterized in terms of water content, calorific value, pH value, ultimate analysis, FTIR, and GC-MS. Kinematic viscosity at 40 ^{o}C was also measured. The additive of 10% methanol decreased the viscosity from 12.20 cst to 3.60 cst. After the aging process, the viscosity was recorded as 20.36 cst and 4.62 cst for

unstabilized and stabilized bio-oil, respectively. GC-MS results showed that there was a diminishment in the major functional groups like alcohols, phenols, aldehydes, ketones, and aromatics whereas a steep increase was found in the concentration of carboxylic acids. Methanol addition reduced the variation in the concentration of components after aging which showed that fewer reactions took place during aging which in turn confirmed that the bio-oil was stable [91].

5.3. Bio-oil Storage Stability and Rheological Properties

W. Cai et al. [41] investigated the bio-oil stability that was produced from rice husk using fast pyrolysis method. Bio-oil aged for two years under three different conditions: at 4 ^{o}C in a refrigerator, at 25 ^{o}C at room temperature, and outdoors in natural conditions. Due to phase separation happened in the bio-oil sample, three samples were collected from each layer (upper, middle, and the bottom) before the aging process. The results show that low temperature may prevent the process of degradation from occurring during storage. Storage at room temperature was the most severe storage condition on bio-oil in terms of viscosity. The change in the viscosity was recorded to be the highest in the bottom layer of the bio-oil stored at 25 ^{o}C as 348.5 $mm^2.s^{-1}$, which is 50.8 times higher than that of the original bio-oil. FT-IR and GC/MS were used to determine the functional groups and chemical compositions in each layer pre- and post-aging process. The highest relative peak areas of phenols, aldehydes, and ketones were found in the middle layer of bio-oil. Alcohols, furans, or hydrocarbons accumulated in the bottom layer of bio-oil. Acids or others (chemicals with N, S, or Si) were found in the upper layer of bio-oil.

The rheological behavior of bio-oil produced from different biomasses was investigated by Nolte et al. [75]. Shear rate ramp (1000 to 0.001 s^{-1} carried out at temperatures -5, 10, 25, 40 and 55 ^{o}C) and frequency sweep (0.001-100 Hz) tests were experimented. Moreover, water content and pH values were measured. Arrhenius type relationship used to give a model for viscosity and inverse temperature linear relationship. The slope of the resulted equation is known as activation energy and it was calculated to be 67, 66, and 24 $kJ.mol^{-1}$ for poplar, oak-based bio-oil produced at a pyrolysis temperature of 500 ^{o}C and 600 ^{o}C, respectively. Bio-oil was found to be Newtonian fluid and the measurement temperature and the water content were found to have a strong effect on the viscosity of bio-oil. The

change in viscosity with water content fits a power law equation as ($\eta = 9300WC^{-3.8}$) where; WC is the water content in bio-oil.

The thermophysical and rheological properties of clean woody-based bio-oil in comparison with light and heavy crude oils were studied and analyzed by Y. Yadykova et. al. [77]. At 30 ^{o}C, the loss modulus (G″) was found to be much higher than the storage modulus (G′), in other words, bio-oil behaves as a liquid under these conditions. However, bio-oil behaved as a pseudoplastic fluid at higher temperatures: the viscosity decreased at a shear stress of about 10 Pa. Using Arrhenius equation, the activation energy was calculated as 86.7, 22.1, 82.9 kJ.mol^{-1} for bio, light and heavy oils, respectively. In addition, binary blends of bio-oil with fossil oils were analyzed with ratios from 20 to 80 wt%. The results showed that mixing light crude oil with bio-oil is not rational in terms of improving the rheology of any of these oils, while the combination of bio-oil with heavy crude oil can slightly reduce the viscosity of the latter.

Table 5.2 summarizes the kinematic and dynamic viscosities of bio-oil produced from different biomasses and crude oil measured at different temperatures. Bio-oil produced from different biomasses exhibits a unique rheological behavior, e.g., at 40 ^{o}C, the viscosity of forestry and Calophyllum inophyllum seed-based bio-oils are 30 and 12.2 cst, respectively. Compared to fossil oil, bio-oils have lower viscosities.

Table 5.2. *Viscosities of different bio-oils and fossil fuels*

Source	Temperature (°C)	Viscosity	Reference
Forestry Residue	20	100 cst	[92]
	40	30 cst	
Calophyllum inophyllum seed cake	40	12.2 cst	[91]
Rice husk	55	6.86 cst	[41]
Poplar	25	350 cP	[75]
Oak	25	196 cP	
Heavy fuel oil	50	180 cP	[56]
Light crude oil	20	<100 cP	[77]
Gasoline	40	0.2-0.5 cP	
Diesel fuel	40	1-20 cP	

6. MATERIALS AND METHODS

6.1. Chemicals Used in Experimental Studies

- Methanol: CAS 67-56-1 (Riedel-de Haën)
- Furfural: CAS 98-01-1 (Merck)
- 1,2,3,4- Tetrahydronaphthalene: CAS 119-64-2 (Sigma-Aldrich)
- Dichloromethane: CAS 75-09-2 (Sigma-Aldrich)

6.2. Equipment Used in Experimental Studies

Devices and brand models used in experimental studies are listed in Table 6.1.

Table 6.1. *Devices used during experiments.*

Application	Manufacturer
Balance	Precisa XB 220A
Drying Oven	MMM Medcenter Einrichtungen GmbH
Gas Chromatography–Mass Spectroscopy (GC-MS)	Agilent Technologies 7820A-5977B
Thermogravimetric Analysis (TGA)	LABSYS EVO SETARAM
Ultimate Analysis	Leco CHN680
Fourier-Transform Infrared Spectroscopy (FTIR)	Thermo Fisher Scientific Nicolet iS10
Kinexus Ultra+ (Rheometer)	Malvern
MSE_Pyrolysis_850 (Pyrolysis)	MSE Teknoloji

6.3. Analysis Applied on the Feedstock

The pomace used in this study as feedstock was collected from Manisa city located in the Aegean Region, west of Turkey, during the 2019 season. The feedstock was dried at room temperature for a few days before pyrolysis to extract any excess water content. The moisture (ASTMD 2016-74), ash (ASTMD 1102-84), and volatile matter (ASTME 897-82) were determined as 7.1, 3.4, and 82.3 wt. %, respectively [93]. The thermogravimetric analysis was carried out using Setaram Labsys-Evo to investigate the thermal decomposition behavior of the raw material.

6.4. Bio-oil Production via Pyrolysis

Pyrolytic oil was obtained from olive residue via slow pyrolysis using a fixed bed reactor (see Figure 6.1). The reactor was fixed in an electrically heated oven to obtain the desired pyrolysis temperature. The reactor temperature was maintained at around 500 °C using a PID controller with a thermocouple placed on the top of the sample. After the reactor was filled with feedstock its upper chamber was sealed carefully to ensure that there are no gas leakages. The final temperature of the reactor was set to 500 °C at a heating rate of 10 °C.min^{-1}. After reaching the final temperature, a holding period of 15 minutes was sustained. The volatiles produced during pyrolysis was swept out using nitrogen that flows in the reactor at 100 cm^3.min^{-1} and passed through four-cylinder vessels placed in an ice bath. The condensed volatiles were collected as bio-oil with a certain amount of water, which was separated using a separation funnel (Figure 6.2). The water-free, pure bio-oil was transferred to a closed glass vessel and kept in the refrigerator at 4^{o}C for further analyses. All analyses for fresh bio-oil were carried out using the bio-oil without any treatment except water separation.

Figure 6.1. *Pyrolysis reactor*

Figure 6.2. *Separation of water - bio-oil*

6.5. Aging Process

In this study, bio-oil samples were aged under two different conditions: (i) at room temperature for 7 days and (ii) at 80 °C known as accelerated aging, for 24 and 168 hours. In addition to this, the non-aged samples were kept in the refrigerator at 4 ºC for further analysis. During aging, all samples were placed in separate brown-colored glass bottles, which were tightly sealed and stored in a dark environment.

6.6. Bio-oil Upgrading Using Additives

Pure bio-oil was aged and analyzed at the first stage, without any solvent addition. To investigate the effect of solvent addition, methanol, furfural, and tetrahydronaphthalene were selected as the chemicals. Each solvent was added to the bio-oil sample with 5, 10, and 15 wt.%. Each percentage of each additive was separated into 4 samples, 3 of the samples were aged under different conditions – explained in the section above - and the 4th sample (non-aged) was kept in the refrigerator at 4 ºC for further analysis (Figure 6.3).

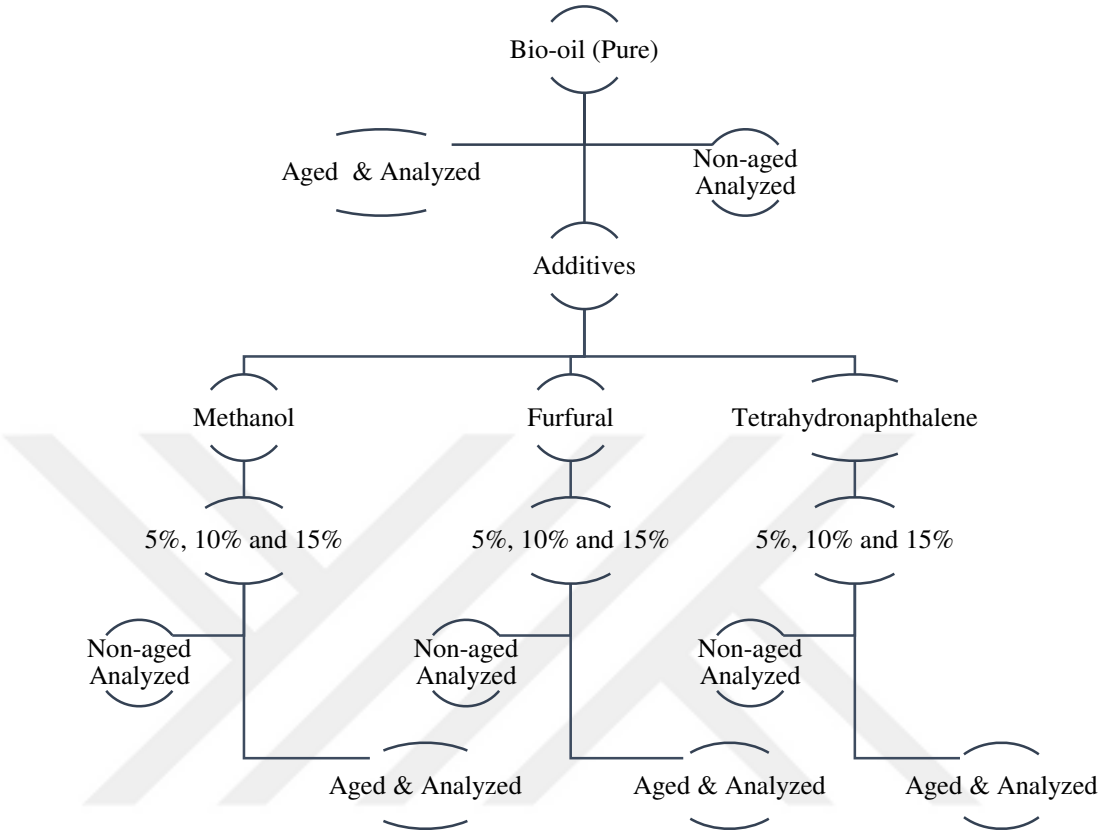

Figure 6.3. *Sample preparation diagram*

Figure 6.4 shows the descriptions of the sample's name (e.g., additive used, percentage added, and duration and aging condition).

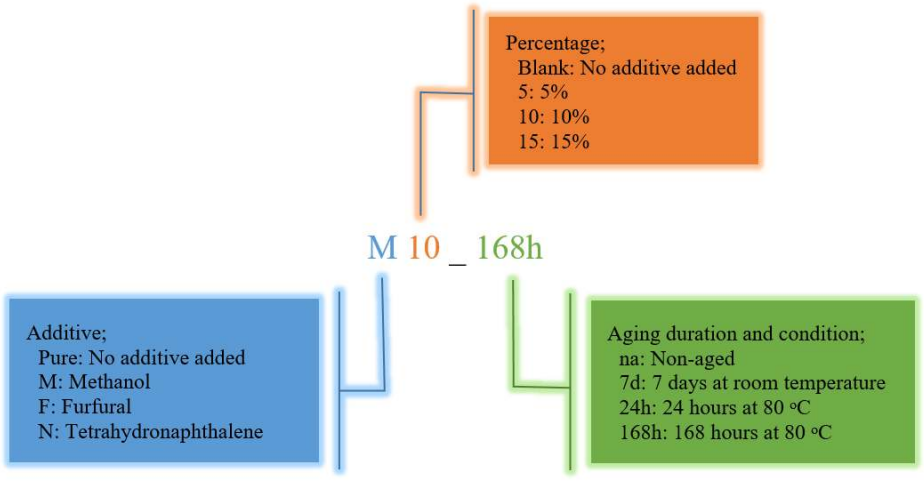

Figure 6.4. *Naming of the samples*

6.7. Bio-oil Characterization

Pure and stabilized bio-oil samples that have 10% of additives were characterized by the devices and techniques mentioned in this section.

6.7.1. Ultimate analysis

The elemental composition, C, H, N, and O content (wt.%) of each sample, was determined using a LECO CHN-628 elemental analyzer. Oxygen content was calculated by difference (100% – (C+H+N)).

6.7.2. Calorific value

The determination of the calorific value of bio-oil samples was accomplished by using the Dulong equation (Eq. 6.1) [94]:

$$Q_{GCV}\left(\frac{MJ}{kg}\right) = 33.83C + 144.3\left(H - \frac{O}{8}\right) \quad (6.1)$$

where C, H, and O are the mass fractions of carbon, hydrogen, and oxygen, respectively and Q_{GCV} is the gross calorific value in MJ/kg.

6.7.3. Fourier-transform infrared spectroscopy

Fourier Transform Infrared Spectroscopy (FTIR) was used to analyze the organic functional groups in the bio-oil samples before and after the aging process. A Thermo Fisher Scientific Nicolet iS10 FTIR spectrometer with a resolution of 4 cm^{-1} and 32 scans were used for analyzing samples between 4000 and 500 cm^{-1} wavelengths.

6.7.4. Thermogravimetric analysis

Thermogravimetric Analysis (TGA) experiments were carried out using Labsys Eyo (SETARAM Instrumentation). Approximately 10 ± 1.0 mg of sample was loaded into a 100 µL alumina crucible. 20 $mL.min^{-1}$ of nitrogen was used as the sweeping gas. Each test was carried in 3 steps, 1st step for 35 minutes at room temperature to reach stability, 2nd step increasing the temperature of the sample from room temperature to 1000 °C by 20 $°C.min^{-1}$ heating rate, followed by the cooling step.

6.7.5. Gas chromatography–mass spectrometry

The analysis was carried out on each sample using Agilent Technologies 7820A Gas Chromatography (GC) – 5977B Mass Spectroscopy (MS) equipped with a 30m x 0.25mm x 0.25μm HP-5MS column. The temperature of GC oven was programmed to hold at 40 ^{o}C for 3 minutes, then, the temperature was increased at a rate of 2 ^{o}C.min^{-1} to hold for 30 minutes after reaching 270 ^{o}C as the final temperature. A 1 μL sample injection was adopted. Helium flow rate was adjusted as 1 mL.min^{-1}. W9N11 mass spectral library was used to identify the obtained peaks. Sample preparation was done using dichloromethane solvent. Around 0.01 g of bio-oil was used with approximately 2 ml of solvent.

6.7.6. Dynamic viscosity and rheological behavior

All bio-oil samples were analyzed in terms of their rheological behavior.

The dynamic viscosity of bio-oil samples was determined by using Kinexus ultra+ (Malvern UK). Two different tests were applied to each sample, shear rate ramp at different temperatures and temperature ramp at constant shear stress. Shear rate ramp tests were applied between 5 to 580 s^{-1} on each sample at different temperatures of 20, 25, 30, 35, 40, 50, and 60 °C, with a residence time of 5 minutes to reach a steady state. Temperature ramp tests were applied between 20 to 60 °C to each sample with a 1 °C.min^{-1} heating rate at constant shear stress (1 Pa). The temperature is controlled using an Active Hood Peltier plate cartridge with 0.01^{o}C temperature resolution and ±0.1^{o}C temperature stability. A mineral oil standard was used to find the error in viscosity measurements to be %2.45 or less. Cone plate stainless-steel geometry was used with a 40mm diameter and 4^{o} angle. This geometry requires a small sample volume and generates a homogeneous shear field on the sample compared to different geometries [84]. During tests, the cone-plate gap was fixed to 0.1498 mm and a sample volume of 1.19 mL was used.

6.7.6.1. *Aging index*

The change in the dynamic viscosity, known as the aging index was calculated using the following equation [95,96]:

$$\Delta\eta = \frac{\eta_{\text{Aged}} - \eta_{\text{Fresh}}}{\eta_{\text{Fresh}}} \times 100\% \quad (6.2)$$

where (η_{Aged}) is the dynamic viscosity (cP) of aged bio-oil and (η_{Fresh}) is the dynamic viscosity of pure non-aged bio-oil (cP). Lower values are preferred in the aging indexes.

7. RESULTS AND DISCUSSIONS

7.1. Feedstock Analysis Results

7.1.1. Ultimate analysis

The ultimate analysis results of the olive pomace sample are given in Table 7.1. Uzun et al. [94] previously reported the carbon, hydrogen, nitrogen, and oxygen content of pomace olive pomace feedstock as 49.08, 5.59, 1.14, and 44.19% on DAF basis, respectively.

Table 7.1. *Elemental analysis results of olive pomace sample (as received, wt. %)*

Element	Content
C	59.45
H	6.96
N	5.37
O[i]	28.22
Q_{GCV}[ii] (MJ/kg)	25.07

[i] By difference

[ii] Gross calorific value

7.1.2. Thermogravimetric analysis

The thermogravimetric analysis was carried out to investigate the thermal decomposition behavior of the feedstock. The sample was heated from room temperature to 1000 °C in an N_2 atmosphere with a flow rate of 20 ml.min^{-1}, at a heating rate of 10 °C.min^{-1}, and the thermogram curves are given in Figure 7.1. The main pyrolysis reactions started around 170°C and completed at 560°C, giving a maximum decomposition rate of 6.4 % per minute at 322°C. The total mass loss was recorded as 77.4 wt.%. According to the thermal decomposition data, the pyrolysis temperature to produce bio-oil was selected to be 500 °C for the further bench-scale experiments.

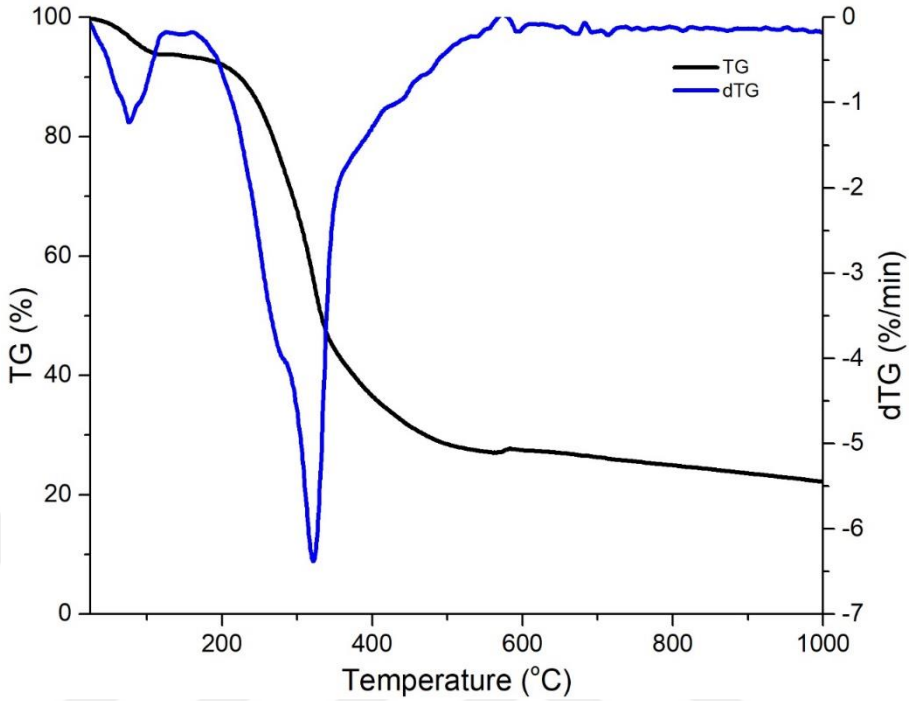

Figure 7.1. *Thermal decomposition behavior of olive pomace*

7.2. Bio-oil Characterization

7.2.1. Ultimate analysis

The ultimate analysis results of bio-oil samples are given in Table 7.2. The analyses showed that all aged pure bio-oil samples contained almost the same percentages of carbon, hydrogen, nitrogen, and oxygen. All results were in the accuracy range specified by the standard materials used for calibration. Aged bio-oil samples were carefully sealed to prevent any contact with air/oxygen to prevent or minimize oxidation reactions. As a result, the oxygen content of aged bio-oil samples showed minor changes to that of fresh bio-oil samples. Separating bio-oil from water content immediately after the pyrolysis resulted in higher carbon and lower oxygen contents compared to other studies [97]. Separating water content from bio-oil as soon as the bio-oil was produced, makes it possible to lower the oxygen ratio and eliminate phase separation during storage. However, still, the oxygen content of bio-oil is around 15 wt. %, which is one of the main problems with its utilization as an alternative to petroleum-derived oils. A higher oxygen ratio means a lower gross calorific value. Moreover, oxygenated chemical compounds, in bio-oil are highly reactive

and can lead to undesirable reactions during storage, in other words, the presence of oxygenated compounds in bio-oil is another influencing factor for bio-oil aging [64,65,98,99].

The high ratio of atomic carbon to hydrogen (C/H) is critical to having a high calorific value. As seen in Table 7.2, the average gross calorific value of pure bio-oil samples was calculated as 35.74 $MJ.kg^{-1}$, which is close to that of petroleum products [100].

As shown in Table 7.2, the addition of 10% of methanol, furfural, and tetrahydronaphthalene to bio-oil samples, resulted in some changes in carbon, oxygen, and nitrogen content. Adding methanol and furfural, increased the oxygen and decreased the carbon contents. However, methanol-stabilized bio-oil showed a lower carbon ratio compared to furfural-stabilized bio-oil. This affects the gross calorific values in a negative way for both additives. On the other hand, tetrahydronaphthalene increased the carbon content and decreased the oxygen content, which resulted in an increase in the gross calorific values compared to pure bio-oil and other additives.

The highest gross calorific value was calculated for tetrahydronaphthalene-stabilized bio-oil that has been aged at room temperature for 7 days as 38.76 $MJ.kg^{-1}$. Whereas the lowest gross calorific value was recorded for methanol-stabilized bio-oil as 33.47 $MJ.kg^{-1}$.

Compared to non-aged bio-oil samples, storage at room temperature for 7 days shows a decrease in the gross calorific value for both methanol and furfural-stabilized bio-oil.

Table 7.2 *Elemental analysis results of bio-oil samples (as received, wt. %)*

Sample	C	H	N	O^i	H/C	O/C	Q_{GCV} (MJ/kg)
Pure Bio-oil							
Pure_na	73.36	9.34	2.17	15.13	0.13	0.21	35.56
Pure_7d	74.05	9.26	2.20	14.49	0.13	0.20	35.80
Pure_24h	73.74	9.44	2.23	14.60	0.13	0.20	35.93
Pure_168h	73.40	9.39	2.16	15.05	0.13	0.21	35.67
10% Methanol							
M10_na	69.61	10.06	2.18	18.16	0.14	0.26	34.79
M10_7d	68.05	9.80	1.68	20.48	0.14	0.30	33.47
M10_24h	69.61	9.85	1.74	18.79	0.14	0.27	34.38
M10_168h	70.50	9.68	1.64	18.17	0.14	0.26	34.55

Table 7.2 (Continued) *Elemental analysis results of bio-oil samples (as received, wt. %)*

Sample	C	H	N	O[i]	H/C	O/C	Q_{GCV} (MJ/kg)
10% Furfural							
F10_na	70.42	9.13	1.58	18.88	0.13	0.27	33.59
F10_7d	71.53	9.19	1.68	17.60	0.13	0.25	34.28
F10_24h	72.90	9.30	1.74	16.06	0.13	0.22	35.18
F10_168h	74.42	9.14	1.76	14.68	0.12	0.20	35.72
10% Tetrahydronaphthalene							
N10_na	73.95	9.63	1.53	14.89	0.13	0.20	36.22
N10_7d	77.14	9.99	3.21	9.66	0.13	0.13	38.76
N10_24h	76.15	9.56	1.68	12.61	0.13	0.17	37.28
N10_168h	76.60	9.72	1.68	11.99	0.13	0.16	37.78

[i] By difference

7.2.2. Fourier-transform infrared spectroscopy

The functional groups of bio-oil samples were detected by FT-IR spectroscopy (Figure 7.2 to Figure 7.5) and the qualitative analysis of these groups is listed in Table 7.3. During the aging process, although a series of reactions took place, all major bands attributed to similar functional groups are observed in the spectra due to the negligible change in the composition of pure, pre- and post-aged bio-oil samples. Moreover, the presence of oxygenated compounds is observed from the spectra through the carboxyl and carbonyl groups' vibration bands.

The O-H stretching vibrations between 3200 and 3570 cm^{-1} observed in all FT-IR spectra indicate the presence of hydroxyl groups in alcohols and phenols. The weak peaks at around 3010 cm^{-1} are related to the aromatic =C-H vibrations from the aromatic ring [101]. The symmetric and asymmetric stretching vibration associated with the peaks at around 2925 and 2854 cm^{-1} of C-H are attributed to methyl and methylene groups. The only difference between the fresh and aged bio-oil samples is the relative intensities and sharpness of these vibration bands. The C=O group is arising mainly from the aldehydes, ketones, and carboxylic acids, and the stretching bands are observed between 1685 and 1760 cm^{-1}. The strong peak at 1711 cm^{-1} observed for all samples is assigned to the stretching vibrations of carboxylic acid, which is a common characteristic of edible oil and is further confirmed by GC-MS analysis [102]. The 1340–1470 cm^{-1} C–H bending vibrations correspond to alkyl and aliphatic groups. The stretching vibrations associated with the peaks at 1242 and 1264

cm^{-1} are likely indicative of C–O stretching vibration in organic acids, ethers, and alcohol groups. The presence of –OH groups is confirmed by the stretching vibrations of C-OH at 1110 cm^{-1}. The stretching vibrations between 1060-1030 cm^{-1} are attributed to stretching vibrations of C-O belonging to the carboxyl (-COOH) group. Table 7.3 represents detailed functional groups of bio-oil [97,101,103].

Table 7.3. *The main functional groups of bio-oil*

Wavenumber (cm^{-1})	Functional group	Compounds
3200-3570 (broad)	O-H stretch	Hydrogen-bonded alcohols, phenols
3000-3100	C-H stretch	Aromatic rings
2850-2970	C-H stretch	CH_2 or CH_3 groups
1690-1760	C=O stretch	Aldehydes, ketones, carboxylic acids
1500-1600	C=C stretch	Aromatic rings
1340-1470	C-H bend	Alkyl, aliphatic
1050-1300	C-O stretch	Alcohols, ethers, carboxylic acids
1000-1200	C-H bend	Aromatic rings
1000-1060	C-O stretch	Ethers, alcohols, phenols

The addition of 10% methanol, furfural, and tetrahydronaphthalene to bio-oil did not make a notable change in the overall FT-IR spectra (Figure 7.3 to Figure 7.5). However, at 3377 cm^{-1}, the width of the peak is becoming smaller in the post-aged sequences with respect to pre-aged. The content of chemicals (like water, alcohols, acids, or phenols) in the aged methanol, furfural, and tetrahydronaphthalene-stabilized samples is lower, this can be due to the esterification reactions that took place between alcohols and organic acids and transesterification reactions occurred among alcohols, acids, and esters in the methanol and tetrahydronaphthalene-stabilized samples and homopolymerization reactions among aldehydes in the furfural-stabilized samples [41,54].

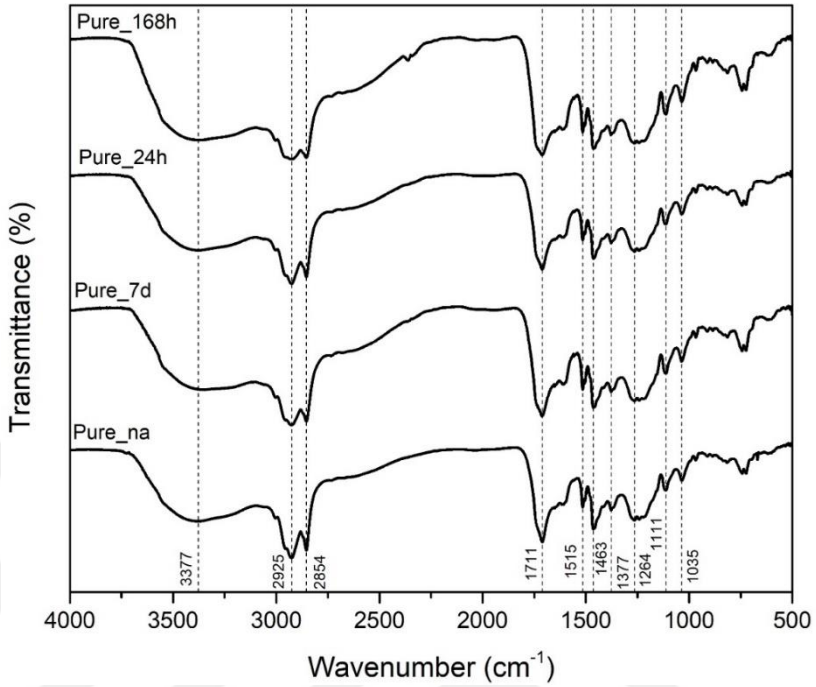

Figure 7.2. *FT-IR spectra of pure bio-oil samples*

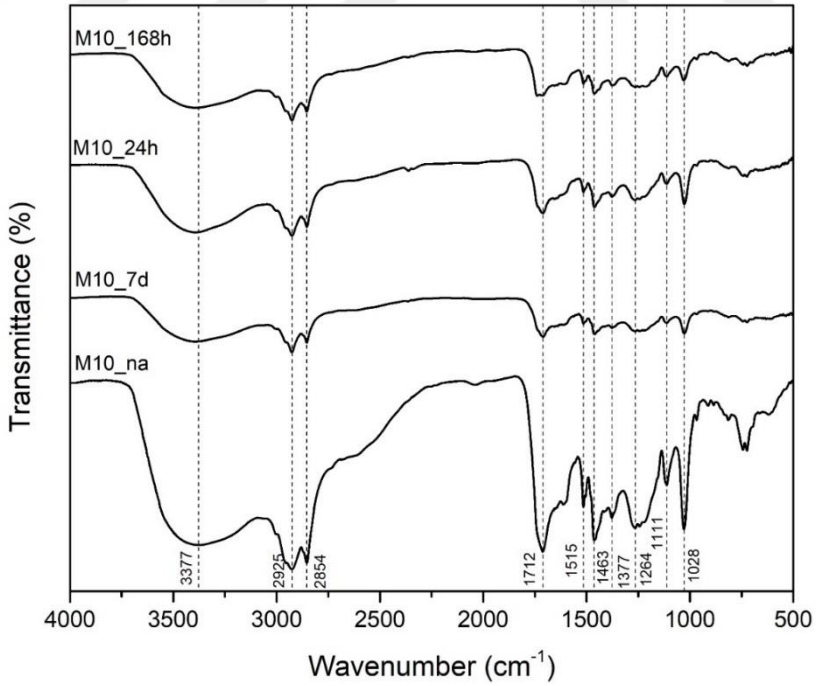

Figure 7.3. *FT-IR spectra of 10% methanol added bio-oil samples*

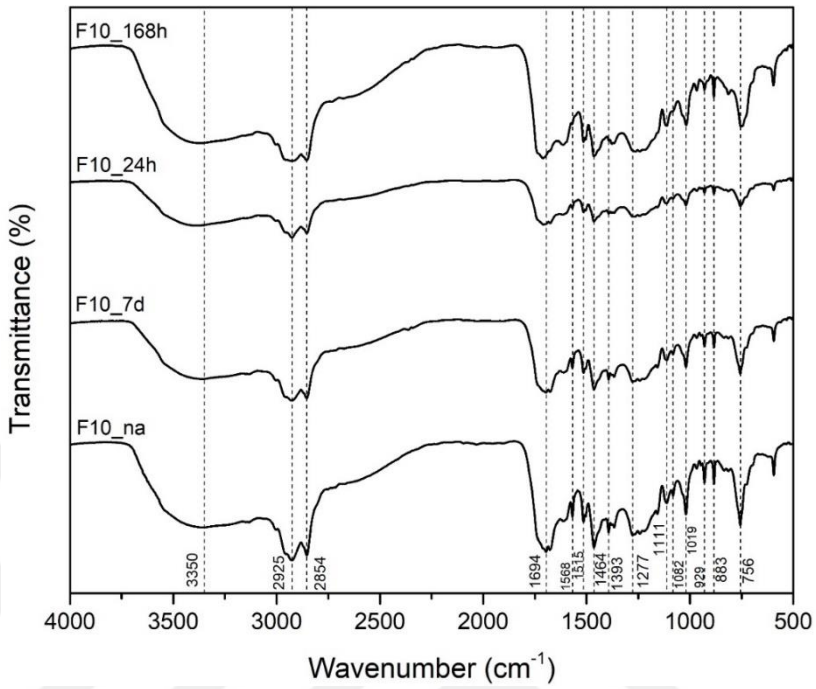

Figure 7.4. *FT-IR spectra of 10% furfural added bio-oil samples*

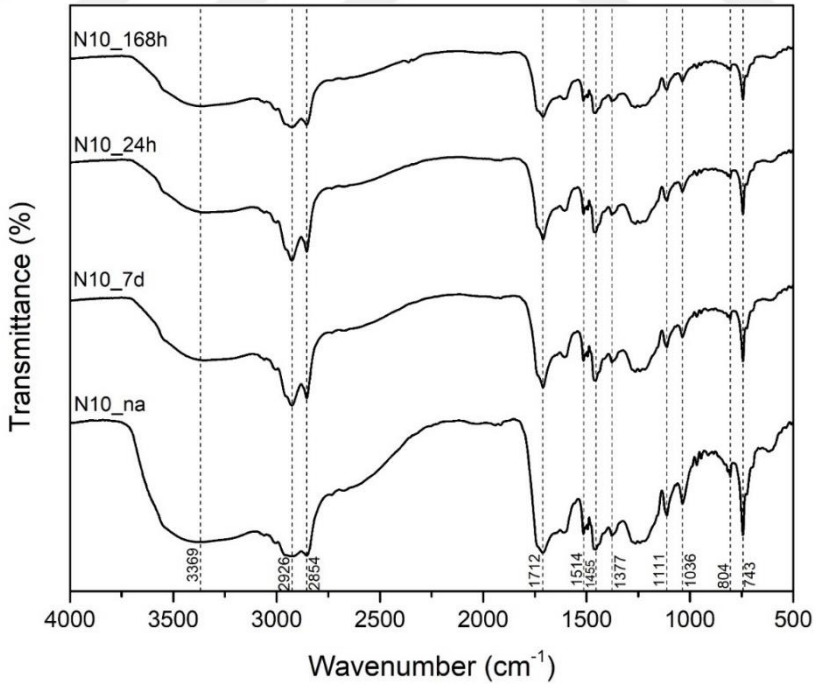

Figure 7.5. *FT-IR spectra of 10% tetrahydronaphthalene added bio-oil samples*

7.2.3. Thermogravimetric analysis

TGA can be used to characterize the evaporation, thermal decomposition, and combustion properties of bio-oils. The experimental data of the weight loss (TG) and weight loss rates (dTG) of pure and 10% stabilized bio-oil samples are illustrated in Figure 7.6. Table 7.4 summarizes the decomposition temperatures at a 20 °C.min^{-1} heating rate.

It is seen that around 93 wt. % of the pure bio-oil samples were decomposed at the final temperature of 1000 ºC and all aged pure bio-oil samples exhibit almost the same mass loss. The decomposition of bio-oil was accomplished in a single step between around 45 ºC and 510 ºC. Lower molecular weight hydrocarbons such as aldehydes, alcohols, and carboxylic acids were volatilized at temperatures between 45 and 130 ºC, and higher molecular weight hydrocarbons volatilized at a temperature higher than 130 ºC. The TG curves of aged pure bio-oil samples shifted to the right which was due to the formation of a higher molecular weight tar sample during the aging process as a result of the polymerization reactions. According to the dTG curves - shown at the right of Figure 7.6 - the maximum decomposition rate increased by 17 °C from 281 °C to 298 °C for Pure_na and Pure-168h. The main decomposition occurred in a single step, followed by a shoulder between approximately 360 and 520 ºC. The magnitude of the shoulder increased significantly for Pure_168h. The degradation of higher molecular weight compounds and aromatic structures is more difficult than the simple short-chain hydrocarbons having lower boiling points. After 500 ºC, the mass-loss rate decreased and both TG and dTG curves became almost flat. Pure_7d showed a similar decomposition behavior to Pure_168h and the decomposition of Pure_24h was found to be similar to Pure_na (Table 7.4).

On the other hand, stabilized bio-oil with 10% additives showed similar behavior to pure bio-oil with a minor difference. While methanol and furfural stabilized bio-oil samples showed a decrease in the total mass loss (wt. %), tetrahydronaphthalene-stabilized bio-oil samples exhibited a slight increase in the total mass loss compared to that of pure bio-oil.

No significant changes were recorded regarding start temperature, maximum temperature, shoulder temperature, and final temperature of decomposition of all additive stabilized-bio-oil samples.

M10_168h dTG curve showed a small peak at 115 °C, which could be due to the formation of H_2O from esterification reactions between alcohols and organic acids. F10_na and F10_7d dTG curves showed a small peak at around 152 °C, which could be due to the furfural decomposition that has a boiling point of around 162 °C [104]. This peak is getting lower with the aging process due to homopolymerization and hydration reactions. All tetrahydronaphthalene-stabilized bio-oil samples showed a small peak between 195 and 213 °C, which could be attained through the decomposition of tetrahydronaphthalene that has a boiling point around 207 °C.

Table 7.4. *Thermal decomposition characteristics of pure and stabilized bio-oil samples; pre- and post-aging process*

Sample	T_i[i]	T_{max}[ii]	T_{sh}[iii]	T_f[iv]	Total mass loss (wt. %)
Pure Bio-oil					
Pure_na	43	281	376	519	93.2
Pure_7d	44	295	389	526	94.1
Pure_24h	44	281	380	515	92.5
Pure_168h	46	298	392	518	93.1
10% Methanol					
M10_na	32	290	384	515	84.7
M10_7d	40	293	383	513	90.3
M10_24h	33	289	380	520	89.1
M10_168h	35	280	374	518	85.2
10% Furfural					
F10_na	34	293	381	525	87.2
F10_7d	40	293	386	529	93.8
F10_24h	33	286	385	530	88.6
F10_168h	41	291	389	533	89
10% Tetrahydronaphthalene					
N10_na	38	295	394	515	93.1
N10_7d	41	299	384	517	92.9
N10_24h	40	293	377	522	95
N10_168h	39	292	380	513	94.9

[i] T_i : Temperature at which the decomposition started (°C)
[ii] T_{max} : Temperature at which the highest decomposition rate observed (°C)
[iii] T_{sh} : Temperature at the shoulder after the main decomposition (°C)
[iv] T_f : Temperature at which the decomposition completed (°C)

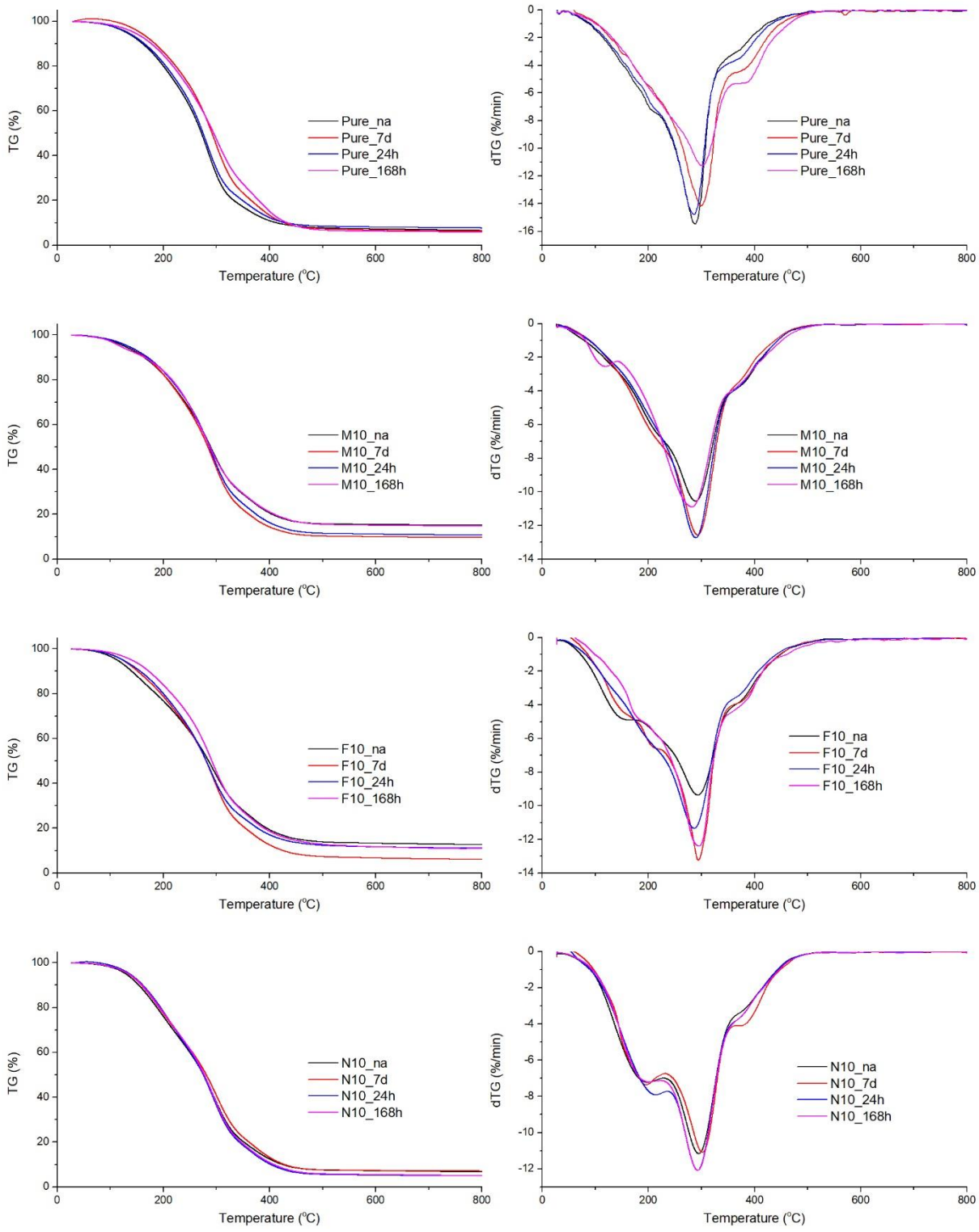

Figure 7.6. *Thermal decomposition of bio-oil samples: TG (left) and dTG (right) curves*

7.2.4. Gas chromatography–mass spectrometry

The chemical compounds detected via GC–MS are given in Table 7.5 - Table 7.8 for pure, methanol, furfural, and tetrahydronaphthalene-stabilized bio-oil samples, respectively. GC/MS chromatograms are given in Appendix A.

GC-MS analysis provides information about the components of bio-oil samples to understand the changes in the composition due to the possible chemical reactions during the aging process. The substances detected were classified as phenols, carboxylic acids, alkanes, ketones, esters, alcohols, aldehydes, and aromatics.

GC-MS results for non-aged pure bio-oil showed that the main groups are carboxylic acids, phenols, and esters with percentages of 58.4, 16.8, and 16.5, respectively (Figure 7.7). After aging, there were few changes in the concentration of compounds compared to non-aged bio-oil. Figure 7.7 shows the change in the total percentages of the main groups in pure bio-oil. It is noticed that the total percentage of carboxylic acids decreased slightly and an increment was recorded for phenols, esters, and aromatics groups percentages. Most notably, all carboxylic acid compounds were reduced in concentration after aging. However, several new compounds were evident. Specifically, Decane, Undecane, Dodecane, Tridecane, Hexadecane, 2,4,6-Octatriene, 2,6-dimethyl-, 2,3,5-Trimethoxytoluene, 9-Octadecenoic acid (Z)-, 2,3-dihydroxypropyl ester, 2-Cyclopenten-1-one, 2-methyl-, 2-Cyclopenten-1-one, 2-hydroxy-3-methyl-, 2,4-Dihydroxypropiophenone, (Phenol, 2-methoxy-3-methyl-), 1,2-Benzenediol, Phenol, 2-methoxy-4-(1-propenyl)-, Phenol, 2-methoxy-4-propyl-, and Phenol, 2-methoxy-4-(1-propenyl)- were identified in aged bio-oil samples. In addition, Ethylbenzene (aromatics) disappeared after the aging process.

Table 7.5. *GC-MS results for pure bio-oil: pre- and post-aging process*

Compounds	Molecular formula	Area (%)			
		Pure_na	Pure_7d	Pure_24h	Pure_168h
Alcohols					
2-Furanmethanol	$C_5H_6O_2$	0.17	0.38	0.36	0.31
Aldehydes					
9-Tetradecenal, (Z)-	$C_{14}H_{26}O$	ND*	0.80	ND	0.81
Alkanes					
Octane	C_8H_{18}	0.22	0.15	0.21	0.19
Nonane	C_9H_{20}	0.18	0.20	0.16	0.14
Decane	$C_{10}H_{22}$	ND	0.26	0.16	0.15
Undecane	$C_{11}H_{24}$	ND	0.24	0.23	0.30
Dodecane	$C_{12}H_{26}$	ND	0.26	0.27	0.26
Tridecane	$C_{13}H_{28}$	ND	0.36	0.29	0.27
Tetradecane	$C_{14}H_{30}$	0.31	0.32	0.34	0.32
Pentadecane	$C_{15}H_{32}$	0.46	0.48	0.46	0.45
Hexadecane	$C_{16}H_{34}$	ND	0.27	0.27	0.25
Aromatics					
Toluene	C_7H_8	0.45	0.41	0.34	0.30
Ethylbenzene	C_8H_{10}	0.18	ND	ND	ND
Benzene, 1,3-dimethyl-	C_8H_{10}	0.16	0.13	0.13	0.12
Styrene	C_8H_8	0.05	0.12	0.11	0.09
p-Xylene	C_8H_{10}	0.20	0.19	0.18	0.15
2,4,6-Octatriene, 2,6-dimethyl-	$C_{10}H_{16}$	ND	0.19	0.25	0.25
2,3,5-Trimethoxytoluene	$C_{10}H_{14}O_3$	ND	ND	ND	1.01
Squalene	$C_{30}H_{50}$	1.47	1.42	1.43	1.36
Carboxylic Acids					
3,5-Dimethoxy-4-hydroxyphenylacetic acid	$C_{10}H_{12}O_5$	0.18	0.25	0.11	0.11
Oleic Acid	$C_{18}H_{34}O_2$	46.80	41.94	44.46	42.55
n-Hexadecanoic acid	$C_{16}H_{32}O_2$	11.39	12.43	9.75	10.30
Esters					
Hexadecanoic acid, methyl ester	$C_{17}H_{34}O_2$	2.53	2.36	2.51	2.54
9,12-Octadecadienoic acid (Z,Z)-, methyl ester	$C_{19}H_{34}O_2$	1.06	1.10	1.04	1.07
9-Octadecenoic acid, methyl ester	$C_{19}H_{36}O_2$	12.95	11.75	12.36	12.74
9-Octadecenoic acid (Z)-, 2,3-dihydroxypropyl ester	$C_{21}H_{40}O_4$	ND	1.02	1.10	1.08

Table 7.5. (Continued) *GC-MS results for pure bio-oil: pre- and post-aging process*

Compounds	Molecular formula	Area (%)			
		Pure_na	Pure_7d	Pure_24h	Pure_168h
Ketons					
2-Cyclopenten-1-one, 2-methyl-	C_6H_8O	ND	0.19	0.17	0.15
Butyrolactone	$C_4H_6O_2$	0.21	0.24	0.22	0.20
2-Cyclopenten-1-one, 2-hydroxy-3-methyl-	$C_6H_8O_2$	ND	0.43	0.25	0.42
2,4-Dihydroxypropiophenone	$C_9H_{10}O_3$	ND	0.12	0.14	0.13
2-Propanone, 1-(4-hydroxy-3-methoxyphenyl)-	$C_{10}H_{12}O_3$	0.46	0.44	0.42	0.47
Phenols					
Phenol	C_6H_6O	0.71	0.76	0.74	0.70
Phenol, 2-methyl-	C_7H_8O	0.59	0.52	0.61	0.54
Phenol, 3-methyl-	C_7H_8O	0.91	0.81	0.81	0.86
Phenol, 2-methoxy-	$C_7H_8O_2$	3.62	3.46	3.45	3.40
Phenol, 2-ethyl-	$C_8H_{10}O$	0.33	0.31	0.32	0.30
Phenol, 3,4-dimethyl-	$C_8H_{10}O$	0.24	0.31	0.31	0.29
Phenol, 2,4-dimethyl-	$C_8H_{10}O$	0.19	0.27	0.29	0.28
Phenol, 4-ethyl-	$C_8H_{10}O$	0.36	0.21	0.30	0.41
Phenol, 3-ethyl-	$C_8H_{10}O$	0.37	0.22	0.29	0.42
Phenol, 2-methoxy-3-methyl-	$C_8H_{10}O_2$	ND	ND	ND	0.15
Creosol	$C_8H_{10}O_2$	0.77	0.98	1.00	1.15
1,2-Benzenediol	$C_6H_6O_2$	ND	ND	ND	0.28
Phenol, 4-ethyl-3-methyl-	$C_9H_{12}O$	0.17	0.19	0.24	0.36
Phenol, 4-ethyl-2-methoxy-	$C_9H_{12}O_2$	1.44	1.36	1.53	1.49
2-Methoxy-4-vinylphenol	$C_9H_{10}O_2$	0.70	0.63	0.62	0.51
Phenol, 2,6-dimethoxy-	$C_8H_{10}O_3$	2.59	2.47	2.61	2.47
Phenol, 2-methoxy-4-(1-propenyl)-	$C_{10}H_{12}O_2$	ND	ND	0.36	0.35
Phenol, 2-methoxy-4-propyl-	$C_{10}H_{14}O_2$	ND	0.56	0.59	0.55
Phenol, 2-methoxy-4-(1-propenyl)-	$C_{10}H_{12}O_2$	ND	0.33	0.35	0.34
Phenol, 2-methoxy-4-(1-propenyl)-	$C_{10}H_{12}O_2$	1.84	1.63	1.73	1.66
2,6-Dimethoxy-4-vinylphenol	$C_{10}H_{12}O_3$	0.31	0.43	0.41	0.30
Phenol, 2,6-dimethoxy-4-(2-propenyl)-	$C_{11}H_{14}O_3$	ND	ND	ND	0.16
2,6-Dimethoxy-4-propylphenol	$C_{11}H_{16}O_3$	0.34	0.38	0.40	0.37
Phenol, 2,6-dimethoxy-4-(2-propenyl)-	$C_{11}H_{14}O_3$	1.31	1.41	1.23	1.37
Polycyclic aromatic hydrocarbons					
Naphthalene, 1,2,3,4-tetrahydro-2,2,5,7-tetramethyl-	$C_{14}H_{20}$	ND	0.27	0.26	0.25
Pyridine, 3-ethyl-	C_7H_9N	0.17	0.32	0.34	0.28

*ND Not detected

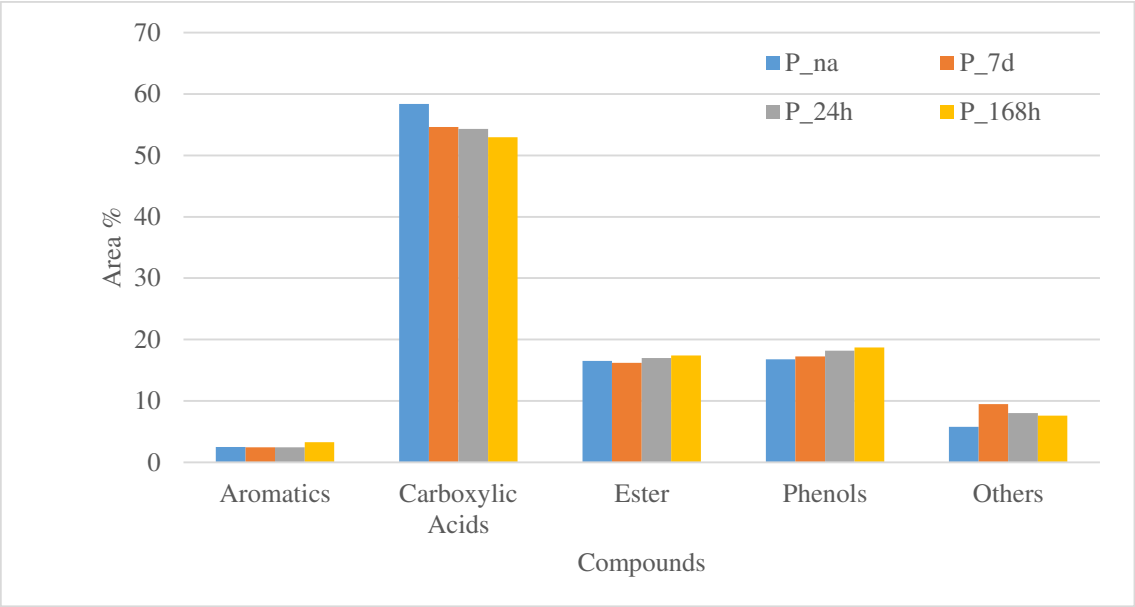

Figure 7.7. *Variations in the composition of pure bio-oil: pre- and post-aging process*

Non-aged methanol-stabilized bio-oil sample showed an increase in the percentage of esters and aromatics groups, and a decrease in phenols (Figure 7.8). Carboxylic acids remain the same compared to non-aged pure bio-oil. However, after aging, a significant change was observed during aging process represented by an increase in ester groups from 19% to 55.7% with a decrease in the carboxylic acids from 58.8% to 27.7% for M10_na and M10_168h, respectively. These changes are indicators of esterification reactions occurred between alcohols and acids in bio-oil to form esters and water during the aging process. Some substances became less significant or even disappeared after the aging process and some appeared after the aging process. Methyl palmitoleate, 9-Octadecenoic acid (Z)-, ethyl ester, Eicosanoic acid, methyl ester, 9-Octadecenoic acid (Z)-, 2,3-dihydroxypropyl ester appeared in the M10_168h sample. In addition, several substances disappeared (e.g., Octane, Tetradecane, Hexadecanamide, Benzene, 1,3-dimethyl-, 3,5-Dimethoxy-4-hydroxyphenylacetic acid, Phenol, 4-ethyl-3-methyl-, 2-Methoxy-4-vinylphenol and 2,6-Dimethoxy-4-vinylphenol) (Table 7.6). Furthermore, the addition of methanol can significantly affect the acidity, which has a crucial catalytic role in many aging reactions (e.g., homopolymerization and copolymerization) [40].

Table 7.6. *GC-MS results for methanol-stabilized bio-oil: pre- and post-aging process*

Compounds	Molecular formula	Area %			
		M10_na	M10_7d	M10_24h	M10_168h
Alcohols					
2-Furanmethanol	$C_5H_6O_2$	ND	0.20	ND	0.15
Benzeneethanol, 2-methoxy-	$C_9H_{12}O_2$	1.24	1.27	1.25	1.31
Alkanes					
Octane	C_8H_{18}	0.17	ND	ND	ND
Tetradecane	$C_{14}H_{30}$	0.31	0.32	ND	ND
Pentadecane	$C_{15}H_{32}$	0.50	0.56	0.49	0.39
Amides					
Hexadecanamide	$C_{16}H_{33}NO$	0.42	0.52	0.55	ND
9-Octadecenamide	$C_{18}H_{35}NO$	1.19	1.39	1.19	0.62
Aromatics					
Toluene	C_7H_8	0.36	0.25	0.26	0.21
Ethylbenzene	C_8H_{10}	0.22	0.23	0.23	0.15
Benzene, 1,3-dimethyl-	C_8H_{10}	0.12	0.16	ND	ND
o-Xylene	C_8H_{10}	0.18	ND	0.17	0.11
2,3,5-Trimethoxytoluene	$C_{10}H_{14}O_3$	0.95	1.12	1.01	0.83
Squalene	$C_{30}H_{50}$	1.65	1.50	1.51	1.25
Carboxylic Acids					
3,5-Dimethoxy-4-hydroxyphenylacetic acid	$C_{10}H_{12}O_5$	0.11	ND	ND	ND
n-Hexadecanoic acid	$C_{16}H_{32}O_2$	14.70	11.10	11.70	5.20
Oleic Acid	$C_{18}H_{34}O_2$	43.97	46.33	39.79	22.46
Esters					
Methyl palmitoleate	$C_{17}H_{32}O_2$	ND	ND	ND	0.56
Hexadecanoic acid, methyl ester	$C_{17}H_{34}O_2$	2.76	2.71	4.77	8.96
9,12-Octadecadienoic acid (Z,Z)-, methyl ester	$C_{19}H_{34}O_2$	1.24	1.20	1.82	4.17
9-Octadecenoic acid, methyl ester, (E)-	$C_{19}H_{36}O_2$	14.12	13.51	20.39	36.66
Methyl stearate	$C_{19}H_{38}O_2$	0.86	0.94	1.38	2.63
9-Octadecenoic acid (Z)-, ethyl ester	$C_{20}H_{38}O_2$	ND	ND	ND	1.31
Eicosanoic acid, methyl ester	$C_{21}H_{42}O_2$	ND	ND	ND	0.32
9-Octadecenoic acid (Z)-, 2,3-dihydroxypropyl ester	$C_{21}H_{40}O_4$	ND	1.16	ND	1.12
Ketons					
2-Propanone, 1-(4-hydroxy-3-methoxyphenyl)-	$C_{10}H_{12}O_3$	0.41	0.50	0.41	0.30

Table 7.6. (Continued) *GC-MS results for methanol-stabilized bio-oil: pre- and post-aging process*

Compounds	Molecular formula	Area %			
		M10_na	M10_7d	M10_24h	M10_168h
Phenols					
Phenol	C_6H_6O	0.70	0.46	0.62	0.68
Phenol, 2-methyl-	C_7H_8O	0.44	0.43	0.54	0.36
Phenol, 3-methyl-	C_7H_8O	0.71	0.78	0.83	0.67
Phenol, 2-methoxy-	$C_7H_8O_2$	3.24	3.59	3.53	2.84
Phenol, 3,4-dimethyl-	$C_8H_{10}O$	0.71	0.63	0.35	0.51
Creosol	$C_8H_{10}O_2$	0.82	0.70	0.70	0.54
Phenol, 4-ethyl-3-methyl-	$C_9H_{12}O$	0.12	ND	ND	ND
2-Methoxy-4-vinylphenol	$C_9H_{10}O_2$	0.55	0.55	0.38	ND
Phenol, 2,6-dimethoxy-	$C_8H_{10}O_3$	2.36	2.43	2.34	1.93
Phenol, 2-methoxy-4-propyl-	$C_{10}H_{14}O_2$	0.60	0.54	0.52	0.42
Phenol, 2-methoxy-4-(1-propenyl)-	$C_{10}H_{12}O_2$	1.65	1.78	1.73	1.40
2,6-Dimethoxy-4-vinylphenol	$C_{10}H_{12}O_3$	0.33	0.36	ND	ND
2,6-Dimethoxy-4-propylphenol	$C_{11}H_{16}O_3$	0.30	0.35	0.33	0.26
Phenol, 2,6-dimethoxy-4-(2-propenyl)-	$C_{11}H_{14}O_3$	1.20	1.24	1.19	0.93

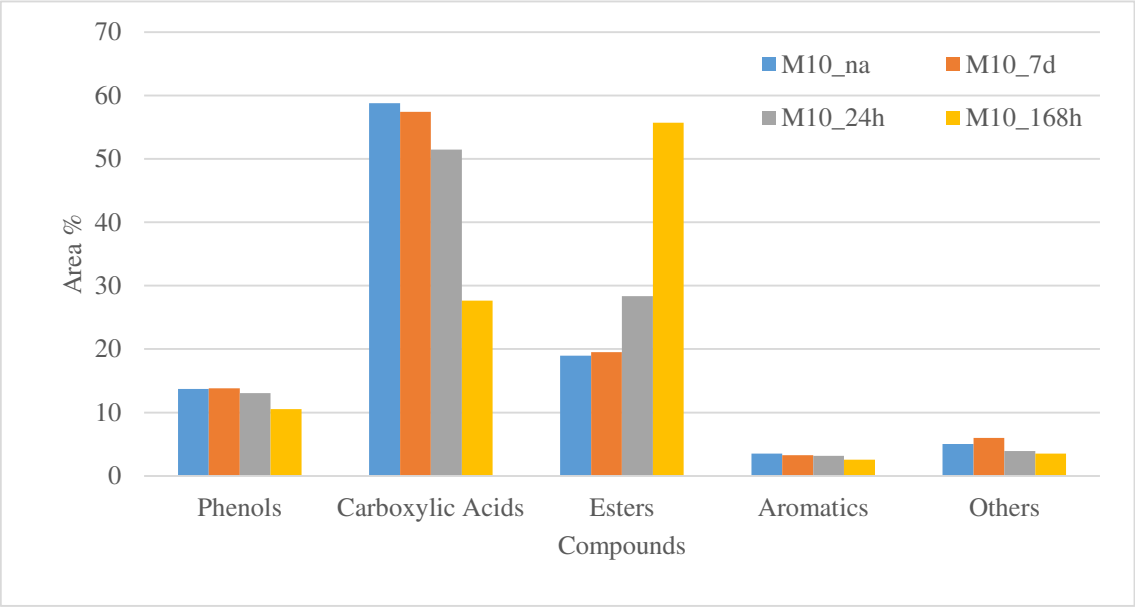

Figure 7.8. *Variations in the composition of methanol-stabilized bio-oil: pre- and post-aging process*

Non-aged furfural-stabilized bio-oil sample showed a slight increase in the percentage of ester and aromatic groups and a decrease in carboxylic acids and phenols compared to non-aged pure bio-oil. Furfural (aldehyde group) was detected as 10%, which is the same

percentage added to the bio-oil sample (Figure 7.9). After aging, a significant change is represented by a crucial decrease in the furfural percentage from 10.84% to 2.56% in both F10_na and F10_168h samples. This indicates that furfural may directly participate in the aging reaction, which ultimately leads to the consumption of this substance. Furthermore, ester, phenol, and aromatic groups' percentages increased slightly after aging. However, carboxylic acids percentage remained almost the same, which showed that furfural didn't affect the acidity of bio-oil samples. Comparing the four samples, it can be seen that some substances became less significant or even disappeared after the aging process and some appeared. Tridecane, Ethylbenzene, and Phenol, 2-ethyl- appeared in post-aged samples. In addition, several substances disappeared such as 2-Furanmethanol, Decane, Hexadecanamide, Homovanillic acid, Methyl laurate, and 2-Methoxy-4-vinylphenol as given in Table 7.7.

Table 7.7. *GC-MS results for furfural-stabilized bio-oil: pre- and post-aging process*

Compounds	Molecular formula	Area %			
		F10_na	F10_7d	F10_24h	F10_168h
Alcohols					
2-Furanmethanol	$C_5H_6O_2$	0.21	0.36	0.35	ND
Benzeneethanol, 2-methoxy-	$C_9H_{12}O_2$	1.19	1.19	1.22	1.78
Aldehyde					
Furfural	$C_5H_4O_2$	10.84	10.93	6.98	2.56
Alkanes					
Octane	C_8H_{18}	0.24	0.16	0.17	0.16
Nonane	C_9H_{20}	0.23	0.23	0.17	0.24
Decane	$C_{10}H_{22}$	0.24	ND	ND	ND
Tridecane	$C_{13}H_{28}$	ND	0.27	0.27	0.33
Tetradecane	$C_{14}H_{30}$	0.31	0.30	0.31	0.39
Pentadecane	$C_{15}H_{32}$	0.50	0.50	0.52	0.78
Amides					
Hexadecanamide	$C_{16}H_{33}NO$	0.48	0.48	0.33	ND
9-Octadecenamide, (Z)-	$C_{18}H_{35}NO$	1.15	1.21	1.00	0.61
Aromatics					
Toluene	C_7H_8	0.53	0.36	0.35	0.44
Ethylbenzene	C_8H_{10}	ND	ND	ND	0.30
Benzene, 1,3-dimethyl-	C_8H_{10}	0.26	0.18	0.17	0.24
Styrene	C_8H_8	0.13	0.09	0.11	0.13
o-Xylene	C_8H_{10}	0.24	0.24	0.20	0.27

Table 7.7. (Continued) *GC-MS results for furfural-stabilized bio-oil: pre- and post-aging process*

Compounds	Molecular formula	Area %			
		F10_na	F10_7d	F10_24h	F10_168h
2,3,5-Trimethoxytoluene	$C_{10}H_{14}O_3$	0.92	0.90	0.93	0.93
Squalene	$C_{30}H_{50}$	1.31	1.51	1.35	1.39
Carboxylic Acids					
n-Hexadecanoic acid	$C_{16}H_{32}O_2$	9.64	10.26	10.32	9.64
Oleic Acid	$C_{18}H_{34}O_2$	40.51	39.37	41.13	41.15
Homovanillic acid	$C_9H_{10}O_4$	0.36	0.35	0.30	ND
Esters					
Hexadecanoic acid, methyl ester	$C_{17}H_{34}O_2$	2.53	2.43	2.73	3.63
9,12-Octadecadienoic acid (Z,Z)-, methyl ester	$C_{19}H_{34}O_2$	1.09	1.04	1.31	1.58
Methyl laurate	$C_{13}H_{26}O_2$	0.24	ND	ND	ND
9-Octadecenoic acid, methyl ester, (E)-	$C_{19}H_{36}O_2$	12.25	12.12	13.24	16.28
Methyl stearate	$C_{19}H_{38}O_2$	0.87	0.85	0.92	1.17
Oleic acid, 3-hydroxypropyl ester	$C_{21}H_{40}O_3$	ND	ND	1.13	ND
Ketons					
2-Cyclopenten-1-one, 2-methyl-	C_6H_8O	ND	0.21	ND	ND
Phenols					
Phenol	C_6H_6O	0.76	0.44	0.47	0.63
Phenol, 2-methyl-	C_7H_8O	0.51	0.44	0.50	0.64
Phenol, 3-methyl-	C_7H_8O	0.86	0.82	0.85	1.06
Phenol, 2-methoxy-	$C_7H_8O_2$	3.36	3.38	3.43	4.28
Phenol, 2-ethyl-	$C_8H_{10}O$	ND	0.30	0.33	0.42
Phenol, 3,4-dimethyl-	$C_8H_{10}O$	0.27	0.06	0.28	0.22
Phenol, 4-ethyl-	$C_8H_{10}O$	0.35	0.28	0.34	0.34
Phenol, 3-ethyl-	$C_8H_{10}O$	0.37	0.33	0.35	0.31
Creosol	$C_8H_{10}O_2$	0.65	0.56	0.62	0.85
2-Methoxy-4-vinylphenol	$C_9H_{10}O_2$	0.48	0.46	0.32	ND
Phenol, 2,6-dimethoxy-	$C_8H_{10}O_3$	2.18	2.84	2.45	2.64
Phenol, 2-methoxy-4-propyl-	$C_{10}H_{14}O_2$	0.52	0.71	0.62	0.64
Phenol, 2-methoxy-4-(1-propenyl)-	$C_{10}H_{12}O_2$	1.56	1.59	1.61	1.95
2,6-Dimethoxy-4-vinylphenol	$C_{10}H_{12}O_3$	ND	0.30	ND	ND
2,6-Dimethoxy-4-propylphenol	$C_{11}H_{16}O_3$	0.32	0.33	0.38	0.38
Phenol, 2,6-dimethoxy-4-(2-propenyl)-	$C_{11}H_{14}O_3$	1.16	1.10	1.14	1.39

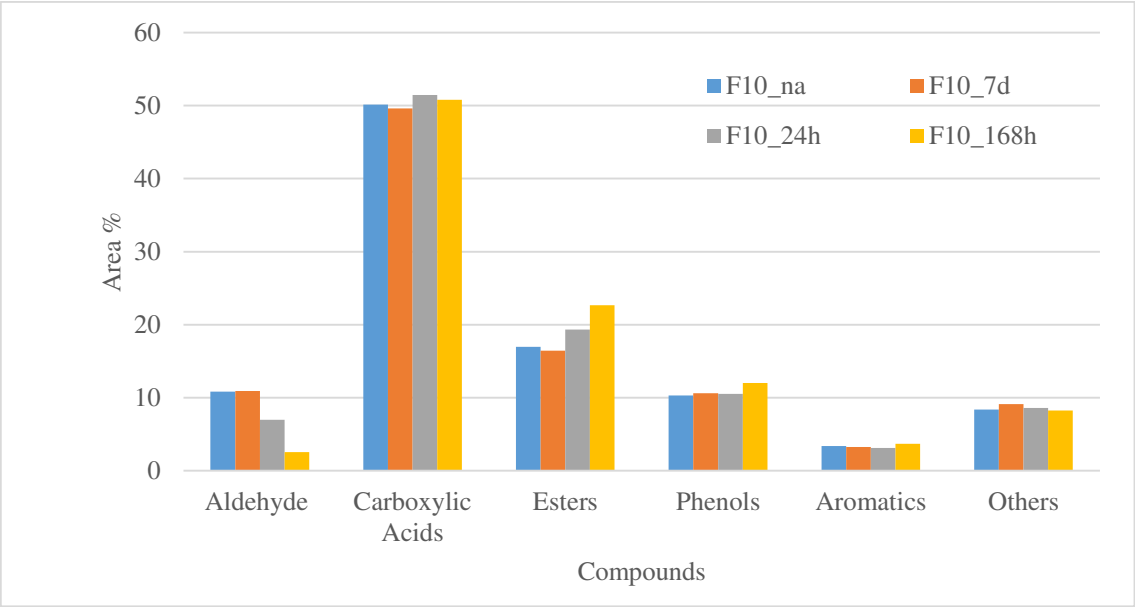

Figure 7.9. *Variations in the composition of furfural-stabilized bio-oil: pre- and post-aging process*

Non-aged tetrahydronaphthalene-stabilized bio-oil sample showed a slight decrease in the percentage of ester, phenol, carboxylic acid, and aromatic groups and significant formation of polycyclic aromatic hydrocarbons represented by 1,2,3,4 – tetrahydronaphthalene with 23.56% compared to non-aged pure bio-oil (Figure 7.10). A slight change for the polycyclic aromatic hydrocarbons was observed during the aging process represented by a small increase in the percentages of 23.88%, 28.87%, 28.12%, and 26.65% for N10_na, N10_7d, N10_24h, and N10_168h, respectively. Furthermore, an increase in the ester group was recorded from 14.28% to 17.86% for N10_na and N10_168h, respectively. While the percentage of phenol didn't change during the aging process, carboxylic acid content decreased from 45.11% to 37.51% for N10_na and N10_168h, respectively. The increase in the ester group indicates that esterification reactions occurred during the aging process. Comparing the four samples, it can be seen that some compounds become less significant or even disappeared and some appeared after the aging process. For instance, Nonane, Ethylbenzene, Homovanillic acid, 2-Methoxy-4-vinylphenol, and 2,6-Dimethoxy-4-vinylphenol disappeared in post-aged bio-oil samples. In addition, several new compounds such as Methyl laurate, Oleic acid, 3-hydroxypropyl ester, keton compounds, Phenol, 2-ethyl- and Phenol, 3-(1-methylethyl)- formed during the aging process (Table 7.8).

Table 7.8. *GC-MS results for tetrahydronaphthalene-stabilized bio-oil: pre- and post-aging process*

Compounds	Molecular formula	Area %			
		N10_na	N10_7d	N10_24h	N10_168h
Alcohols					
Benzeneethanol, 2-methoxy-	$C_9H_{12}O_2$	0.85	0.95	0.98	0.94
Alkanes					
Octane	C_8H_{18}	0.17	0.11	ND	0.10
Nonane	C_9H_{20}	0.14	0.16	ND	ND
Dodecane	$C_{12}H_{26}$	0.22	ND	ND	0.27
Tridecane	$C_{13}H_{28}$	0.27	0.23	ND	0.23
Tetradecane	$C_{14}H_{30}$	0.27	0.25	ND	0.23
Pentadecane	$C_{15}H_{32}$	0.51	0.40	0.42	0.39
Hexadecane	$C_{16}H_{34}$	0.09	ND	ND	0.21
Amides					
Hexadecanamide	$C_{16}H_{33}NO$	0.31	0.40	0.41	0.34
9-Octadecenamide, (Z)-	$C_{18}H_{35}NO$	0.83	0.98	0.97	0.78
Aromatics					
Toluene	C_7H_8	0.36	0.23	0.23	0.22
Ethylbenzene	C_8H_{10}	0.14	0.15	ND	ND
p-Xylene	C_8H_{10}	0.13	0.12	0.19	0.12
Styrene	C_8H_8	0.17	0.08	ND	0.20
Squalene	$C_{30}H_{50}$	0.96	0.98	1.10	1.04
Carboxylic Acids					
Homovanillic acid	$C_9H_{10}O_4$	0.32	0.30	0.29	ND
n-Hexadecanoic acid	$C_{16}H_{32}O_2$	8.71	9.55	8.28	7.07
Oleic Acid	$C_{18}H_{34}O_2$	36.08	31.57	33.13	30.44
Esters					
Methyl laurate	$C_{13}H_{26}O_2$	ND	ND	0.15	0.12
Hexadecanoic acid, methyl ester	$C_{17}H_{34}O_2$	2.14	1.95	2.21	2.94
9,12-Octadecadienoic acid (Z,Z)-, methyl ester	$C_{19}H_{34}O_2$	0.92	0.86	0.95	1.13
9-Octadecenoic acid, methyl ester, (E)-	$C_{19}H_{36}O_2$	10.54	9.71	10.72	12.18
Methyl stearate	$C_{19}H_{38}O_2$	0.68	0.69	0.76	0.81
Oleic acid, 3-hydroxypropyl ester	$C_{21}H_{40}O_3$	ND	ND	ND	0.69
Ketons					
2-Cyclopenten-1-one, 2-methyl-	C_6H_8O	ND	ND	ND	0.12
Butyrolactone	$C_4H_6O_2$	ND	ND	ND	0.17
2-Propanone, 1-(4-hydroxy-3-methoxyphenyl)-	$C_{10}H_{12}O_3$	ND	ND	ND	0.29

Table 7.8. (Continued) *GC-MS results for tetrahydronaphthalene-stabilized bio-oil: pre- and post-aging process*

Compounds	Molecular formula	Area %			
		N10_na	N10_7d	N10_24h	N10_168h
Phenols					
Phenol	C_6H_6O	0.39	0.33	0.46	0.45
Phenol, 2-methyl-	C_7H_8O	0.41	0.35	0.39	0.43
Phenol, 3-methyl-	C_7H_8O	0.54	0.67	0.70	0.65
Phenol, 2-methoxy-	$C_7H_8O_2$	2.35	2.79	2.79	2.64
Phenol, 2-ethyl-	$C_8H_{10}O$	ND	0.25	ND	0.25
Phenol, 4-ethyl-	$C_8H_{10}O$	0.23	0.31	0.26	0.29
Creosol	$C_8H_{10}O_2$	0.43	0.63	0.51	0.69
Phenol, 3-(1-methylethyl)-	$C_9H_{12}O$	ND	ND	ND	0.22
2-Methoxy-4-vinylphenol	$C_9H_{10}O_2$	0.43	0.38	0.28	ND
Phenol, 2,6-dimethoxy-	$C_8H_{10}O_3$	1.83	1.72	1.71	1.72
Phenol, 2-methoxy-4-propyl-	$C_{10}H_{14}O_2$	0.46	0.43	0.44	0.41
Phenol, 2-methoxy-4-(1-propenyl)-	$C_{10}H_{12}O_2$	1.34	1.23	1.25	1.24
2,6-Dimethoxy-4-vinylphenol	$C_{10}H_{12}O_3$	0.24	0.24	ND	ND
2,6-Dimethoxy-4-propylphenol	$C_{11}H_{16}O_3$	0.25	0.26	0.24	0.29
Phenol, 2,6-dimethoxy-4-(2-propenyl)-	$C_{11}H_{14}O_3$	0.97	0.78	0.91	0.87
Polycyclic aromatic hydrocarbons					
Naphthalene, 1,2,3,4-tetrahydro-	$C_{10}H_{12}$	23.56	28.42	27.72	26.26
Naphthalene	$C_{10}H_8$	0.32	0.45	0.39	0.40

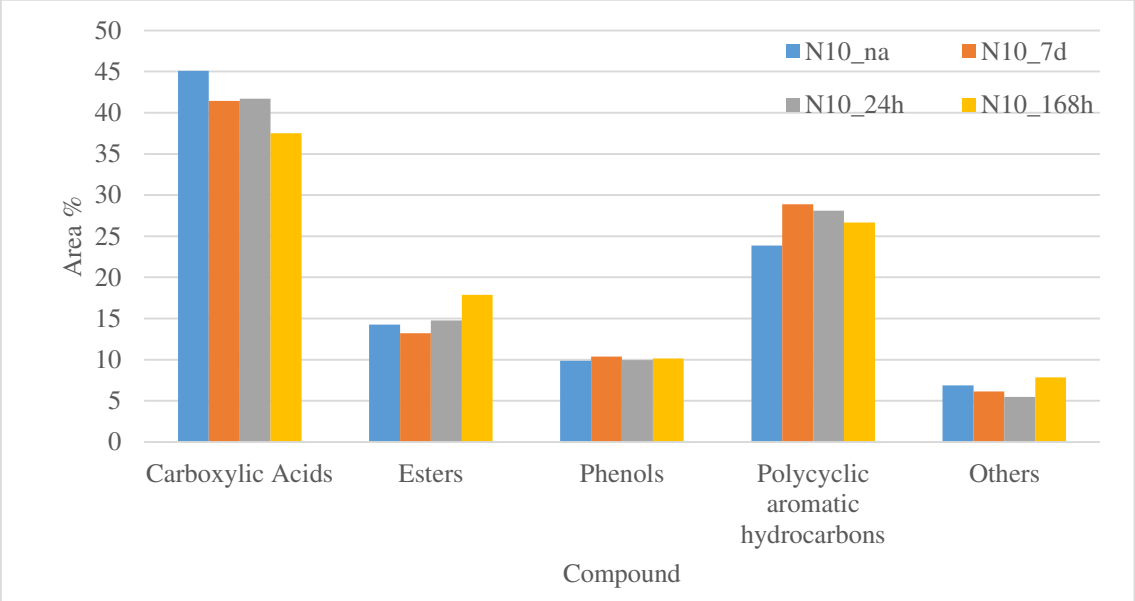

Figure 7.10. *Variations in the composition of tetrahydronaphthalene-stabilized bio-oil: pre- and post-aging process*

7.2.5. Dynamic viscosity and rheological behavior

The dynamic viscosity values of bio-oil samples were measured at different temperatures at shear rates ramp of 5 to 580 s^{-1} (Figure 7.11 - Figure 7.14). It's seen that the dynamic viscosity of post-aged pure and stabilized bio-oil samples increased after the aging process. All samples at all temperatures began to shear thickening at +˜200 s^{-1}, therefore the average viscosity was calculated at a shear rate between 10 and 50 s^{-1}, where the dynamic viscosity was almost constant as shown in Table 7.9, Table 7.10, Table 7.11, and Table 7.12 for pure, methanol-stabilized, furfural-stabilized and tetrahydronaphthalene-stabilized bio-oil samples, respectively. Using the mean of the dynamic viscosity, the aging index was calculated using eq. 6.2 for each sample at all temperatures. Aging index gives an idea about the change in the dynamic viscosity of bio-oil taking the pure non-aged bio-oil as a reference point.

The dynamic viscosities of pure non-aged bio-oil produced from olive pomace biomass were measured as 75.74, 57.86, 45.34, 36.34, 29.82, 20.88, and 15.55 cP at 20, 25, 30, 35, 40, 40, 50 and 60 ºC respectively. The dynamic viscosity of all samples decreases with the increase in temperature because of the increasing Brownian motion of their constituent molecules, and generally, the higher the viscosity, the greater the rate of decrease [73]. Aging indexes were calculated for aged bio-oil samples, results indicate that the highest value recorded was for Pure_168h at 20 ºC with a change of 46.8% compared to pure non-aged bio-oil. The higher the temperature, the lower the aging index for bio-oil aged at 80 ºC for 24 hours and 168 hours. However, bio-oil aged at room temperature for 7 days shows the opposite behavior. The increase in the dynamic viscosity when aging at room temperature for 7 days was confirmed to be similar to the increase determined in the accelerated aging test of 24 hours at 80 ºC.

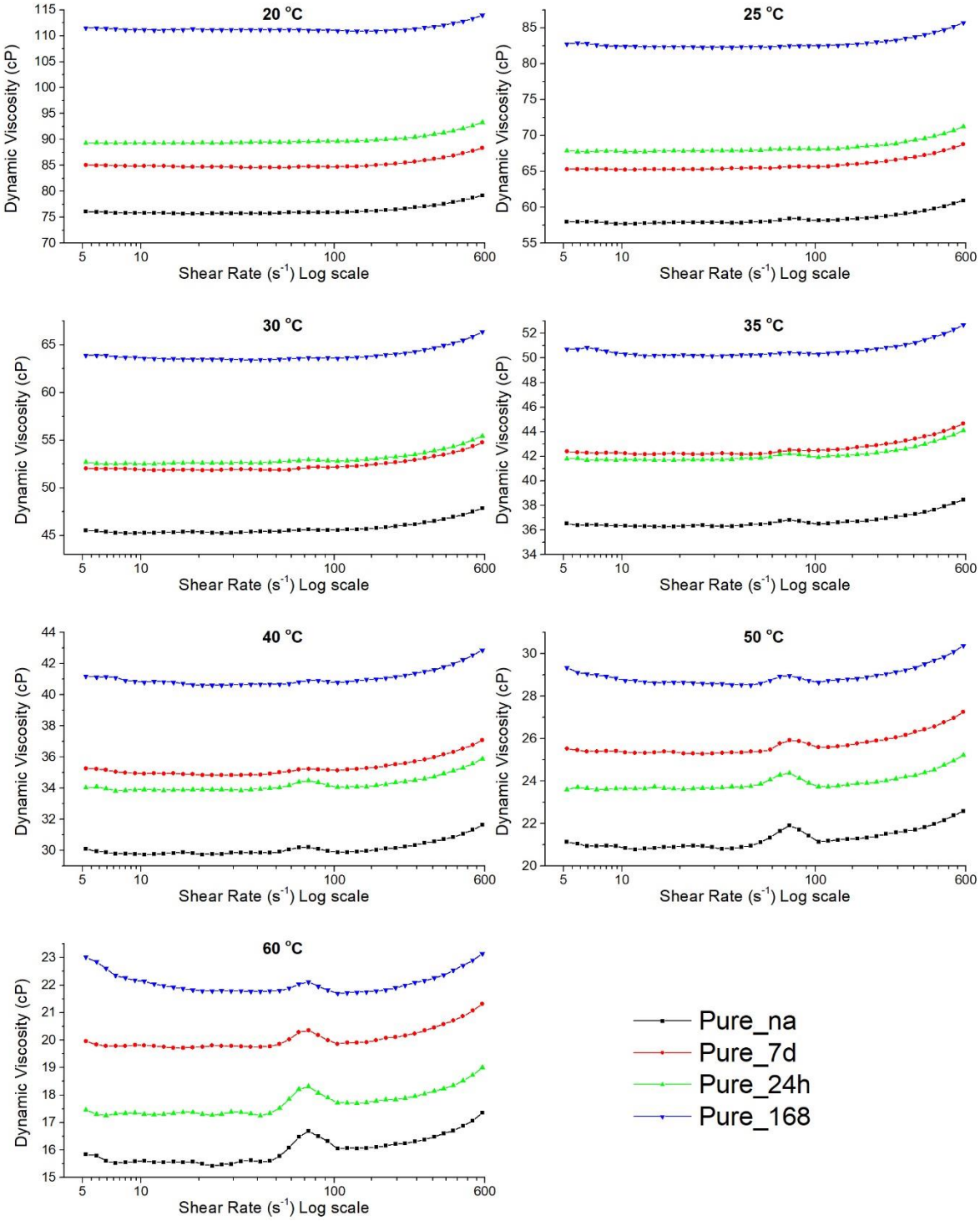

Figure 7.11. *Shear rate dependences of the dynamic viscosity of pure bio-oil: pre- and post-aged at different temperatures*

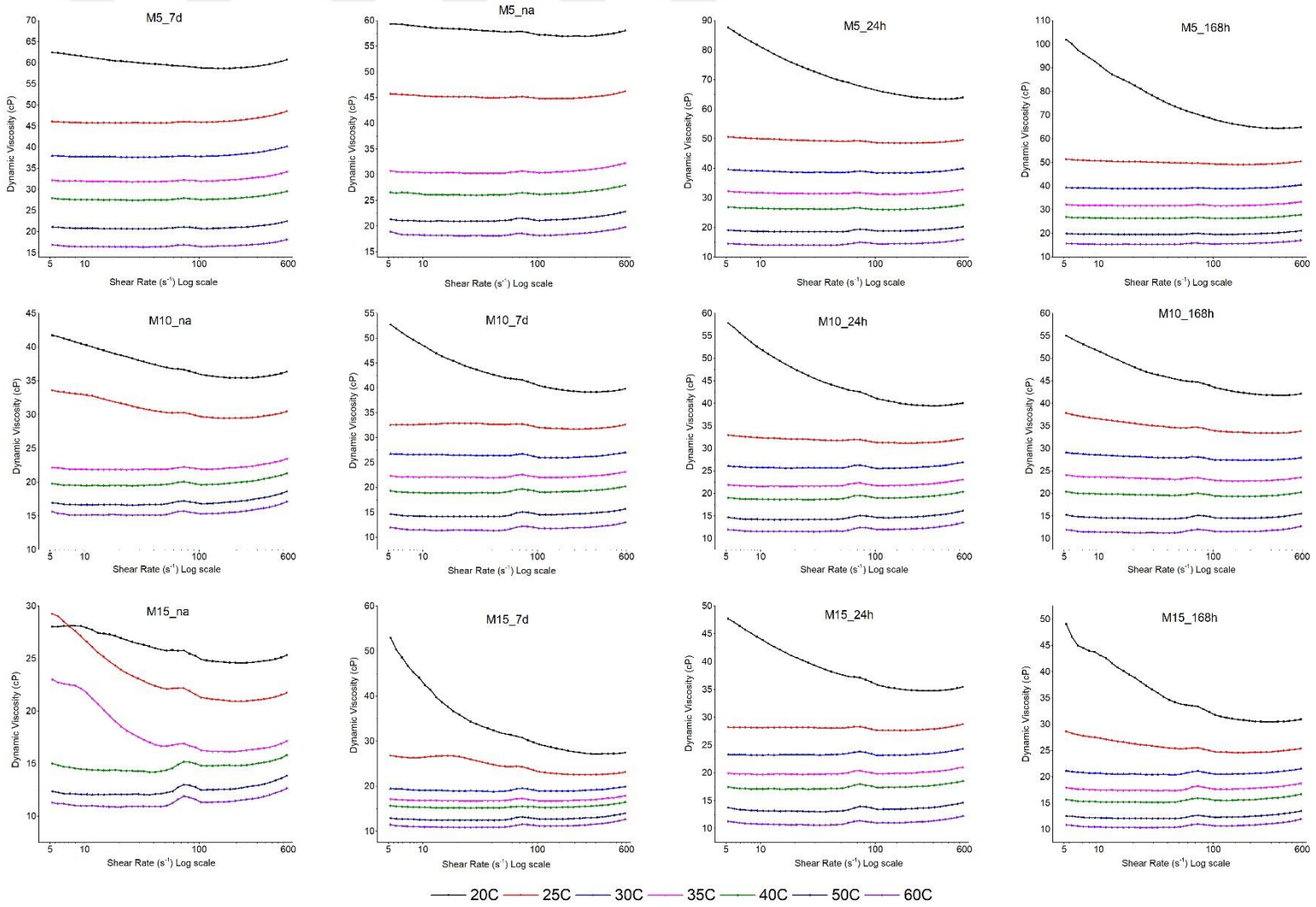

Figure 7.12. *Shear rate dependences of the dynamic viscosity of methanol-stabilized bio-oil: pre- and post-aged at different temperatures*

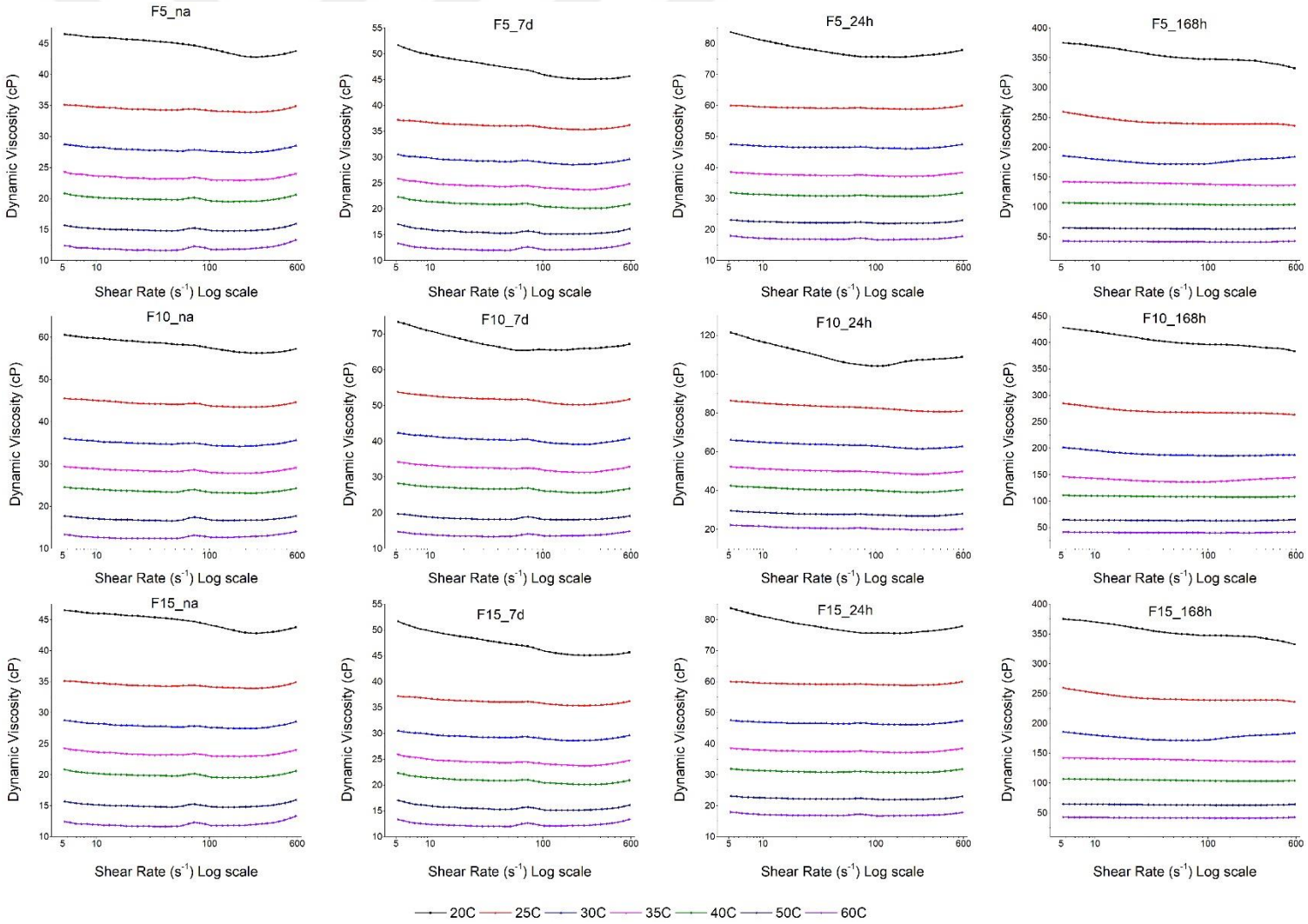

Figure 7.13. *Shear rate dependences of the dynamic viscosity of furfural-stabilized bio-oil: pre- and post-aged at different temperatures*

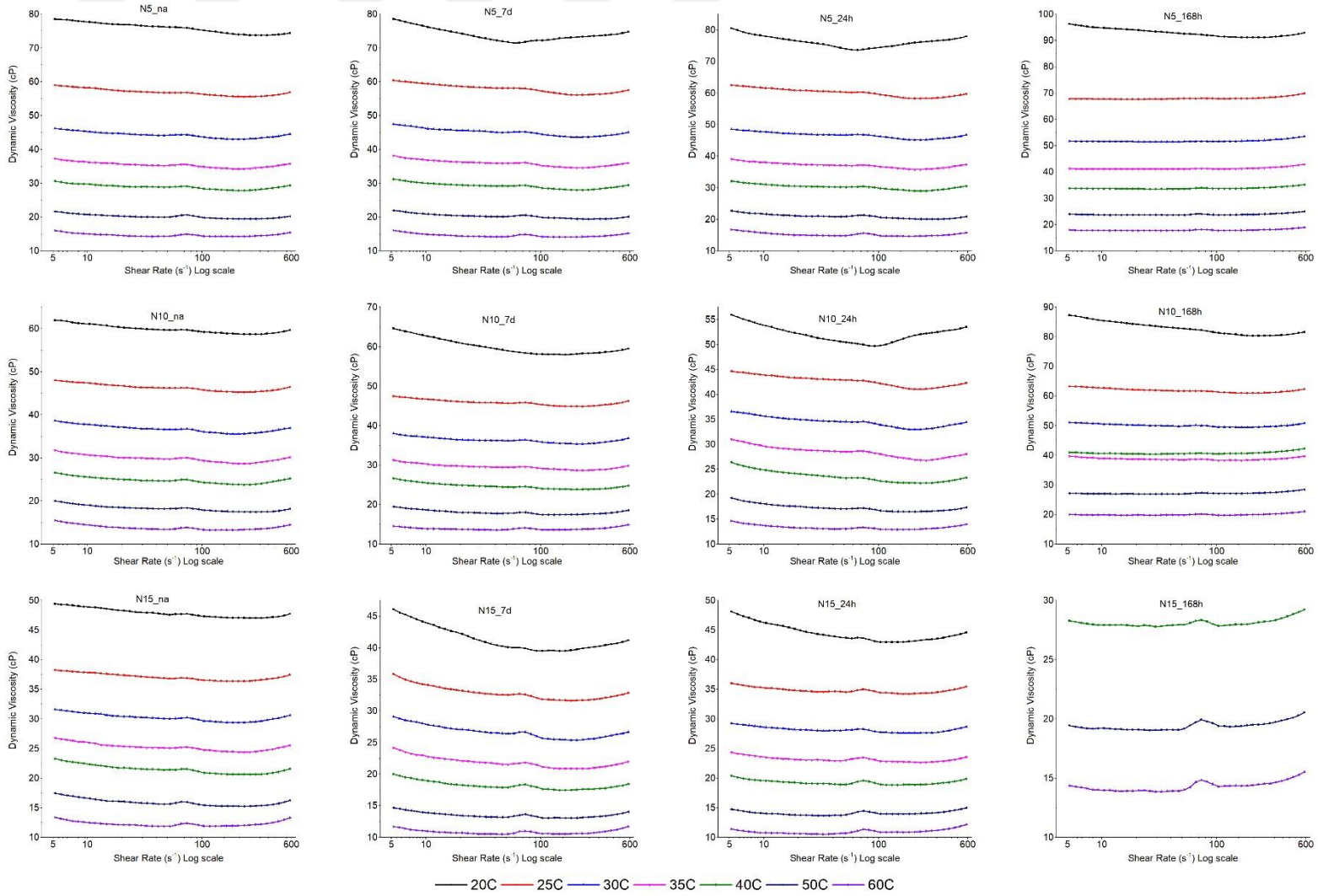

Figure 7.14. *Shear rate dependences of the dynamic viscosity of tetrahydronaphthalene-stabilized bio-oil: pre- and post-aged at different temperatures*

Table 7.9. *Mean viscosities and aging index for pure bio-oil: pre- and post-aging process*

Sample		20 °C	25 °C	30 °C	35 °C	40 °C	50 °C	60 °C
Pure_na	η	75.74	57.86	45.34	36.34	29.82	20.88	15.55
Pure_7d	η	84.73	65.32	51.9	42.19	34.89	25.34	19.76
	AI*,%	11.9	12.9	14.5	16.1	17.0	21.4	27.1
Pure_24h	η	89.37	67.85	52.61	41.74	33.91	23.68	17.33
	AI, %	18.0	17.3	16.0	14.9	13.7	13.4	11.4
Pure_168h	η	111.19	82.35	63.5	50.22	40.7	28.63	21.86
	AI, %	46.8	42.3	40.1	38.2	36.5	37.1	40.6

*AI Aging Index

The presence of additive improved bio-oil stability in terms of the dynamic viscosity as represented by the aging indexes.

The addition of 5%, 10%, and 15% of methanol, furfural, and tetrahydronaphthalene to bio-oil decreased the dynamic viscosity of non-aged bio-oil at all temperatures. Furthermore, the decrease in the dynamic viscosity was recorded the most at low temperatures, and (as expected) the higher the additive ratio, the lower the dynamic viscosity become. Non-aged methanol stabilized bio-oil samples showed the highest decrease in dynamic viscosities among the other additives. Compared to the Pure_na sample, 10% methanol, furfural, and tetrahydronaphthalene addition showed an improvement in the dynamic viscosity at 25 °C by 45.40%, 23.12%, and 19.31%, respectively.

After the aging process, compared to pure bio-oil, the aging index values of the methanol-stabilized bio-oil samples at 25 °C were calculated to be -43.33%, -44.66%, and -38.68% for M10_7d, M10_24h, and M10_168h, respectively. 10% furfural addition, the aging index values were calculated to be -9.97%, 45.18%, and 369.08% at 25 °C for F10_7d, F10_24h, and F10_168h, respectively. The aging indexes for 10% tetrahydronaphthalene addition, were calculated to be -20.32%, -25.13%, and 11.08% at the same temperature for N10_7d, N10_24h, and N10_168h, respectively. Table 7.10 – 7.12 summarize the change in the dynamic viscosities at all measurement temperatures and for each additive ratio for methanol, furfural and tetrahydronaphthalene additives.

Table 7.10. *Mean viscosities and aging index for methanol-stabilized bio-oil: pre- and post-aging process*

Methanol									
Age	**Percentage**		**20 ºC**	**25 ºC**	**30 ºC**	**35 ºC**	**40 ºC**	**50 ºC**	**60 ºC**
Non-Aged	5%	η	58.29	45.12	36.42	30.34	26.07	20.97	18.15
		AI,%	-23.04	-22.02	-19.67	-16.51	-12.58	0.43	16.72
	10%	η	38.68	31.59	25.54	21.88	19.52	16.66	15.13
		AI,%	-48.93	-45.40	-43.67	-39.79	-34.54	-20.21	-2.70
	15%	η	26.85	24.04	20.53	18.73	14.33	12.07	10.93
		AI,%	-64.55	-58.45	-54.72	-48.46	-51.95	-42.19	-29.71
7 Days	5%	η	60.37	45.76	37.68	31.86	27.50	20.71	16.40
		AI,%	-20.29	-20.91	-16.89	-12.33	-7.78	-0.81	5.47
	10%	η	44.93	32.79	26.50	22.04	18.91	14.19	11.40
		AI,%	-40.68	-43.33	-41.55	-39.35	-36.59	-32.04	-26.69
	15%	η	36.14	25.99	18.95	16.77	15.20	12.44	10.87
		AI,%	-52.28	-55.08	-58.20	-53.85	-49.03	-40.42	-30.10
24 Hours	5%	η	74.91	49.51	38.73	31.50	26.26	18.56	14.01
		AI, %	-1.10	-14.43	-14.58	-13.32	-11.94	-11.11	-9.90
	10%	η	47.31	32.02	25.68	21.60	18.67	14.19	11.56
		AI,%	-37.54	-44.66	-43.36	-40.56	-37.39	-32.04	-25.66
	15%	η	40.59	28.13	23.25	19.77	17.13	13.10	10.68
		AI,%	-46.41	-51.38	-48.72	-45.60	-42.56	-37.26	-31.32
168 Hours	5%	η	81.72	50.22	38.96	31.72	26.40	19.53	15.35
		AI,%	7.90	-13.20	-14.07	-12.71	-11.47	-6.47	-1.29
	10%	η	48.00	35.48	28.17	23.39	19.71	14.45	11.29
		AI,%	-36.63	-38.68	-37.87	-35.64	-33.90	-30.80	-27.40
	15%	η	38.46	26.25	20.48	17.41	15.17	12.08	10.35
		AI,%	-49.22	-54.63	-54.83	-52.09	-49.13	-42.15	-33.44

Table 7.11. *Mean viscosities and aging index for furfural-stabilized bio-oil: pre- and post-aging process*

Furfural									
Age	**Percentage**		**20 ºC**	**25 ºC**	**30 ºC**	**35 ºC**	**40 ºC**	**50 ºC**	**60 ºC**
Non-Aged	5%	η	77.12	56.88	44.11	35.35	28.98	20.49	15.26
		AI,%	1.82	-1.69	-2.71	-2.72	-2.82	-1.87	-1.86
	10%	η	59.04	44.48	34.99	28.51	23.65	16.79	12.49
		AI,%	-22.05	-23.12	-22.83	-21.55	-20.69	-19.59	-19.68
	15%	η	45.59	34.45	27.93	23.37	19.96	14.94	11.75
		AI,%	-39.81	-40.46	-38.40	-35.69	-33.07	-28.45	-24.44
7 Days	5%	η	90.51	67.68	52.27	41.47	33.69	23.19	16.70
		AI,%	19.50	16.97	15.28	14.12	12.98	11.06	7.40
	10%	η	68.21	52.09	40.77	32.77	26.91	18.39	13.54

Table 7.11. (Continued) *Mean viscosities and aging index for furfural-stabilized bio-oil: pre- and post-aging process*

Furfural									
Age	**Percentage**		**20 ºC**	**25 ºC**	**30 ºC**	**35 ºC**	**40 ºC**	**50 ºC**	**60 ºC**
7 Days		AI,%	-9.94	-9.97	-10.08	-9.82	-9.76	-11.93	-12.93
	15%	η	48.55	36.30	29.40	24.57	21.06	15.56	12.15
		AI,%	-35.90	-37.26	-35.16	-32.39	-29.38	-25.48	-21.86
24 Hours	5%	η	130.79	97.22	72.56	55.59	43.71	28.78	20.03
		AI,%	72.68	68.03	60.04	52.97	46.58	37.84	28.81
	10%	η	111.77	84.00	64.14	50.53	40.80	28.06	20.80
		AI,%	47.57	45.18	41.46	39.05	36.82	34.39	33.76
	15%	η	78.69	59.27	46.63	37.63	31.01	22.30	16.94
		AI,%	3.89	2.44	2.85	3.55	3.99	6.80	8.94
168 Hours	5%	η	321.79	222.84	156.78	113.54	84.88	50.92	33.19
		AI,%	324.86	285.14	245.79	212.44	184.64	143.87	113.44
	10%	η	410.19	271.41	190.26	139.39	109.27	63.56	40.37
		AI,%	441.58	369.08	319.63	283.57	266.43	204.41	159.61
	15%	η	360.59	244.30	175.23	140.42	105.55	63.87	41.91
		AI,%	376.09	322.23	286.48	286.41	253.96	205.89	169.52

Table 7.12. *Mean viscosities and aging index for tetrahydronaphthalene-stabilized bio-oil: pre- and post-aging process*

Tetrahydronaphthalene									
Age	**Percentage**		**20 ºC**	**25 ºC**	**30 ºC**	**35 ºC**	**40 ºC**	**50 ºC**	**60 ºC**
Non-Aged	5%	η	76.86	57.34	44.61	35.66	29.14	20.27	14.54
		AI,%	1.48	-0.90	-1.61	-1.87	-2.28	-2.92	-6.50
	10%	η	60.33	46.69	37.11	30.14	25.01	18.48	13.80
		AI,%	-20.35	-19.31	-18.15	-17.06	-16.13	-11.49	-11.25
	15%	η	48.26	37.34	30.45	25.40	21.75	16.00	12.11
		AI,%	-36.28	-35.46	-32.84	-30.10	-27.06	-23.37	-22.12
7 Days	5%	η	74.02	58.63	45.57	36.28	29.50	20.41	14.44
		AI,%	-2.27	1.33	0.51	-0.17	-1.07	-2.25	-7.14
	10%	η	60.82	46.10	36.50	29.75	24.91	18.08	13.72
		AI,%	-19.70	-20.32	-19.50	-18.13	-16.47	-13.41	-11.77
	15%	η	41.98	33.20	27.05	22.13	18.31	13.46	10.67
		AI,%	-44.57	-42.62	-40.34	-39.10	-38.60	-35.54	-31.38
24 Hours	5%	η	76.24	60.87	47.09	37.45	30.52	21.13	15.08
		AI,%	0.66	5.20	3.86	3.05	2.35	1.20	-3.02

Table 7.12. (Continued) *Mean viscosities and aging index for tetrahydronaphthalene-stabilized bio-oil: pre- and post-aging process*

			Tetrahydronaphthalene						
Age	**Percentage**		**20 ºC**	**25 ºC**	**30 ºC**	**35 ºC**	**40 ºC**	**50 ºC**	**60 ºC**
24 Hours	10%	η	52.06	43.32	34.98	28.96	24.03	17.48	13.27
		AI,%	-31.26	-25.13	-22.85	-20.31	-19.42	-16.28	-14.66
	15%	η	44.92	34.80	28.20	23.14	19.20	13.79	10.63
		AI,%	-40.69	-39.85	-37.80	-36.32	-35.61	-33.96	-31.64
168 Hours	5%	η	93.77	67.70	51.50	41.12	33.60	23.67	17.74
		AI,%	23.81	17.01	13.59	13.15	12.68	13.36	14.08
	10%	η	84.13	62.12	50.13	38.69	40.49	26.93	19.80
		AI,%	11.08	7.36	10.56	6.47	35.78	28.98	27.33
	15%	η	46.18	NA*	NA	NA	27.89	19.10	13.93
		AI,%	-39.03	NA	NA	NA	-6.47	-8.52	-10.42

*Not Available

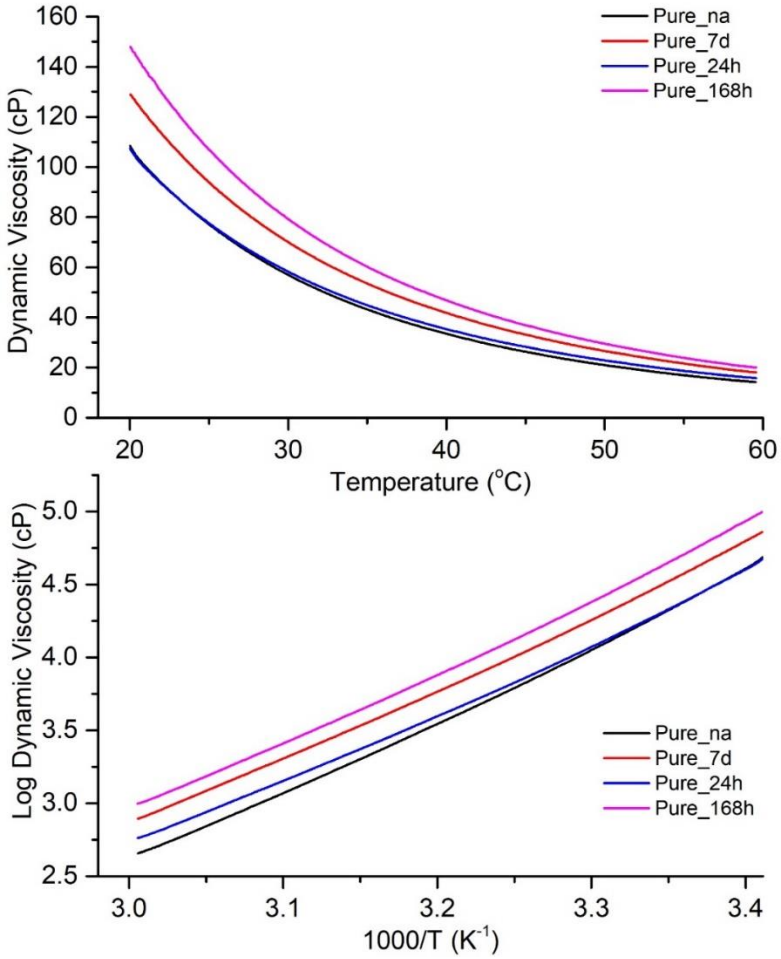

Figure 7.15. *Arrhenius plots for pure bio-oil: pre- and post-aging process*

The relationship between temperature and dynamic viscosity is represented by Arrhenius equation for bio-oil samples in Figure 7.15-7.18 for pure, methanol-stabilized, furfural-stabilized, and tetrahydronaphthalene-stabilized samples, respectively. (Plots of log (η) versus 1000/T.).

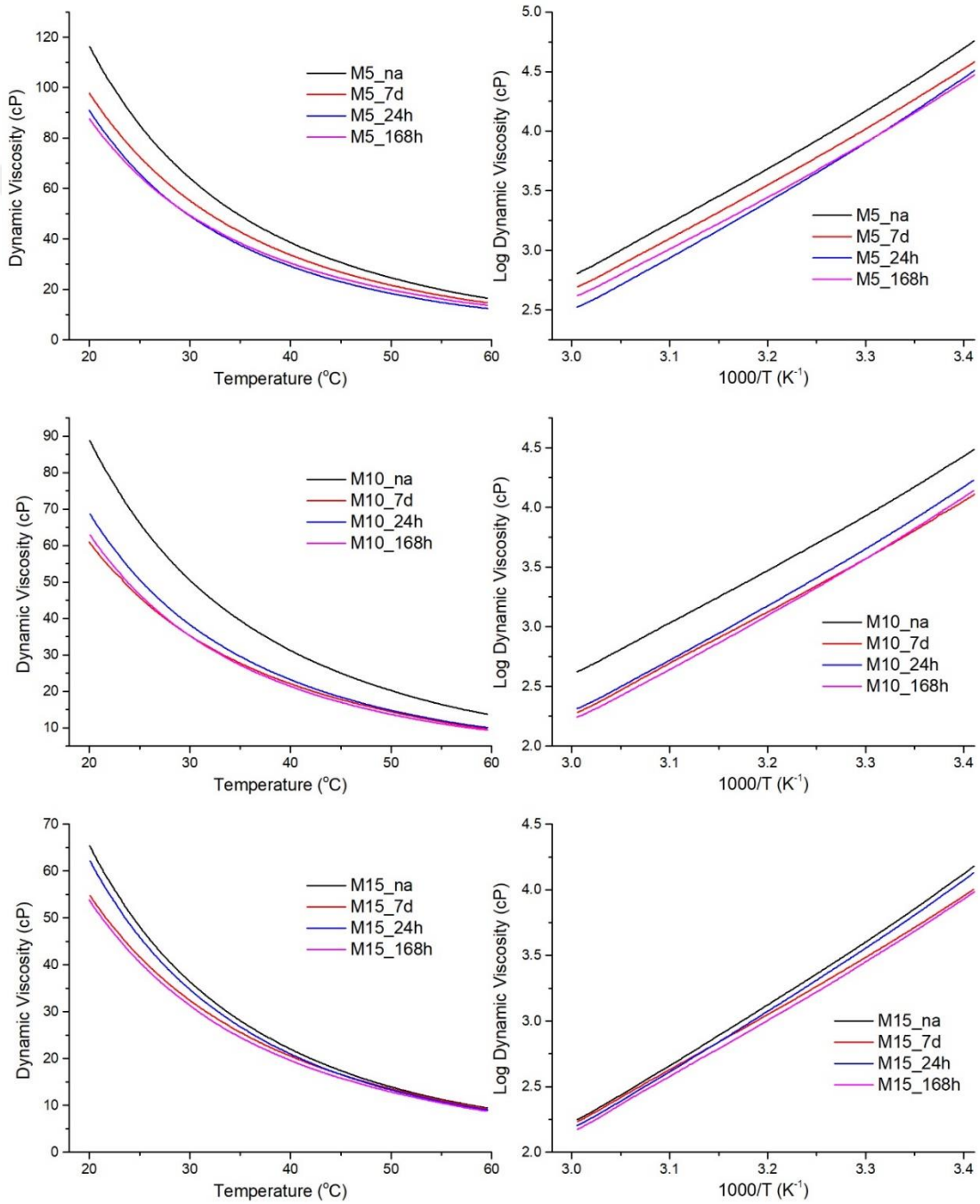

Figure 7.16. *Arrhenius plots for methanol-stabilized bio-oil: pre- and post-aging process*

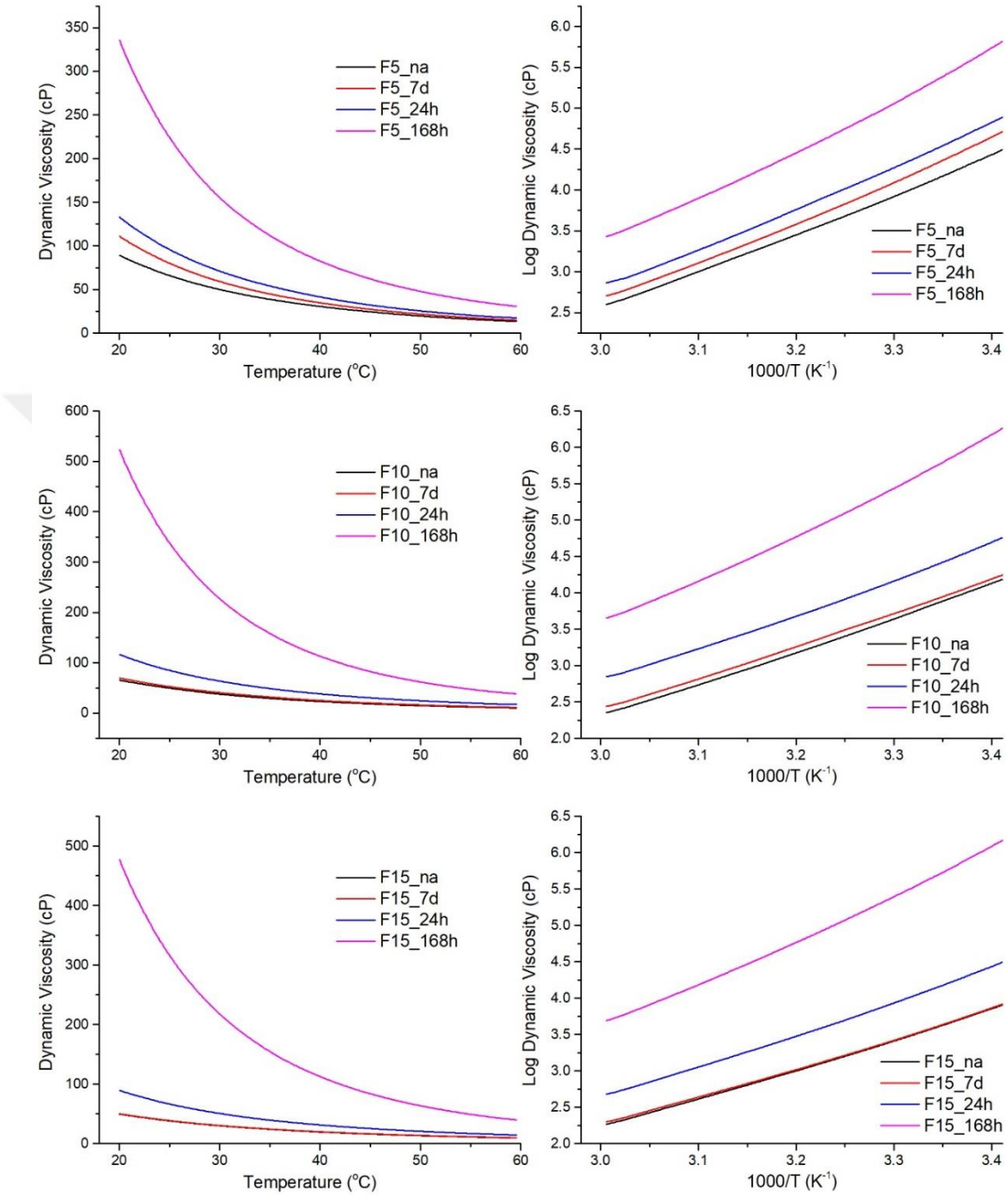

Figure 7.17. *Arrhenius plots for furfural-stabilized bio-oil: pre- and post-aging process*

Using eq. 4.2 and eq. 4.3 the activation energy (E) and the intercept were calculated as given in Table 7.13. The activation energy of pre- and post-aged pure bio-oil are nearly the same being 41.26, 39.95, 38.78 and 40.76 kJ.mol^{-1}, respectively.

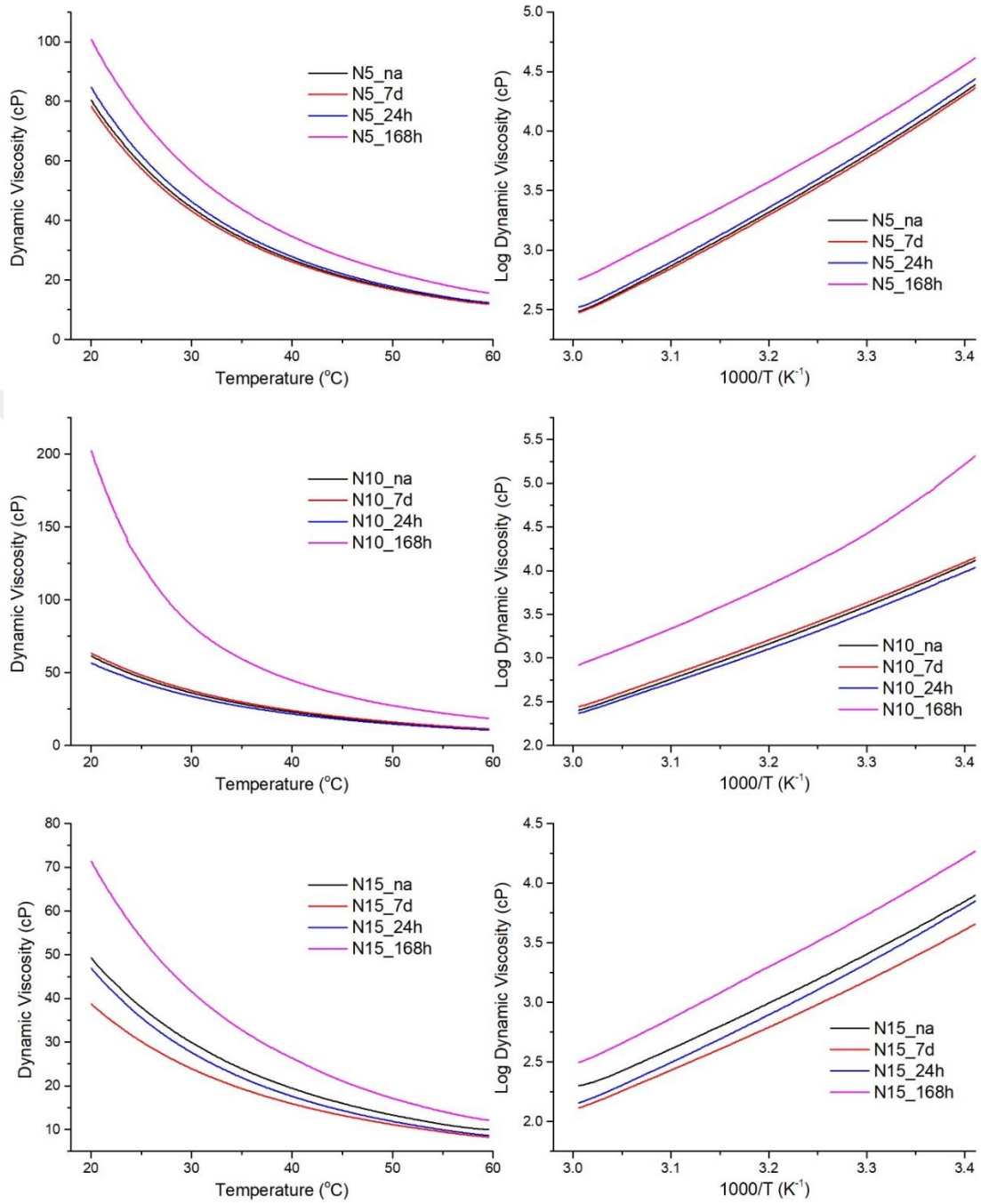

Figure 7.18. *Arrhenius plots for tetrahydronaphthalene-stabilized bio-oil: pre- and post-aging process*

Despite the solvent used, the addition of solvent to bio-oil decreased the activation energy. When the ratio of the additive increased, the activation energy decreased significantly. However, the addition of furfural increased the activation energy significantly only for 168 hours' samples. Moreover, 5% of furfural increased the activation energy. This

could be due to the homopolymerization reactions that happened with aldehydes to form polymers.

Table 7.13. *Arrhenius coefficients and activation energies of bio-oil samples*

Additive	%	Age	Intercept	E/R	R^2	E (kJ.mol^{-1})
Pure	-	Non-Aged	1.42E-04	4.96	0.9981	41.26
	-	7 Days	2.93E-04	4.81	0.9984	39.95
	-	24 Hours	1.23E-03	4.66	0.9980	38.78
	-	168 Hours	2.40E-04	4.90	0.9983	40.76
Methanol	5%	Non-Aged	9.79E-06	4.76	0.9991	39.59
	10%		1.52E-05	4.56	0.9994	37.87
	15%		5.88E-06	4.74	0.9993	39.44
	5%	7 Days	1.28E-05	4.64	0.9992	38.54
	10%		1.44E-05	4.46	0.9996	37.11
	15%		2.04E-05	4.33	0.9996	36.01
	5%	24 Hours	5.22E-06	4.87	0.9987	40.50
	10%		6.98E-06	4.71	0.9991	39.14
	15%		5.72E-06	4.74	0.9992	39.39
	5%	168 Hours	1.61E-05	4.53	0.9988	37.68
	10%		7.10E-06	4.68	0.9990	38.89
	15%		1.48E-05	4.42	0.9995	36.73
Furfural	5%	Non-Aged	1.12E-05	4.64	0.9992	38.62
	10%		1.19E-05	4.54	0.9990	37.76
	15%		5.24E-05	4.02	0.9990	33.45
	5%	7 Days	4.98E-06	4.94	0.9982	41.09
	10%		1.52E-05	4.49	0.9995	37.32
	15%		6.55E-05	3.96	0.9987	32.91
	5%	24 Hours	4.31E-06	5.04	0.9988	41.91
	10%		1.18E-05	4.70	0.9981	39.10
	15%		2.15E-05	4.45	0.9983	37.01
	5%	168 Hours	6.41E-07	5.86	0.9973	48.71
	10%		1.43E-07	6.43	0.9975	53.45
	15%		4.08E-07	6.10	0.9980	50.69

Table 7.13. (Continued) Arrhenius coefficients and activation energies of bio-oil samples

Additive	%	Age	Intercept	E/R	R^2	E (kJ.mol^{-1})
Tetrahydro-naphthalene	5%	Non-Aged	8.67E-06	4.69	0.9984	38.97
	10%		3.37E-05	4.21	0.9987	35.02
	5%		8.67E-06	4.69	0.9984	38.97
	10%		3.37E-05	4.21	0.9987	35.02
	15%		5.95E-05	3.98	0.9983	33.11
	5%	7 Days	9.45E-06	4.65	0.9980	38.68
	10%		3.72E-05	4.19	0.9990	34.87
	15%		9.01E-05	3.79	0.9984	31.51
	5%	24 Hours	7.65E-06	4.74	0.9983	39.39
	10%		4.66E-05	4.09	0.9984	34.03
	15%		2.89E-05	4.18	0.9982	34.73
	5%	168 Hours	1.69E-05	4.56	0.9985	37.89
	10%		6.34E-07	5.68	0.9885	47.23
	15%		2.27E-05	4.37	0.9993	36.37

Bio-oil produced from olive pomace exhibited a Newtonian behavior, which means the viscosity does not vary with deformation rate or time. Drawing the data obtained from the rheometer as shear stress vs shear rate a straight line was obtained for all samples (Figure 7.19). Using the Newtonian fluid equation (Eq. 4.1), the slope of each straight line is the mean of the dynamic viscosity given in Table 7.10 – 7.12 (e.g., the slope of the Pure_na, M10_na, F10_na and N10_na at 25 ºC are 57.86, 31.59, 44.48 and 46.69 cP, respectively.

Being Newtonian fluid, make it easier to predict the rheological behavior of the bio-oil under different shear rates, since the dynamic viscosity remains constant. As noted in previous studies, bio-oil produced from different biomasses exhibits similar behavior as olive pomace-based bio-oil. Poplar and oak wood [75], pine and oak bark [105], and clean woody [77] biomass-based bio-oils exhibit Newtonian behavior at relatively high shear rates at a wide range of temperatures that is higher than 20 ºC. However, bio-oil exhibited a non-Newtonian behavior at low shear rates and relatively low temperatures [77,105].

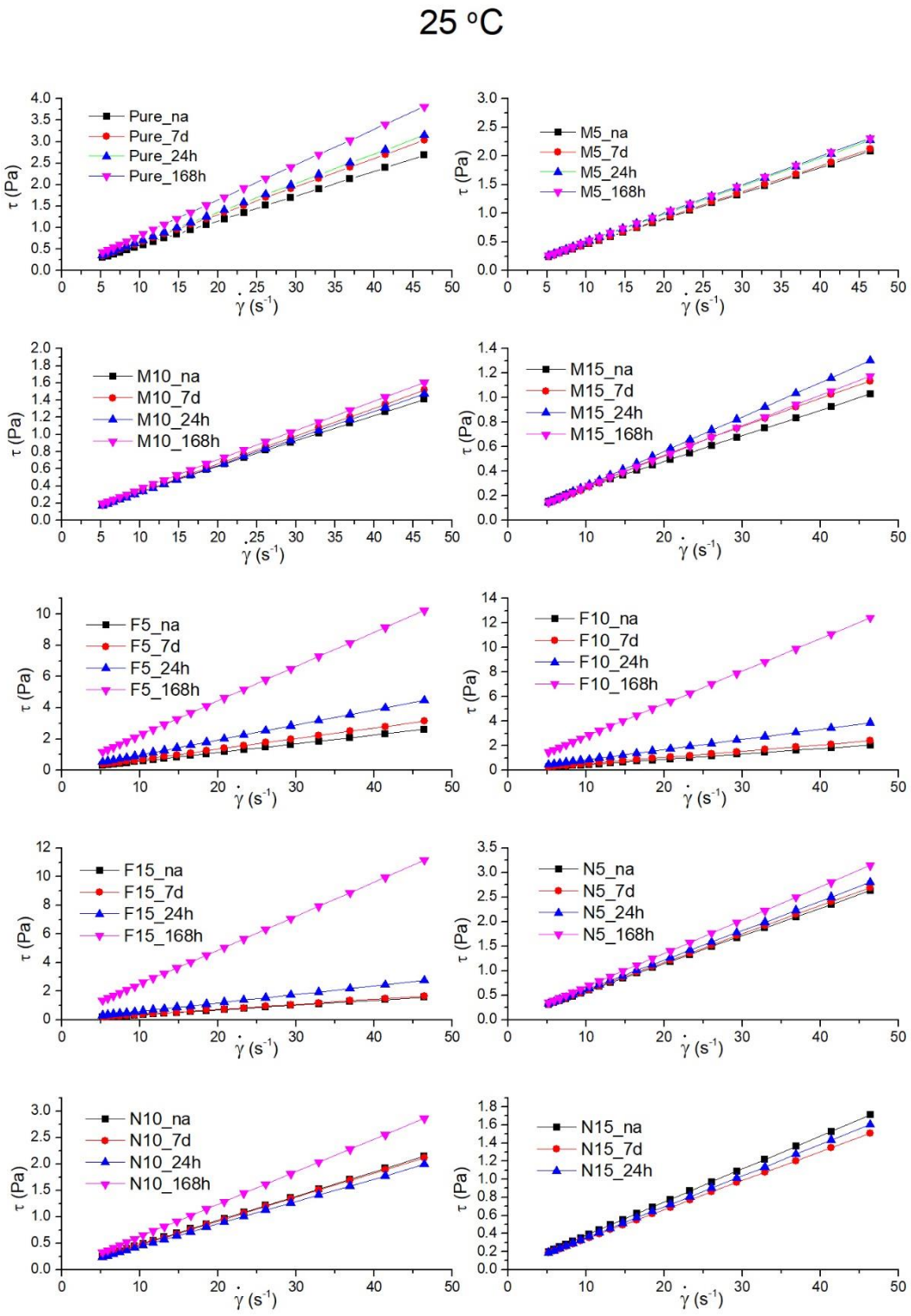

Figure 7.19. *Shear rate versus shear stress of pure and stabilized bio-oil samples pre- and post-aging process at 25 °C*

7.2.6. Full factorial design

Full factorial design gives the ability to study the effects of the combination of more than one factor in the experiment in a random way on a response. The response of interest is the dynamic viscosity (cP). In this study, four factors were studied: additive, measuring temperature, additive percentage, and aging duration. Table 7.14 illustrates these four parameters and their chosen levels for the experiment. Only accelerated aging was considered in this analysis.

Table 7.14. *Experimental factors and their levels*

Factor	Levels	Values
Additive	3	Methanol, Furfural, Tetrahydronaphthalene
Temperature (K)	7	293.15, 298.15, 303.15, 308.15, 313.15, 323.15, 333.15
Percentage (%)	4	0, 5, 10, 15
Aging (hours)	3	0, 24, 168

Minitab© 18.1 statistical software was used to implement a Full Factorial Design (FFD) analysis. FFD assumes that the data is approximately linear over the range of the factor settings chosen. While 4-way interaction analysis could be done, only linear and 2-way interactions were considered in this study. The mathematical model of the FFD could be represented as Eq. 7.1.

$$\hat{y} = \beta_0 + \sum_{i=1}^{n} \beta_i x_i + \sum_{i}^{n} \sum_{j \neq i}^{k} \beta_{ij} x_i x_j + \varepsilon \tag{7.1}$$

where $\hat{y}$ is the predicted values, β_0 is the constant coefficient, n and k are the level size of each factor, β_i is the regression coefficient of i^{th} level, β_{ij} is the regression coefficient of interaction of i^{th} and j^{th} levels, and ε is the error term.

Two hundred fifty-two experiments (3 levels of additive x 7 levels of temperature x 4 levels of percentage x 3 levels of aging) were carried out in random order and in a single replicate, the dynamic viscosity (cP) is measured as the response.

Probability Plot was constructed to check the normality of the data, with a P-value less than 0.05, this indicates that the data is not normal. Johnson Transformation was used to transform the data to follow a normal distribution (Figure 7.20), transformed data has a P-

value greater than 0.05, which indicates that the transformed data follows a normal distribution. Transformation function was generated as given in Eq. 7.2. A normal capability analysis was done on the transformed data to show the histogram and the distribution of the data (Figure 7.21).

$$\eta_T = -3.59124 + 1.09675 \times ln(\eta - 7.15614) \quad (7.2)$$

where η_T is the transformed dynamic viscosity.

To visualize the effect of each factor on the transformed data, main effects plot (Figure 7.22) was constructed. The figure indicates that temperature and aging duration have the highest effect on the mean of the transformed data. It also illustrates that methanol has the highest effect on lowering the value of the transformed data among the other two additives.

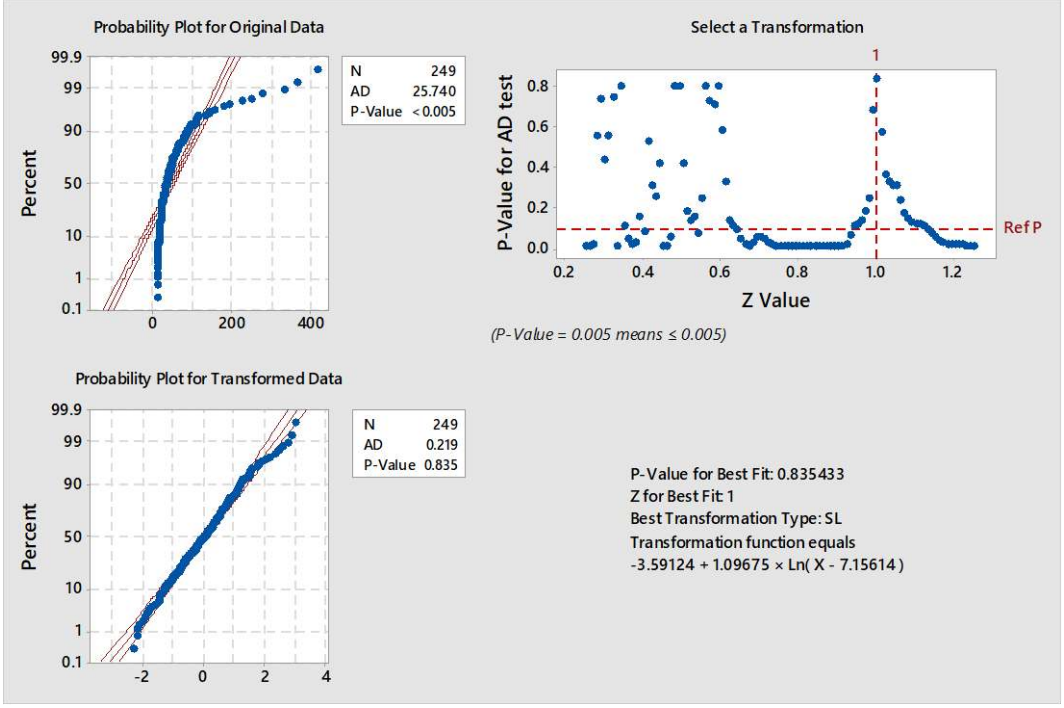

Figure 7.20. *Johnson transformation for dynamic viscosity data*

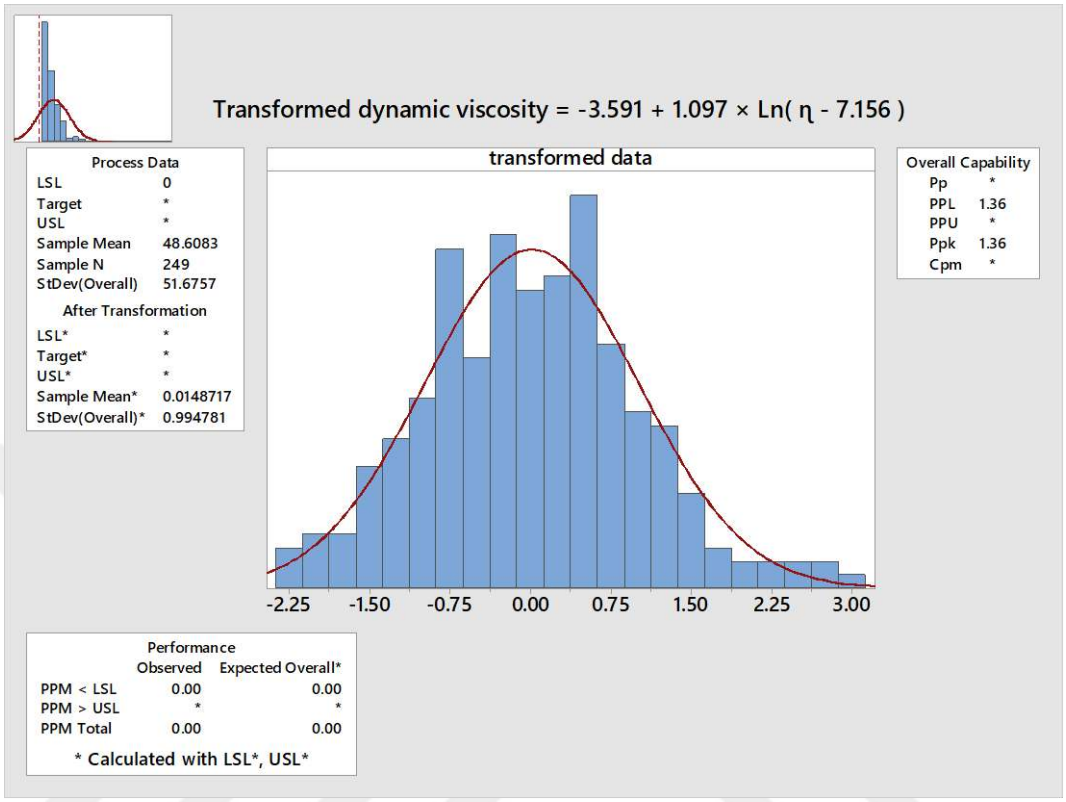

Figure 7.21. *Capability analysis report for dynamic viscosity data using Johnson Transformation*

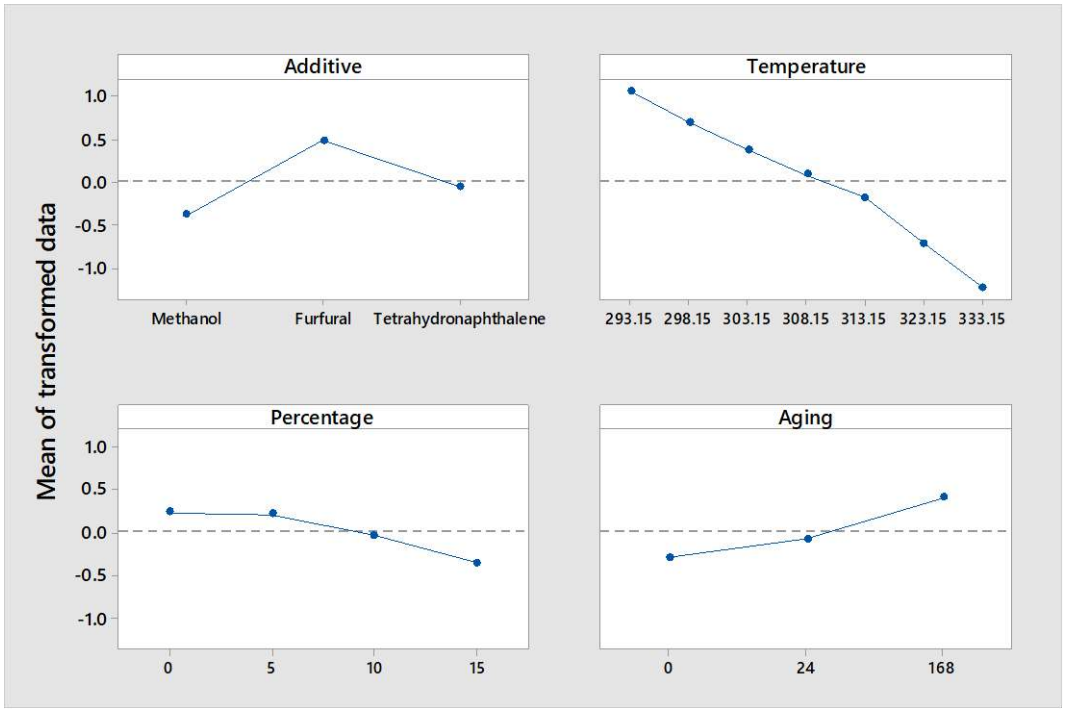

Figure 7.22. *Main effects plot for the mean of the transformed data*

The regression equation was generated using transformed data (Eq. 7.3).

$$\begin{aligned}\eta_T = {} & 17.442 - 0.05568\,T - 0.0546\,P + 0.00617\,A \\ & - 0.409\,S_m + 0.686\,S_f - 0.276\,S_t \\ & + 0.000008\,T*P - 0.000012\,T*A + 0.000162\,P*A \\ & + 0.00173\,T*S_m - 0.00285\,T*S_f + 0.00112\,T*S_t \\ & - 0.04279\,P*S_m + 0.04915\,P*S_f - 0.00636\,P*S_t \\ & - 0.003101\,A*S_m + 0.004708\,A*S_f - 0.001607\,A*S_t \end{aligned} \quad (7.3)$$

where T is the temperature (K), P is the percentage of the additive (wt.%), A is the accelerated aging duration (hours), and S_m, S_f, and S_t are the categorical predictor coding for methanol, furfural, and tetrahydronaphthalene as -1, 0 and 1, respectively.

A regression model could be generated by taking the additives as a category, this will produce a regression model for each additive. The obtained regression model equation for each additive is listed below.

Methanol:

$$\eta_T = 17.033 - 0.05395\,T - 0.0974\,P + 0.00307\,A + 0.000008\,T*P - 0.000012\,T*A + 0.000162\,P*A \quad (7.4)$$

Furfural:

$$\eta_T = 18.128 - 0.05853\,T - 0.0055\,P + 0.01088\,A + 0.000008\,T*P - 0.000012\,T*A + 0.000162\,P*A \quad (7.5)$$

Tetrahydronaphthalene:

$$\eta_T = 17.166 - 0.05456\,T - 0.0610\,P + 0.00456\,A + 0.000008\,T*P - 0.000012\,T*A + 0.000162\,P*A \quad (7.6)$$

Using Figure 7.23, calculated results could be retransformed to the dynamic viscosity (cP) values.

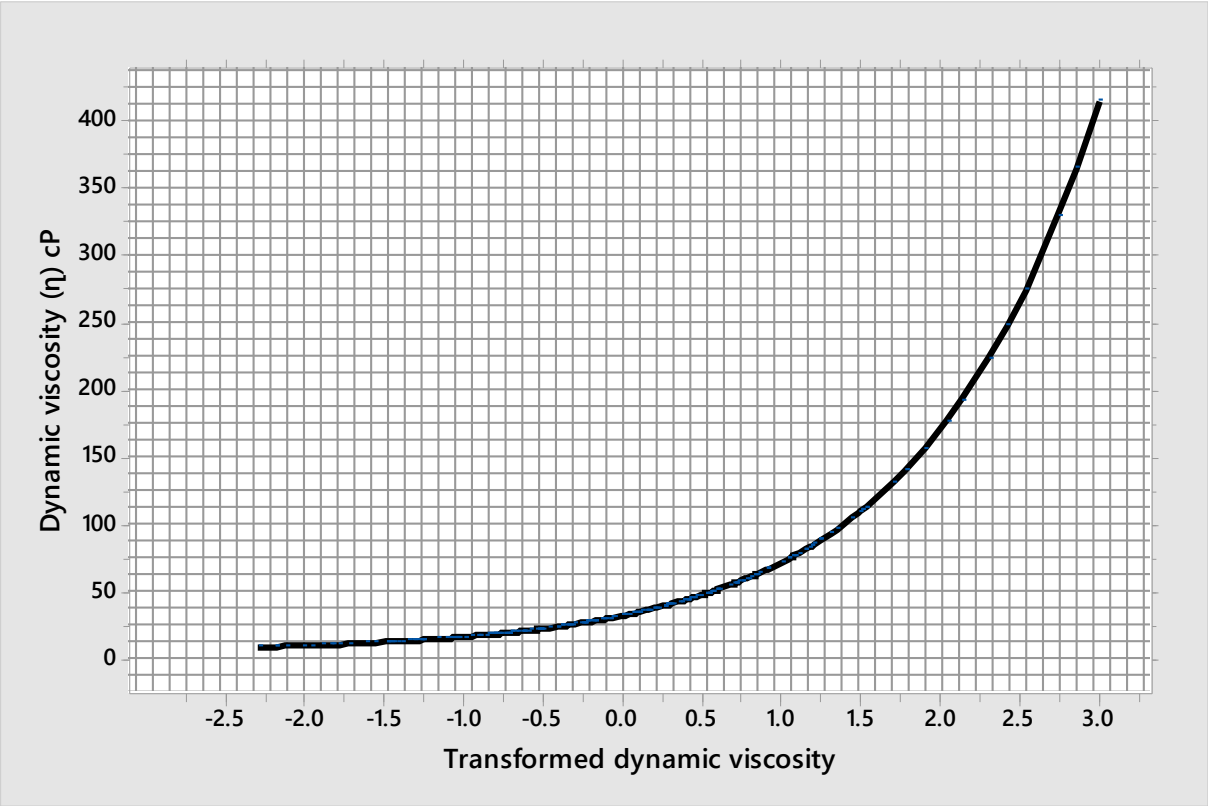

Figure 7.23. *The relationship between the dynamic viscosity and transformed data*

Table 7.15 illustrates the coefficients of determination for this model. The Adjusted coefficient of determination, R-sq(adj), for this model is 93.40%. In other words, 93% of the variability observed in the target variable is explained by the regression model.

Table 7.15. *Fit regression model coefficients of determination values*

Standard deviation	R-sq	R-sq(adj)	R-sq(pred)
0.254044	93.77%	93.40%	92.76%

Analysis of variance (ANOVA) was performed by computing the sums of squares (SS) for each factor. The SS values for model and residual are shown in the second column of the ANOVA, Table 7.16. The first column lists the degrees of freedom (DF) associated with the sum of squares (derived from the effects). The mean square (MS) is the of squares divided by the degrees of freedom. The ratio of mean squares forms the F-value. In the last column, P-value represents the significance of the factor, if the p-value is less than 0.05, providing at least 95% confidence. Temperature, (percentage and aging), (percentage and additive), and

(aging and additive) have a p-value less than 0.05, which means that these factors have a statistically significant effect. The p-value for the rest of the factors is greater than 0.05, which indicates that there is not enough evidence to conclude that these factors are related to the response.

Table 7.16. *ANOVA for the regression model*

Source	DF	Adj SS	Adj MS	F-Value	P-Value
Regression	14	230.198	16.4427	254.77	<0.001
Temperature	1	37.565	37.5651	582.06	<0.001
Percentage	1	0.041	0.0414	0.64	0.424
Aging	1	0.093	0.0929	1.44	0.231
Additive	2	0.105	0.0527	0.82	0.443
Temperature*Percentage	1	0.000	0.0001	0.00	0.971
Temperature*Aging	1	0.032	0.0322	0.50	0.480
Percentage*Aging	1	1.138	1.1379	17.63	<0.001
Temperature*Additive	2	0.178	0.0888	1.38	0.255
Percentage*Additive	2	11.253	5.6264	87.18	<0.001
Aging*Additive	2	15.887	7.9434	123.08	<0.001
Error	237	15.296	0.0645		
Total	251	245.493			

8. CONCLUSION

This thesis aimed to investigate the effect of different storage conditions and different ratios of three additives on bio-oil characterization and rheological behavior. Methanol, furfural, and tetrahydronaphthalene were used as additives each with 5, 10, and 15% added to olive pomace-based bio-oil that was produced using a fixed bed via slow pyrolysis method at around 500 ºC.

Having more than a hundred different chemical compounds, many reactions may occur in the aging process of bio-oil, such as oxidation, transesterification, esterification, and homopolymerization reactions, which cause the main dissimilarities between the fresh and the aged oils.

The characteristics of bio-oil, including viscosity and activation energy, were found to vary across the treated samples. Rheological tests were performed under a wide range of shear rates, and temperature conditions. The results showed that bio-oil has a higher viscosity than fossil fuels and lower viscosity than heavy crude oil. This means that bio-oil can be transferred easier than heavy crude oil. In addition, compared to heavy crude oil, lower activation energy illustrated that bio-oil was less sensitive to the changes in temperature and had a lower resistance to flow.

The addition of stabilizing chemicals to bio-oil leads to an overall improvement in the dynamic viscosity of fresh samples. After the aging process, methanol is found to be the best additive among the others. For instance, with the addition of 10% methanol, furfural, and tetrahydronaphthalene and after 168 hours of accelerated aging the aging indexes are calculated to be -33.90, 266.43, and 35.78% at 40 ºC, respectively. All bio-oil samples are found to exhibit Newtonian or near Newtonian behavior at all testing temperatures and shear rates (the dynamic viscosity is independent of the shear rate).

As a result, it can be conducted that, the rheological behavior and chemical composition of bio-oil depend on the biomass used, water content, temperature, and storage condition. Without a clearly defined standard, it’s difficult to compare the results between different studies. To be able to make a meaningful comparison, it is important to define a standard for biomass pretreatment, bio-oil production (pyrolysis conditions), storage, and testing temperature and shear rate.

To better understand the implications of these results, future studies could analyze water content, acidity and quantitative GC-MS results to determine the effects of additives on bio-oil. Furthermore, a combination of additives could be optimized to have the best results in terms of dynamic viscosity.

REFERENCES

[1] Jacobson, K., Maheria, K.C. and Kumar Dalai, A. (2013) Bio-oil valorization: A review. Renew. Sustain. Energy Rev. Pergamon. p. 91–106.

[2] Cao, W., Wang, Y. and Wang, C. (2019) Fatigue characterization of bio-modified asphalt binders under various laboratory aging conditions. *Construction and Building Materials*, Elsevier. 208, 686–96.

[3] Wei, P.H., Xie, R.H., Fu, L., Zheng, Y.J. and Zhao, H. (2021) Application Research on Crop Straw Biomass Waste in Logistics Packaging System. *Communications in Computer and Information Science*, p. 238–50.

[4] Miao, X., Lin, J. and Bian, F. (2020) Utilization of discarded crop straw to produce cellulose nanofibrils and their assemblies. *Journal of Bioresources and Bioproducts*, 5, 26–36.

[5] Hu, X. and Gholizadeh, M. (2020) Progress of the applications of bio-oil. *Renewable and Sustainable Energy Reviews*, Elsevier Ltd. 134.

[6] Han, X., Wang, H., Zeng, Y. and Liu, J. (2021) Advancing the application of bio-oils by co-processing with petroleum intermediates: A review. *Energy Conversion and Management: X*, 10.

[7] No, S.Y. (2014) Application of bio-oils from lignocellulosic biomass to transportation, heat and power generation - A review. Renew. Sustain. Energy Rev. p. 1108–25.

[8] Zhang, R., You, Z., Ji, J., Shi, Q. and Suo, Z. (2021) A review of characteristics of bio-oils and their utilization as additives of asphalts. *Molecules*, Multidisciplinary Digital Publishing Institute. 26, 5049.

[9] Bridgwater, A. V. (2003) Renewable fuels and chemicals by thermal processing of biomass. *Chemical Engineering Journal*, 91, 87–102.

[10] Guedes, R.E., Luna, A.S. and Torres, A.R. (2018) Operating parameters for bio-oil production in biomass pyrolysis: A review. J. Anal. Appl. Pyrolysis. Elsevier B.V. p. 134–49.

[11] Wu, S., Wang, Z., Yang, H., Zhang, H. and Xiao, R. (2020) The applicability of catalytic esterified biomass-pyrolysis-oil surrogates in diesel engine. *Fuel Processing Technology*, Elsevier. 198, 106251.

[12] Zheng, J.L. and Kong, Y.P. (2010) Spray combustion properties of fast pyrolysis bio-oil produced from rice husk. *Energy Conversion and Management*, Pergamon. 51, 182–8.

[13] Sippula, O., Huttunen, K., Hokkinen, J., Kärki, S., Suhonen, H., Kajolinna, T. et al. (2019) Emissions from a fast-pyrolysis bio-oil fired boiler: Comparison of health-related characteristics of emissions from bio-oil, fossil oil and wood. *Environmental Pollution*, Elsevier. 248, 888–97.

[14] Buffi, M., Cappelletti, A., Rizzo, A.M., Martelli, F. and Chiaramonti, D. (2018) Combustion of fast pyrolysis bio-oil and blends in a micro gas turbine. *Biomass and Bioenergy*, Pergamon. 115, 174–85.

[15] Boucher, M.E., Chaala, A. and Roy, C. (2000) Bio-oils obtained by vacuum pyrolysis of softwood bark as a liquid fuel for gas turbines. Part I: Properties of bio-oil and its blends with methanol and a pyrolytic aqueous phase. *Biomass and Bioenergy*, Pergamon. 19, 337–50.

[16] Boucher, M.E., Chaala, A., Pakdel, H. and Roy, C. (2000) Bio-oils obtained by vacuum pyrolysis of softwood bark as a liquid fuel for gas turbines. Part II: Stability and ageing of bio-oil and its blends with methanol and a pyrolytic aqueous phase. *Biomass and Bioenergy*, Pergamon. 19, 351–61.

[17] Lødeng, R. and Bergem, H. (2018) 7 - Stabilisation of pyrolysis oils. *Direct Thermochemical Liquefaction for Energy Applications*, p. 193–247.

[18] Elliott, D.C., Oasmaa, A., Meier, D., Preto, F. and Bridgwater, A. V. (2012) Results of the IEA round robin on viscosity and aging of fast pyrolysis bio-oils: Long-Term tests and repeatability. *Energy and Fuels*, American Chemical Society. 26, 7362–6.

[19] Oasmaa, A., Sundqvist, T., Kuoppala, E., Garcia-Perez, M., Solantausta, Y., Lindfors,

C. et al. (2015) Controlling the phase stability of biomass fast pyrolysis bio-oils. *Energy and Fuels*, 29, 4373–81.

[20] Houghton, R.A. and Hole, W. (2008) Quantities of Biomass Importance. *Small*, p. 448–53.

[21] Durusoy, T. and Gümüşderelioğlu, M. (2004) Basic Chemical Process Industries. Ankara.

[22] Opia, A.C., Hamid, M.K.B.A., Syahrullail, S., Rahim, A.B.A. and Johnson, C.A.N. (2019) Biomass as a potential source of sustainable fuel, chemical and tribological materials - Overview. *Materials Today: Proceedings*, Elsevier Ltd. 39, 922–8.

[23] Bassham, J.A. and Lambers, H. (2022) Photosynthesis. Encyclopedia Britannica.

[24] (2020) Center for Carbon Management. https://short.boku.ac.at/mdddqk (Access date: December 30, 2020)

[25] Kapellakis, I.E., Tsagarakis, K.P. and Crowther, J.C. (2008) Olive oil history, production and by-product management. *Reviews in Environmental Science and Biotechnology*, 7, 1–26.

[26] Breton, C.M., Warnock, P. and Bervillé, A.J. (2012) Olive Germplasm - The Olive Cultivation, Table Olive and Olive Oil Industry in Italy. In: Muzzalupo I, editor. *Olive Germplasm - The Olive Cultivation, Table Olive and Olive Oil Industry in Italy*, INTECH EUROPE, JANEZA TRDINE9, RIJEKA, 51000, CROATIA. p. 1–372.

[27] Turkish Ministry of Commerce. (2021) Olive and Olive Oil Report.

[28] TSI. (2017) Turkish Statistical Institute. Heal. Stat. https://data.tuik.gov.tr/Kategori/GetKategori?p=saglik-ve-sosyal-koruma-101&dil=1 (Access date: April 11, 2021)

[29] Skaltsounis, A.L., Argyropoulou, A., Aligiannis, N. and Xynos, N. (2015) Recovery of High Added Value Compounds from Olive Tree Products and Olive Processing Byproducts. In: Boskou D, editor. *Olive and Olive Oil Bioactive Constituents*, AOCS Press. p. 333–56.

[30] Sánchez Moral, P. and Ruiz Méndez, M.V. (2006) Production of pomace olive oil. *Grasas y Aceites*, 57, 47–55.

[31] Bridgwater, A. V. (2001) Thermal conversion of biomass and waste: the status. *Bio-Energy Research Group, Aston University, Birmingham, UK*,.

[32] Zhang, L., Xu, C. (Charles) and Champagne, P. (2010) Overview of recent advances in thermo-chemical conversion of biomass. *Energy Conversion and Management*, Pergamon. 51, 969–82.

[33] Demirbaş, A. (2001) Biomass resource facilities and biomass conversion processing for fuels and chemicals. *Energy Conversion and Management*, Pergamon. 42, 1357–78.

[34] Rezaiyan, J. and Cheremisinoff, N.P. (2005) Gasification Technologies. *Gasification Technologies*, CRC Press.

[35] Nachenius, R.W., Ronsse, F., Venderbosch, R.H. and Prins, W. (2013) Biomass Pyrolysis. 1st ed. Adv. Chem. Eng. Elsevier Inc.

[36] Zhang, H., Xiao, R., Wang, D., He, G., Shao, S., Zhang, J. et al. (2011) Biomass fast pyrolysis in a fluidized bed reactor under N 2, CO 2, CO, CH 4 and H 2 atmospheres. *Bioresource Technology*, 102, 4258–64.

[37] Chhiti, Y. and Kemiha, M. (2013) Thermal Conversion of Biomass, Pyrolysis and Gasification. International Journal of Engineering and Science (IJES), 2(3), pp.75-85. *The International Journal of Engineering And Science*, 2, 75–85.

[38] Xiu, S. and Shahbazi, A. (2012) Bio-oil production and upgrading research: A review. Renew. Sustain. Energy Rev. Pergamon. p. 4406–14.

[39] Elliott, D.C. (2007) Historical developments in hydroprocessing bio-oils. Energy and Fuels. American Chemical Society . p. 1792–815.

[40] Yi, W., Wang, X., Zeng, K., Yang, H., Shao, J., Zhang, S. et al. (2021) Improving bio-oil stability by fractional condensation and solvent addition. *Fuel*, Elsevier Ltd. 290, 119929.

[41] Cai, W., Kang, N., Jang, M.K., Sun, C., Liu, R. and Luo, Z. (2019) Long term storage stability of bio-oil from rice husk fast pyrolysis. *Energy*, Elsevier Ltd. 186, 115882.

[42] Khosravanipour Mostafazadeh, A., Solomatnikova, O., Drogui, P. and Tyagi, R.D. (2018) A review of recent research and developments in fast pyrolysis and bio-oil upgrading. Biomass Convers. Biorefinery. p. 739–73.

[43] Demirbas, A. (2007) The influence of temperature on the yields of compounds existing in bio-oils obtained from biomass samples via pyrolysis. *Fuel Processing Technology*, 88, 591–7.

[44] Onay, O. (2007) Influence of pyrolysis temperature and heating rate on the production of bio-oil and char from safflower seed by pyrolysis, using a well-swept fixed-bed reactor. *Fuel Processing Technology*, 88, 523–31.

[45] He, R., Ye, X.P., English, B.C. and Satrio, J.A. (2009) Influence of pyrolysis condition on switchgrass bio-oil yield and physicochemical properties. *Bioresource Technology*, 100, 5305–11.

[46] Bonelli, P.R., Della Rocca, P.A., Cerrella, E.G. and Cukierman, A.L. (2001) Effect of pyrolysis temperature on composition, surface properties and thermal degradation rates of Brazil Nut shells. *Bioresource Technology*, 76, 15–22.

[47] Debdoubi, A., El Amarti, A., Colacio, E., Blesa, M.J. and Hajjaj, L.H. (2006) The effect of heating rate on yields and compositions of oil products from esparto pyrolysis. *International Journal of Energy Research*, 30, 1243–50.

[48] Pütün, A.E., Uzun, B.B., Apaydin, E. and Pütün, E. (2005) Bio-oil from olive oil industry wastes: Pyrolysis of olive residue under different conditions. *Fuel Processing Technology*, Elsevier. 87, 25–32.

[49] Hilten, R.N. and Das, K.C. (2010) Comparison of three accelerated aging procedures to assess bio-oil stability. *Fuel*, Elsevier. 89, 2741–9.

[50] Pandey, A., Bhaskar, T., Stöcker, M. and Sukumaran, R.K. (2015) Recent Advances in Thermochemical Conversion of Biomass. *Recent Advances in Thermochemical*

Conversion of Biomass, Elsevier. 1–491.

[51] Bertero, M., De La Puente, G. and Sedran, U. (2012) Fuels from bio-oils: Bio-oil production from different residual sources, characterization and thermal conditioning. *Fuel*, Elsevier. 95, 263–71.

[52] Diebold, J.P. (2000) A Review of the Chemical and Physical Mechanisms of the Storage Stability of Fast Pyrolysis Bio-Oils. *Nrel/Sr-570-27613*, 59.

[53] Cai, J., Rahman, M.M., Zhang, S., Sarker, M., Zhang, X., Zhang, Y. et al. (2021) Review on Aging of Bio-Oil from Biomass Pyrolysis and Strategy to Slowing Aging. Energy and Fuels. p. 11665–92.

[54] Chen, D., Zhou, J., Zhang, Q. and Zhu, X. (2014) Evaluation methods and research progresses in bio-oil storage stability. *Renewable and Sustainable Energy Reviews*, Elsevier. 40, 69–79.

[55] Chen, D., Zheng, Y. and Zhu, X. (2012) Determination of effective moisture diffusivity and drying kinetics for poplar sawdust by thermogravimetric analysis under isothermal condition. *Bioresource Technology*, Elsevier. 107, 451–5.

[56] Yang, Z., Kumar, A. and Huhnke, R.L. (2015) Review of recent developments to improve storage and transportation stability of bio-oil. Renew. Sustain. Energy Rev. p. 859–70.

[57] Jendoubi, N., Broust, F., Commandre, J.M., Mauviel, G., Sardin, M. and Lédé, J. (2011) Inorganics distribution in bio oils and char produced by biomass fast pyrolysis: The key role of aerosols. *Journal of Analytical and Applied Pyrolysis*, 92, 59–67.

[58] Javaid, A., Ryan, T., Berg, G., Pan, X., Vispute, T., Bhatia, S.R. et al. (2010) Removal of char particles from fast pyrolysis bio-oil by microfiltration. *Journal of Membrane Science*, 363, 120–7.

[59] Moutsoglou, A., Lawburgh, B. and Lawburgh, J. (2018) Fractional condensation and aging of pyrolysis oil from softwood and organosolv lignin. *Journal of Analytical and Applied Pyrolysis*, Elsevier. 135, 350–60.

[60] Ortega, J. V., Renehan, A.M., Liberatore, M.W. and Herring, A.M. (2011) Physical and chemical characteristics of aging pyrolysis oils produced from hardwood and softwood feedstocks. *Journal of Analytical and Applied Pyrolysis*, Elsevier. 91, 190–8.

[61] Oasmaa, A., Kuoppala, E., Selin, J.F., Gust, S. and Solantausta, Y. (2004) Fast pyrolysis of forestry residue and pine. 4. Improvement of the product quality by solvent addition. *Energy and Fuels*, American Chemical Society . 18, 1578–83.

[62] Zhang, Q. (2006) Upgrading bio-oil over solid acid and base by catalytic esterification. *Hefei: University of Science and Technology of China*,.

[63] Xiong, W.M., Fu, Y., Lai, D.M. and Guo, Q.X. (2009) Upgrading of bio-oil via esterification catalysted with acidic ion-exchange resin. *Gaodeng Xuexiao Huaxue Xuebao/Chemical Journal of Chinese Universities*, 30, 1754–8.

[64] Mante, O.D. and Agblevor, F.A. (2012) Storage stability of biocrude oils from fast pyrolysis of poultry litter. *Waste Management*, Pergamon. 32, 67–76.

[65] Cheng, T., Han, Y., Zhang, Y. and Xu, C. (2016) Molecular composition of oxygenated compounds in fast pyrolysis bio-oil and its supercritical fluid extracts. *Fuel*, Elsevier. 172, 49–57.

[66] Wang, H., Lee, S.J., Olarte, M. V. and Zacher, A.H. (2016) Bio-oil Stabilization by Hydrogenation over Reduced Metal Catalysts at Low Temperatures. *ACS Sustainable Chemistry and Engineering*, American Chemical Society. 4, 5533–45.

[67] Otyuskaya, D., Thybaut, J.W., Alexiadis, V., Alekseeva, M., Venderbosch, R., Yakovlev, V. et al. (2018) Fast pyrolysis oil stabilization kinetics over a Ni-Cu catalyst using propionic acid as a model compound. *Applied Catalysis B: Environmental*, Elsevier. 233, 46–57.

[68] Schmitt, C.C., Raffelt, K., Zimina, A., Krause, B., Otto, T., Rapp, M. et al. (2018) Hydrotreatment of Fast Pyrolysis Bio-oil Fractions Over Nickel-Based Catalyst. *Topics in Catalysis*, 61, 1769–82.

[69] Auersvald, M., Shumeiko, B., Vrtiška, D., Straka, P., Staš, M., Šimáček, P. et al. (2019) Hydrotreatment of straw bio-oil from ablative fast pyrolysis to produce suitable refinery intermediates. *Fuel*, Elsevier. 238, 98–110.

[70] Tang, Z., Lu, Q., Zhang, Y., Zhu, X. and Guo, Q. (2009) One step bio-oil upgrading through hydrotreatment, esterification, and cracking. *Industrial and Engineering Chemistry Research*, 48, 6923–9.

[71] Horne, P.A. and Williams, P.T. (1996) Upgrading of biomass-derived pyrolytic vapours over zeolite ZSM-5 catalyst: Effect of catalyst dilution on product yields. *Fuel*, Elsevier. 75, 1043–50.

[72] Olazar, M., Aguado, R., Bilbao, J. and Barona, A. (2000) Pyrolysis of sawdust in a conical spouted-bed reactor with a HZSM-5 catalyst. *AIChE Journal*, AIChE. 46, 1025–33.

[73] Butt, H.J. (2011) Controlling the flow of suspensions. Science (80-.). Institute of Non-Newtonian Fluid Mechanics, University of Wales.

[74] Schurz, J. (1967) Rheological Methods. Polym. Fractionation. Freeman press.

[75] Nolte, M.W. and Liberatore, M.W. (2010) Viscosity of biomass pyrolysis oils from various feedstocks. *Energy and Fuels*, 24, 6601–8.

[76] Yin, R., Liu, R., Mei, Y., Fei, W. and Sun, X. (2013) Characterization of bio-oil and bio-char obtained from sweet sorghum bagasse fast pyrolysis with fractional condensers. *Fuel*, Elsevier. 112, 96–104.

[77] Yadykova, A.Y. and Ilyin, S.O. (2022) Compatibility and rheology of bio-oil blends with light and heavy crude oils. *Fuel*, Elsevier. 314, 122761.

[78] Lu, Q., Yang, X.L. and Zhu, X.F. (2008) Analysis on chemical and physical properties of bio-oil pyrolyzed from rice husk. *Journal of Analytical and Applied Pyrolysis*, 82, 191–8.

[79] Stieger, M. (2019) The Rheology Handbook - For users of rotational and oscillatory rheometers. *Applied Rheology*, 12, 232.

[80] Prasad, K. (2019) Rheology for Chemists – An Introduction. Appl. Rheol. Royal Society of Chemistry.

[81] Malvern Instruments Ltd. (2014) Kinexus series user manual. https://www.equipx.net/uploads/Malvern Instruments/MalvernKinexus-usermanual.pdf (Access date: March 23, 2022)

[82] Bird, R.B., Stewart, W.E. and Lightfoot, E.N. (2006) Transport Phenomena. Revised 2n. John Wiley Sons, Inc.

[83] Apaydin-Varol, E., Pütün, E. and Pütün, A.E. (2007) Slow pyrolysis of pistachio shell. *Fuel*, 86, 1892–9.

[84] Uzun, B.B., Apaydin-Varol, E., Ateş, F., Özbay, N. and Pütün, A.E. (2010) Synthetic fuel production from tea waste: Characterisation of bio-oil and bio-char. *Fuel*, Elsevier. 89, 176–84.

[85] Acikgoz, C. and Kockar, O.M. (2009) Characterization of slow pyrolysis oil obtained from linseed (Linum usitatissimum L.). *Journal of Analytical and Applied Pyrolysis*, Elsevier. 85, 151–4.

[86] Özbay, N., Apaydin-Varol, E., Burcu Uzun, B. and Eren Pütün, A. (2008) Characterization of bio-oil obtained from fruit pulp pyrolysis. *Energy*, Pergamon. 33, 1233–40.

[87] Yin, R., Liu, R., Mei, Y., Fei, W. and Sun, X. (2013) Characterization of bio-oil and bio-char obtained from sweet sorghum bagasse fast pyrolysis with fractional condensers. *Fuel*, Elsevier Ltd. 112, 96–104.

[88] Fei, W.T., Liu, R.H., Zhou, W.Q., Mei, Y.F. and Yin, R.Z. (2014) Influence of methanol additive on bio-oil stability. *International Journal of Agricultural and Biological Engineering*, 7, 83–92.

[89] Diebold, J.P. and Czernik, S. (1997) Additives to lower and stabilize the viscosity of pyrolysis oils during storage. *Energy and Fuels*, American Chemical Society. 11, 1081–91.

[90] Yin, R., Zhang, L., Liu, R., Mei, Y. and Yu, W. (2016) Optimization of composite additives for improving stability of bio-oils. *Fuel*, Elsevier Ltd. 170, 1–8.

[91] Sakthivel, R., Ramesh, K., Mohamed Shameer, P. and Purnachandran, R. (2019) Experimental investigation on improvement of storage stability of bio-oil derived from intermediate pyrolysis of Calophyllum inophyllum seed cake. *Journal of the Energy Institute*, Elsevier B.V. 92, 768–82.

[92] Oasmaa, A. and Kuoppala, E. (2003) Fast pyrolysis of forestry residue. 3. Storage stability of liquid fuel. *Energy and Fuels*, 17, 1075–84.

[93] Vural, E.G. (2019) Lignoselülozik Biyokütlenin Isıl Dönüşümüne Hidrotermal Ön İşlemin Etkilerinin İncelemesi. Eskişehir Teknik Üniversitesi.

[94] Uzun, B.B., Pütün, A.E. and Pütün, E. (2007) Rapid pyrolysis of olive residue. 1. Effect of heat and mass transfer limitations on product yields and bio-oil compositions. *Energy and Fuels*, 21, 1768–76.

[95] Meng, J., Moore, A., Tilotta, D.C., Kelley, S.S., Adhikari, S. and Park, S. (2015) Thermal and Storage Stability of Bio-Oil from Pyrolysis of Torrefied Wood. *Energy and Fuels*, 29, 5117–26.

[96] Meng, J., Park, J., Tilotta, D. and Park, S. (2012) The effect of torrefaction on the chemistry of fast-pyrolysis bio-oil. *Bioresource Technology*, Elsevier Ltd. 111, 439–46.

[97] Uzun, B.B., Pütün, A.E. and Pütün, E. (2007) Composition of products obtained via fast pyrolysis of olive-oil residue: Effect of pyrolysis temperature. *Journal of Analytical and Applied Pyrolysis*, Elsevier. 79, 147–53.

[98] Adjaye, J.D. and Bakhshi, N.N. (1995) Production of hydrocarbons by catalytic upgrading of a fast pyrolysis bio-oil. Part II: Comparative catalyst performance and reaction pathways. *Fuel Processing Technology*, Elsevier. 45, 185–202.

[99] Zhang, Q., Chang, J., Wang, T. and Xu, Y. (2007) Review of biomass pyrolysis oil properties and upgrading research. *Energy Conversion and Management*, Pergamon.

48, 87–92.

[100] Viswanathan, B. (2016) Energy Sources: Fundamentals of Chemical Conversion Processes and Applications. Energy Sources Fundam. Chem. Convers. Process. Appl. Newnes.

[101] Ţucureanu, V., Matei, A. and Avram, A.M. (2016) FTIR Spectroscopy for Carbon Family Study. *Critical Reviews in Analytical Chemistry*, Taylor & Francis. 46, 502–20.

[102] Grioui, N., Halouani, K. and Agblevor, F.A. (2014) Bio-oil from pyrolysis of Tunisian almond shell: Comparative study and investigation of aging effect during long storage. *Energy for Sustainable Development*, Elsevier. 21, 100–12.

[103] El-Hendawy, A.N.A. (2006) Variation in the FTIR spectra of a biomass under impregnation, carbonization and oxidation conditions. *Journal of Analytical and Applied Pyrolysis*, Elsevier. 75, 159–66.

[104] ILO International Chemical Safety Cards (ICSC). (2012) FURFURAL. https://www.ilo.org/dyn/icsc/showcard.display?p_version=2&p_card_id=0276 (Access date: March 10, 2022)

[105] Ingram, L., Mohan, D., Bricka, M., Steele, P., Strobel, D., Crocker, D. et al. (2008) Pyrolysis of wood and bark in an auger reactor: Physical properties and chemical analysis of the produced bio-oils. *Energy and Fuels*, 22, 614–25.

APPENDIX

Appendix A: GC/MS Chromatograms

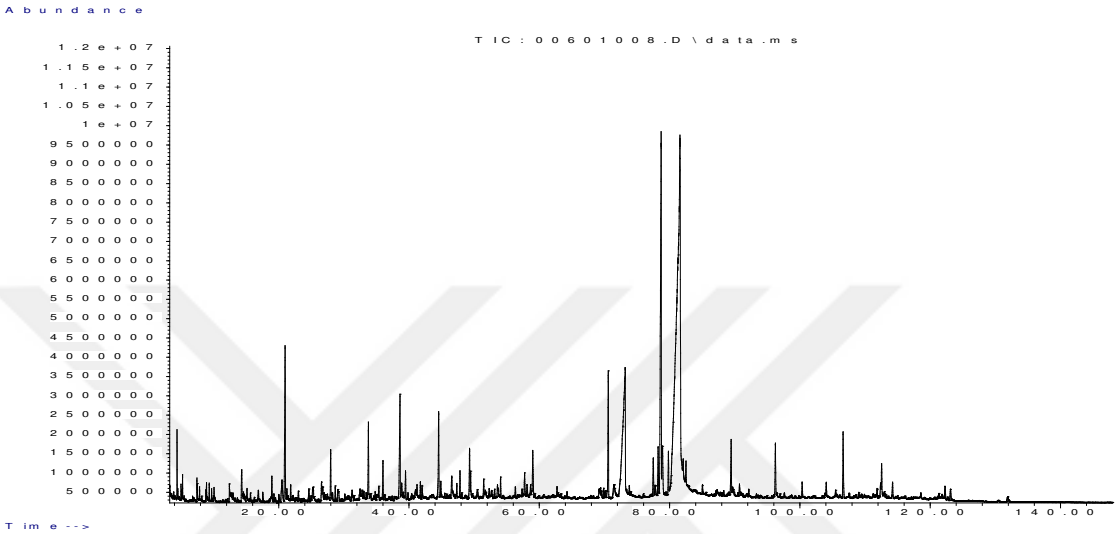

Figure A.1 *GC-MS chromatogram for non-aged pure bio-oil*

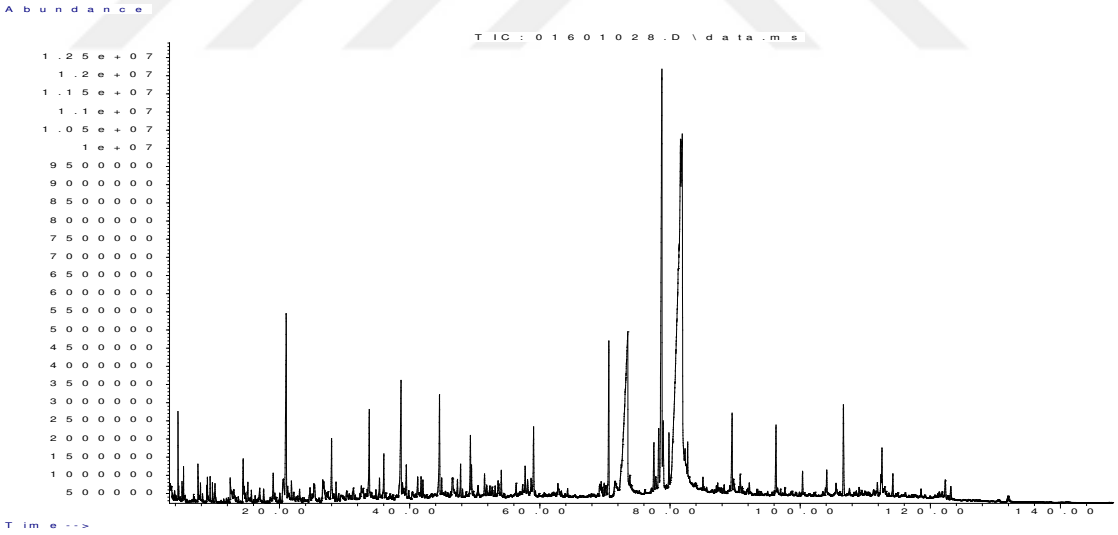

Figure A.2 *GC-MS chromatogram for 7 days-aged pure bio-oil*

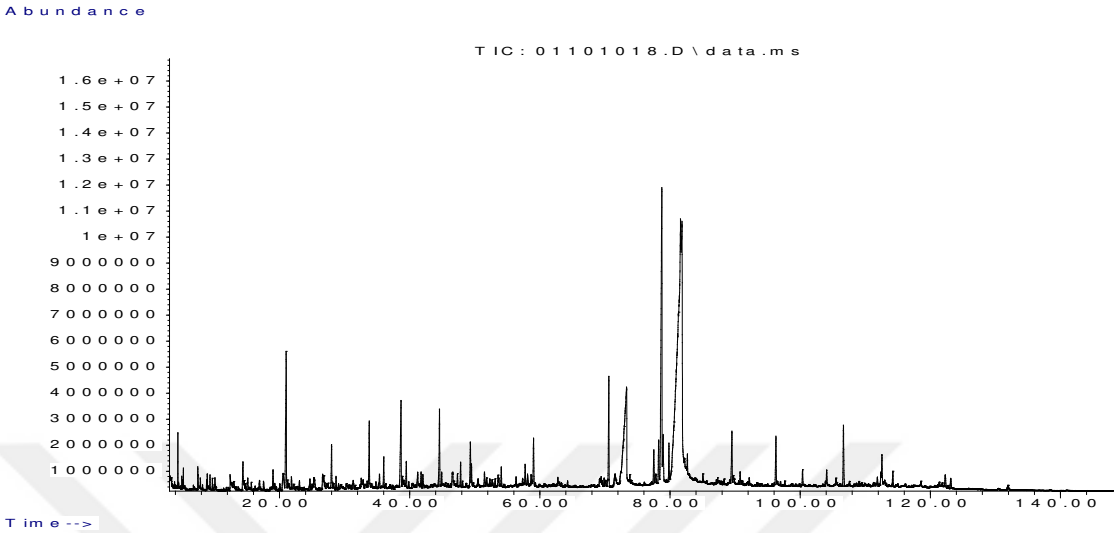

Figure A.3 *GC-MS chromatogram for 24 hours accelerated-aged pure bio-oil*

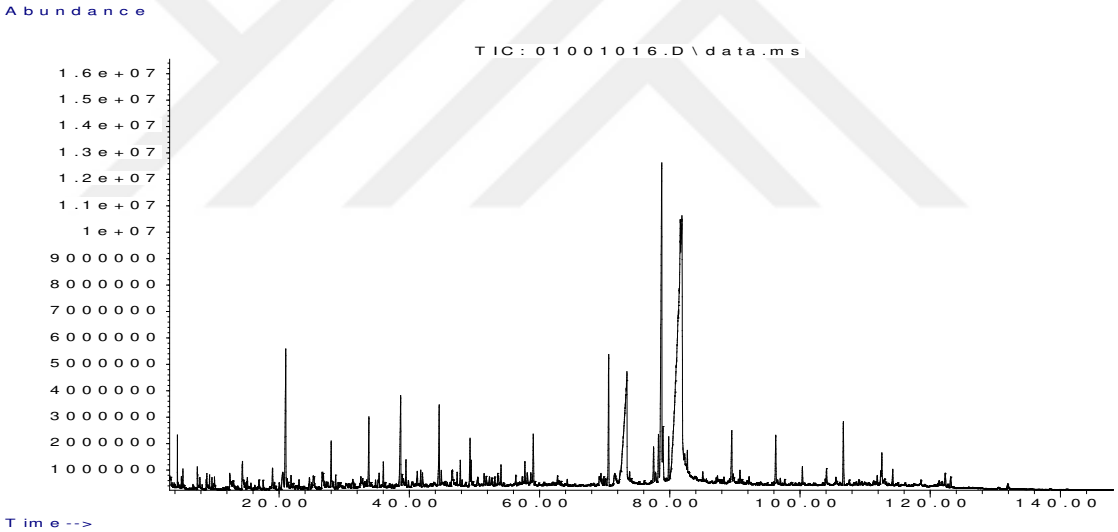

Figure A.4 *GC-MS chromatogram for 168 hours accelerated-aged pure bio-oil*

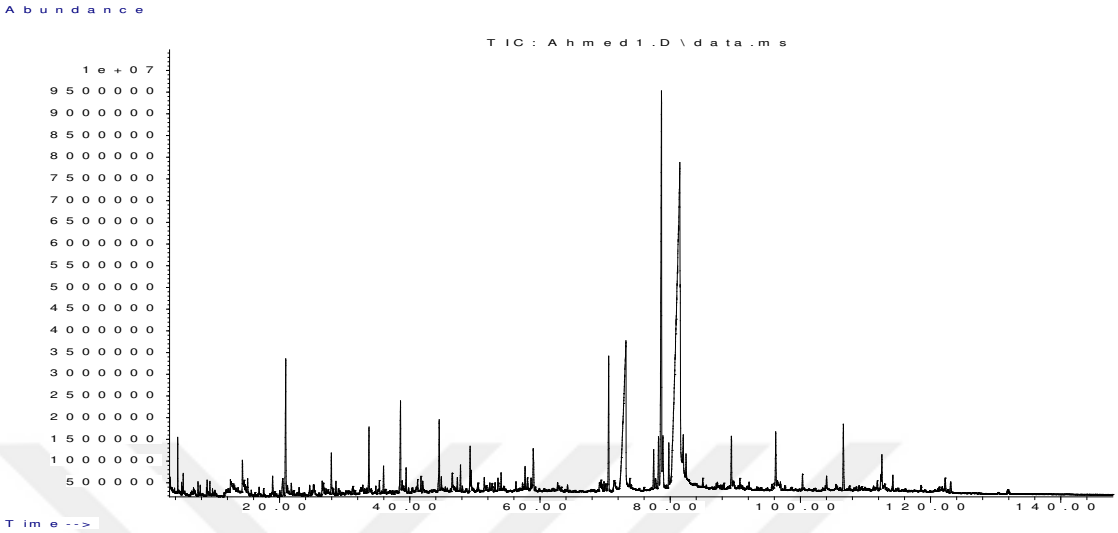

Figure A.5 *GC-MS chromatogram for non-aged methanol-stabilized bio-oil*

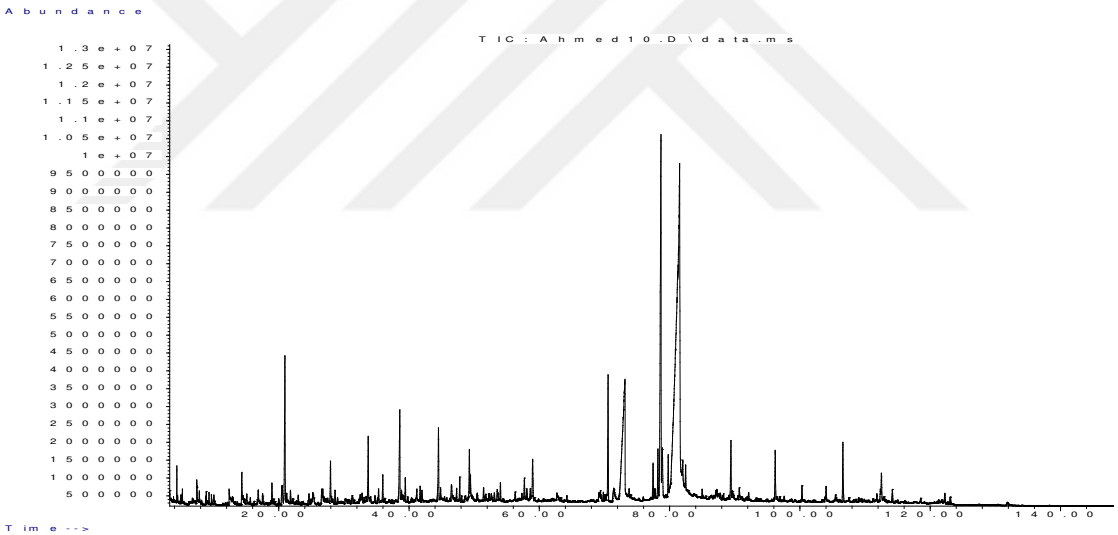

Figure A.6 *GC-MS chromatogram for 7 days-aged methanol-stabilized bio-oil*

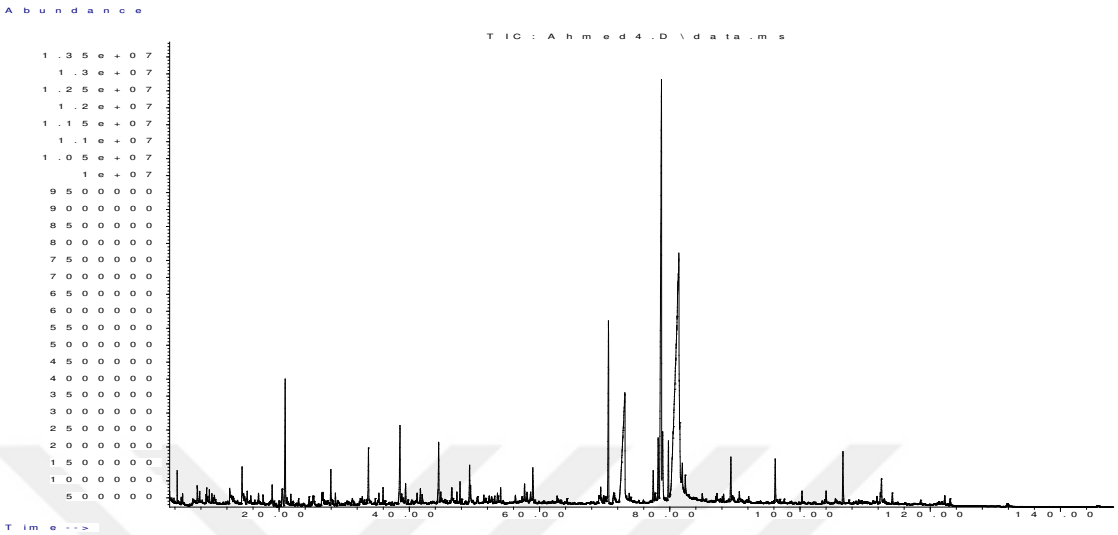

Figure A.7 *GC-MS chromatogram for 24 hours accelerated-aged methanol-stabilized bio-oil*

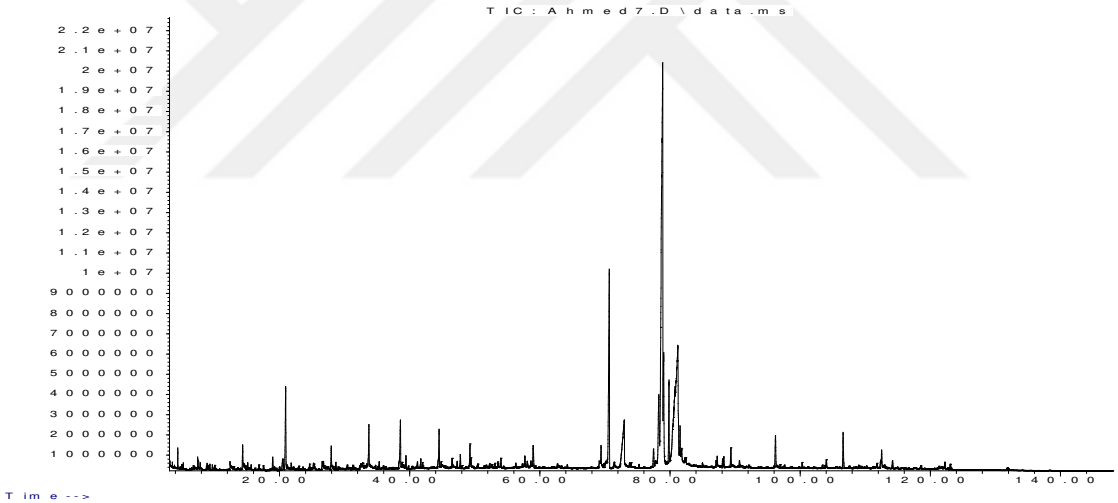

Figure A.8 *GC-MS chromatogram for 168 hours accelerated-aged methanol-stabilized bio-oil*

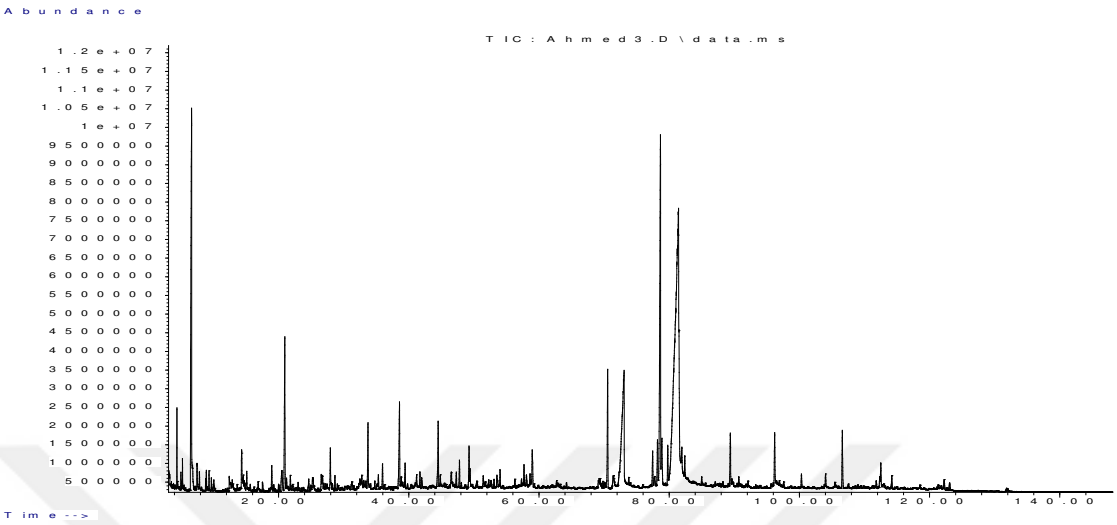

Figure A.9 *GC-MS chromatogram for non-aged furfural-stabilized bio-oil*

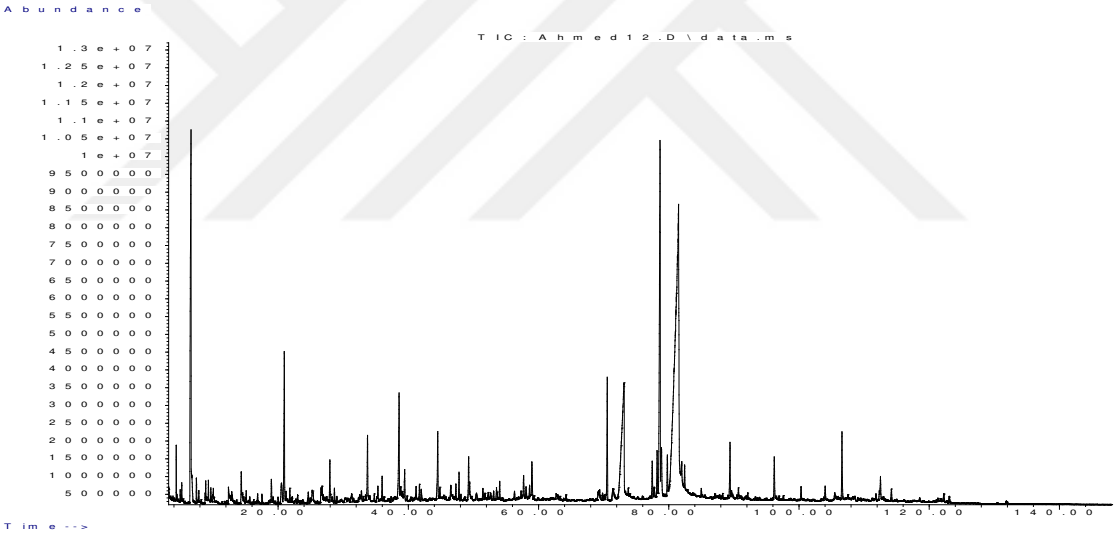

Figure A.10 *GC-MS chromatogram for 7 days-aged furfural-stabilized bio-oil*

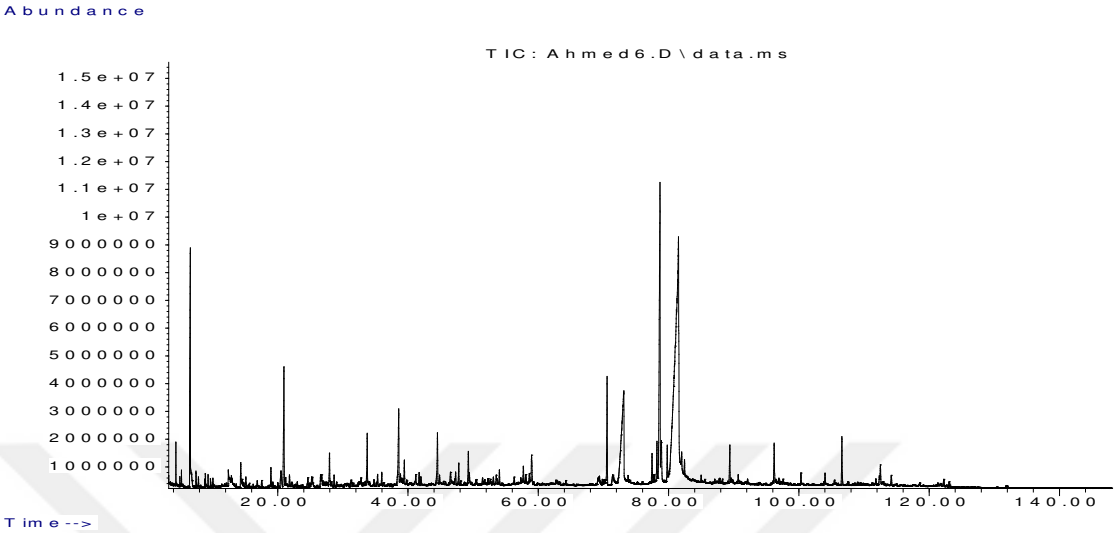

Figure A.11 *GC-MS chromatogram for 24 hours accelerated-aged furfural-stabilized bio-oil*

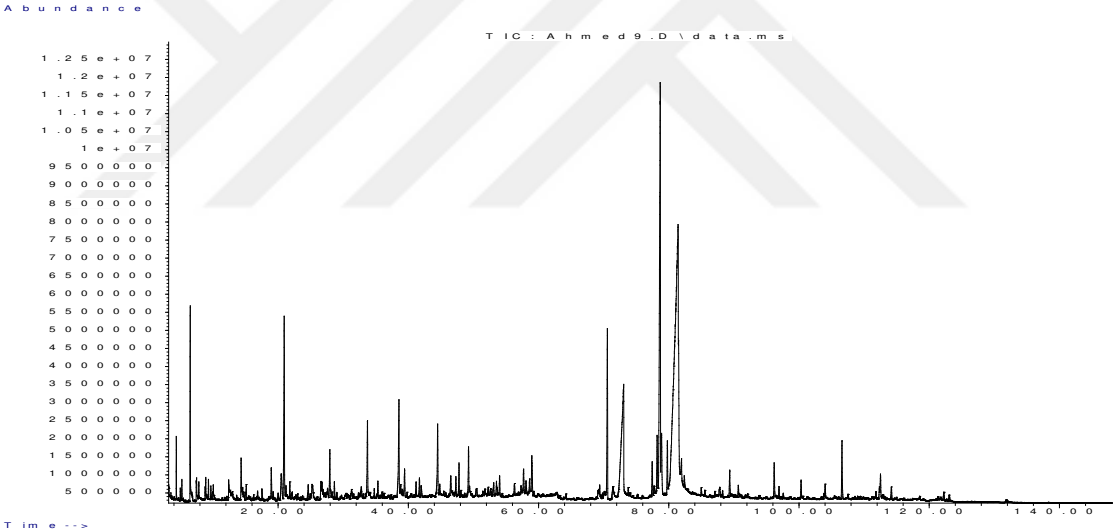

Figure A.12 *GC-MS chromatogram for 168 hours accelerated-aged furfural- stabilized bio-oil*

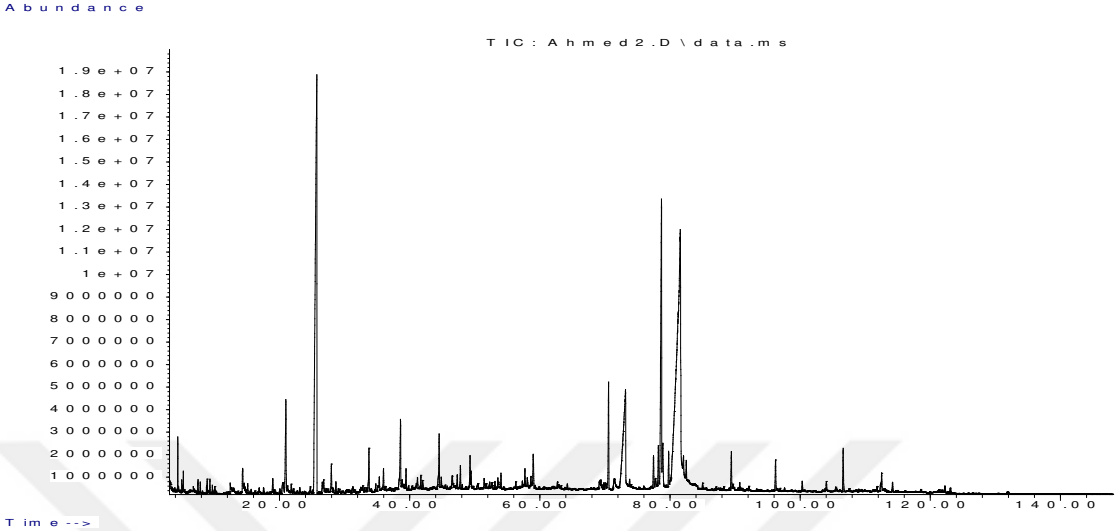

Figure A.13 *GC-MS chromatogram for non-aged tetrahydronaphthalene-stabilized bio-oil*

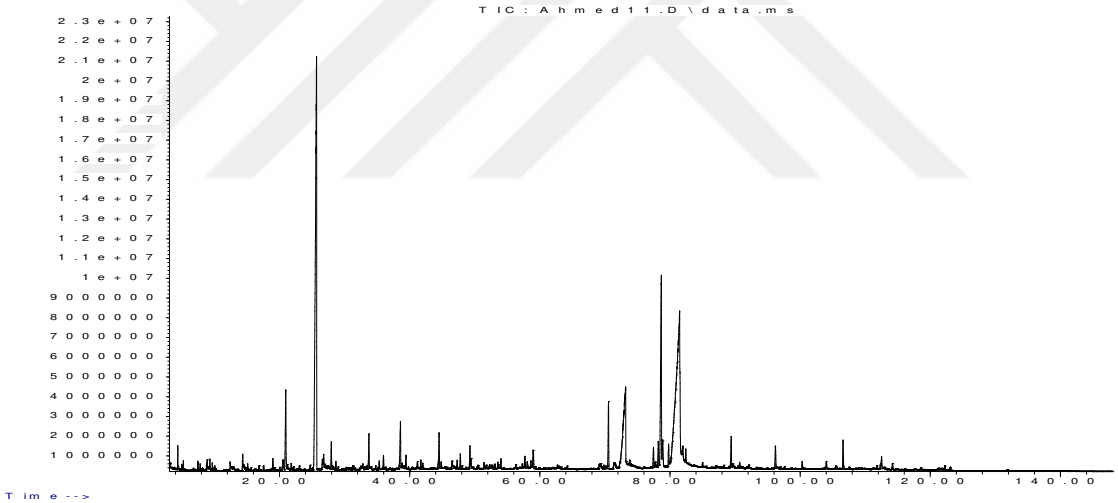

Figure A.14 *GC-MS chromatogram for 7 days-aged tetrahydronaphthalene-stabilized bio-oil*

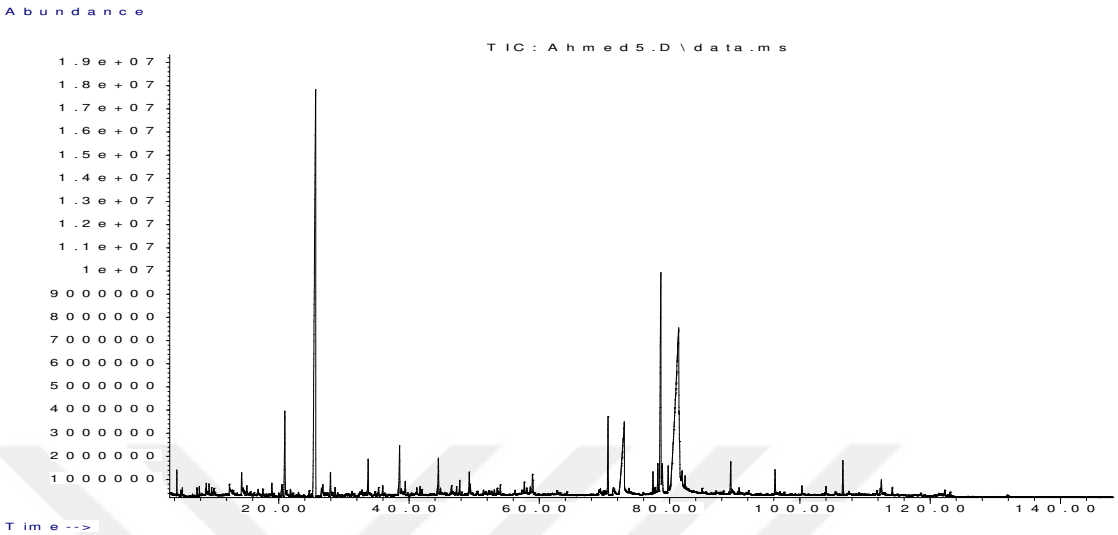

Figure A.15 *GC-MS chromatogram for 24 hours accelerated-aged tetrahydronaphthalene- stabilized bio-oil*

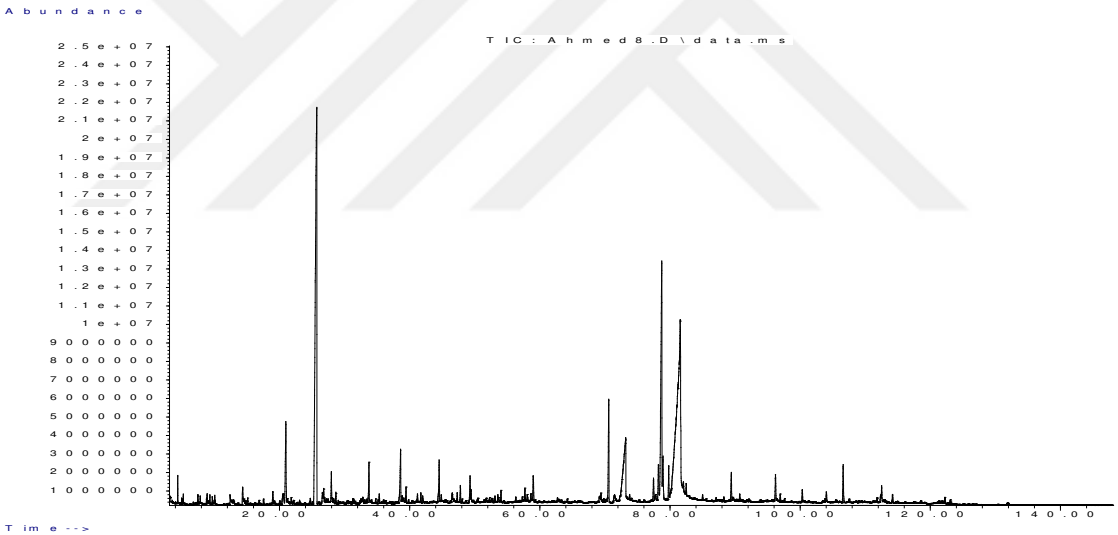

Figure A16 *GC-MS chromatogram for 168 hours accelerated-aged tetrahydronaphthalene- stabilized bio-oil*

CURRICULUM VITAE

Name Surname	**: Ahmed Ayyash**
Orcid Id	: 0000-0001-8102-9937
Languages	: Arabic (Native), Turkish, English

Education and qualifications:

- 2022, Eskişehir Technical University, Institute of Graduate Programs, Chemical Engineering Department.
- 2014, Hacettepe University, Engineering Faculty, Chemical Engineering Department.

Publications:

- Ayyash, A., Varol, E.A., Kılıç, M., Özsin, G. (2022). Influence of aging on the rheological behavior and characteristics of bio-oil produced from olive pomace via slow pyrolysis. *Biomass Conversion and Biorefinery.*
- Ayyash, A., Varol, E., Kılıç, M., Özsin, G. (2020). Characterization and Stability of Pyrolytic Oil Produced from Olive Residue, 15th International Combustion Symposium. Erciyes University